Appendices

Appendix - Chapter 2

Table A.1 Sample clinical metadata for all samples included in the thesis
This table summarizes the metadata for each sample analyzed in the thesis. UID denotes the unique sample identifier following the format Disease.Tissue.Condition-Site.Batch-Individual.Replicate. PID represents a randomly assigned individual identifier (1–999), with checks performed to avoid collisions. Disease abbreviations: As = ankylosing spondylitis; Aa = acute anterior uveitis; Ra rheumatoid arthritis; Ps = peripheral spondyloarthritis; Pa = psoriatic arthritis; Ma = monoarthritis; Hc = healthy control; Ni = no information. Tissue abbreviations: Pb = peripheral blood; Sf = synovial fluid; Sj = sacroiliac joint; Im = ileum; Pe = peri-entheseal bone; Et = entheseal soft tissue; Ey = eye. Treatment status: Bn = biologic-naïve; Bt = biologic-treated; Pb = previously biologic-treated but currently untreated; Ni = no information; Na = not applicable. Medication usage: Y = yes (currently taking); N = no (never taken); P = previous use (not currently taking).

UID	PID	Batch Name	Age	Sex	HLA-B*27 Status	Disease	Tissue	Treatment	Fresh/Frozen
Aa.Ey.Ni-Ox11-242A	242	aqh_eye			Positive	Aa	Ey	Bn	
Aa.Ey.Ni-Ox11-371A	371	aqh_eye			Positive	Aa	Ey	Bn	
Aa.Ey.Ni-Ox11-465A	465	aqh_eye			Positive	Aa	Ey	Bn	
Aa.Ey.Ni-Ox11-709A	709	aqh_eye		F	Positive	Aa	Ey	Bn	
Aa.Ey.Ni-Ox11-964A	964	aqh_eye			Positive	Aa	Ey	Bn	
As.Et.Na-Le10-843B	843	spine_enthesis			Positive	As	Et	Bn	Fresh
As.Et.Ni-Le10-91B	91	spine_enthesis			Positive	As	Et	Bn	Frozen
As.Im.Bn-Na7-263A	263	gut_naples		M	Positive	As	Im	Bn	Frozen

As.Im.Bn-Na7-614A	614	gut_naples		M	Negative	As	Im	Bn	Frozen
As.Im.Bn-Na7-910A	910	gut_naples		M	Negative	As	Im	Bn	Frozen
As.Im.Bn-Ox8-275A	275	gut_tgu		M	Positive	As	Im	Bn	Fresh
As.Im.Bn-Ox8-275B	275	gut_tgu		M	Positive	As	Im	Bn	Fresh
As.Im.Ni-Ox8-35B	35	gut_tgu			Positive	As	Im	Ni	Fresh
As.Pb.Bn-Be6-369A	369	berlin_pb_sf	29	F	Negative	As	Pb	Bn	Frozen
As.Pb.Bn-Be6-453A	453	berlin_pb_sf	68	F	Positive	As	Pb	Bn	Frozen
As.Pb.Bn-Be6-508A	508	berlin_pb_sf	44	M	Positive	As	Pb	Bn	Frozen
As.Pb.Bn-Na7-263B	263	gut_naples		M	Positive	As	Pb	Bn	Frozen
As.Pb.Bn-Na7-614B	614	gut_naples		M	Negative	As	Pb	Bn	Frozen
As.Pb.Bn-Na7-910B	910	gut_naples		M	Negative	As	Pb	Bn	Frozen
As.Pb.Bn-Ox1-134A	134	ox_old_P170676	24	M	Positive	As	Pb	Bn	Frozen
As.Pb.Bn-Ox1-503A	503	ox_old_P170676	47	M	Positive	As	Pb	Bn	Frozen
As.Pb.Bn-Ox1-925A	925	ox_old_P170676	49	M	Negative	As	Pb	Bn	Frozen
As.Pb.Bn-Ox2-598A	598	ox_old_P180407	49	M	Positive	As	Pb	Bn	Frozen

As.Pb.Bn-Ox2-681A	681	ox_old_P180407	42	M	Positive	As	Pb	Bn	Frozen
As.Pb.Bn-Ox4-580A	580	ox_old_P190726	56	M	Positive	As	Pb	Bn	Frozen
As.Pb.Bn-Ox4-600A	600	ox_old_P190726	49	M	Positive	As	Pb	Bn	Frozen
As.Pb.Bn-Ox4-810A	810	ox_old_P190726	66	M	Positive	As	Pb	Bn	Frozen
As.Pb.Bn-Ox5-105A	105	ox_va_pb_sf	39	F	Positive	As	Pb	Bn	Frozen
As.Pb.Bn-Ox5-434A	434	ox_va_pb_sf	44	F	Positive	As	Pb	Bn	Frozen
As.Pb.Bn-Ox5-585A	585	ox_va_pb_sf	65	M	Positive	As	Pb	Bn	Frozen
As.Pb.Bn-Ox5-800A	800	ox_va_pb_sf	65	M	Positive	As	Pb	Bn	Frozen
As.Pb.Bn-Ox5-874A	874	ox_va_pb_sf	20	M	Positive	As	Pb	Bn	Frozen
As.Pb.Bn-Ox9-375B	375	sij		F	Positive	As	Pb	Bn	Fresh
As.Pb.Bn-Ox9-405B	405	sij		F	Positive	As	Pb	Bn	Fresh
As.Pb.Bn-Ox9-495C	495	sij		M	Positive	As	Pb	Bn	Fresh
As.Pb.Bn-Ox9-79B	79	sij		M	Positive	As	Pb	Bn	Fresh
As.Pb.Bt-Be6-609A	609	berlin_pb_sf	61	F	Positive	As	Pb	Bt	Frozen
As.Pb.Bt-Ox1-319A	319	ox_old_P170676	47	M	Positive	As	Pb	Bt	Frozen

As.Pb.Bt-Ox1-473A	473	ox_old_P170676	36	M	Positive	As	Pb	Bt	Frozen
As.Pb.Bt-Ox1-7A	7	ox_old_P170676	22	M	Positive	As	Pb	Bt	Frozen
As.Pb.Bt-Ox2-598B	598	ox_old_P180407	49	M	Positive	As	Pb	Bt	Frozen
As.Pb.Bt-Ox2-681B	681	ox_old_P180407	42	M	Positive	As	Pb	Bt	Frozen
As.Pb.Bt-Ox3-598C	598	ox_old_P190230	49	M	Positive	As	Pb	Bt	Frozen
As.Pb.Bt-Ox3-598D	598	ox_old_P190230	49	M	Positive	As	Pb	Bt	Frozen
As.Pb.Bt-Ox5-109A	109	ox_va_pb_sf	30	M	Positive	As	Pb	Bt	Frozen
As.Pb.Bt-Ox5-120A	120	ox_va_pb_sf	35	M	Positive	As	Pb	Bt	Frozen
As.Pb.Bt-Ox5-447A	447	ox_va_pb_sf	56	M	Positive	As	Pb	Bt	Frozen
As.Pb.Bt-Ox5-497A	497	ox_va_pb_sf	65	M	Positive	As	Pb	Bt	Frozen
As.Pb.Bt-Ox5-50A	50	ox_va_pb_sf	31	M	Positive	As	Pb	Bt	Frozen
As.Pb.Bt-Ox5-744A	744	ox_va_pb_sf	53	M	Positive	As	Pb	Bt	Frozen
As.Pb.Ni-Ox8-35A	35	gut_tgu		M	Positive	As	Pb	Ni	Frozen
As.Pb.Pb-Be6-243A	243	berlin_pb_sf	30	F	Positive	As	Pb	Pb	Frozen
As.Pb.Pb-Be6-929A	929	berlin_pb_sf	62	M	Positive	As	Pb	Pb	Frozen
As.Pb.Pb-Ox1-143A	143	ox_old_P170676	53	F	Positive	As	Pb	Pb	Frozen

As.Pe.Na-Le10-843A	843	spine_enthesis			Positive	As	Pe	Ni	Fresh
As.Pe.Ni-Le10-706A	706	spine_enthesis			Positive	As	Pe	Ni	Frozen
As.Pe.Ni-Le10-706B	706	spine_enthesis			Positive	As	Pe	Ni	Frozen
As.Pe.Ni-Le10-834A	834	spine_enthesis			Positive	As	Pe	Ni	Frozen
As.Pe.Ni-Le10-91A	91	spine_enthesis			Positive	As	Pe	Ni	Frozen
As.Sf.Bn-Be5-102A	102	ox_va_pb_sf	68	F	Positive	As	Sf	Bn	Frozen
As.Sf.Bn-Be6-369B	369	berlin_pb_sf	29	F	Negative	As	Sf	Bn	Frozen
As.Sf.Bn-Be6-453B	453	berlin_pb_sf	68	F	Positive	As	Sf	Bn	Frozen
As.Sf.Bn-Be6-508B	508	berlin_pb_sf	44	M	Positive	As	Sf	Bn	Frozen
As.Sf.Bn-Ox5-800B	800	ox_va_pb_sf	65	M	Positive	As	Sf	Bn	Frozen
As.Sf.Bt-Be6-609B	609	berlin_pb_sf	61	F	Positive	As	Sf	Bt	Frozen
As.Sf.Bt-Ox5-447B	447	ox_va_pb_sf	56	M	Positive	As	Sf	Bt	Frozen
As.Sf.Bt-Ox5-744B	744	ox_va_pb_sf	53	M	Positive	As	Sf	Bt	Frozen
As.Sf.Ni-Be12-190A	190	cd8_sfmc_berlin	35	M	Negative	As	Sf	Ni	
As.Sf.Ni-Be12-518A	518	cd8_sfmc_berlin	26	F	Positive	As	Sf	Ni	
As.Sf.Ni-Be12-528A	528	cd8_sfmc_berlin	41	M	Positive	As	Sf	Ni	
As.Sf.Ni-Be12-560A	560	cd8_sfmc_berlin	34	M	Positive	As	Sf	Ni	
As.Sf.Ni-Be12-714A	714	cd8_sfmc_berlin	35	M	Negative	As	Sf	Ni	
As.Sf.Ni-Ox5-644A	644	ox_va_pb_sf		F	Positive	As	Sf	Ni	Fresh
As.Sf.Ni-Ox5-644B	644	ox_va_pb_sf		F	Positive	As	Sf	Ni	Fresh

As.Sf.Ni-Ox5-721A	721	ox_va_pb_sf		M	Positive	As	Sf	Ni	Fresh
As.Sf.Pb-Be6-243B	243	berlin_pb_sf	30	F	Positive	As	Sf	Pb	Frozen
As.Sf.Pb-Be6-243C	243	berlin_pb_sf	30	F	Positive	As	Sf	Pb	Frozen
As.Sf.Pb-Be6-929B	929	berlin_pb_sf	62	M	Positive	As	Sf	Pb	Frozen
As.Sj.Bn-Ox9-405A	405	sij			Positive	As	Sj	Bn	Fresh
As.Sj.Bn-Ox9-495A	495	sij			Positive	As	Sj	Bn	Fresh
As.Sj.Bn-Ox9-495B	495	sij			Positive	As	Sj	Bn	Fresh
As.Sj.Bn-Ox9-79A	79	sij			Positive	As	Sj	Bn	Fresh
Hc.Et.Na-Le10-192B	192	spine_enthesis		F		Hc	Et	Na	Fresh
Hc.Et.Na-Le10-458B	458	spine_enthesis		F		Hc	Et	Na	Fresh
Hc.Et.Na-Le10-66B	66	spine_enthesis		M		Hc	Et	Na	Fresh
Hc.Et.Na-Le10-838B	838	spine_enthesis		F		Hc	Et	Na	Fresh
Hc.Im.Na-Na7-568A	568	gut_naples		F		Hc	Im	Na	Frozen
Hc.Im.Na-Na7-606A	606	gut_naples		F		Hc	Im	Na	Frozen
Hc.Im.Na-Na7-630A	630	gut_naples		M		Hc	Im	Na	Frozen
Hc.Im.Na-Na7-734A	734	gut_naples		F		Hc	Im	Na	Frozen
Hc.Im.Na-Na7-885A	885	gut_naples		F		Hc	Im	Na	Frozen
Hc.Pb.Na-Na7-568B	568	gut_naples		F		Hc	Pb	Na	Frozen

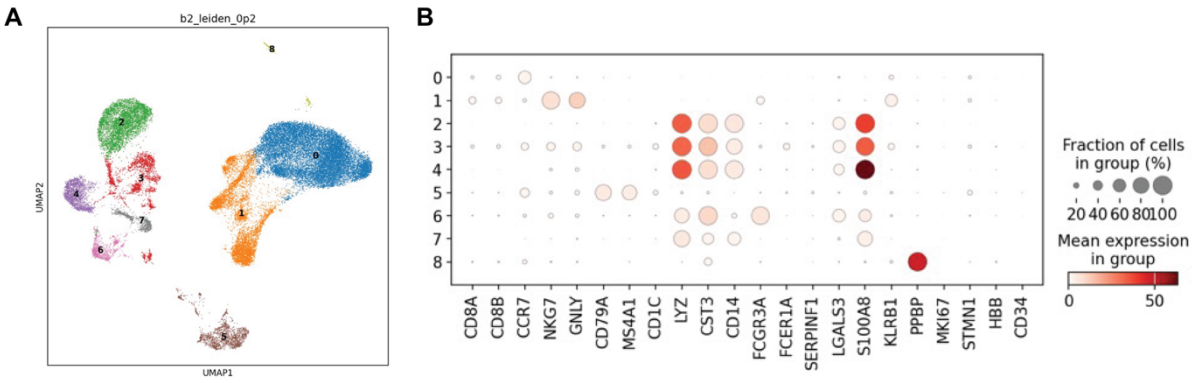
Hc.Pb.Na-Na7-606B	606	gut_naples		F		Hc	Pb	Na	Frozen
Hc.Pb.Na-Na7-630B	630	gut_naples		M		Hc	Pb	Na	Frozen
Hc.Pb.Na-Na7-734B	734	gut_naples		F		Hc	Pb	Na	Frozen
Hc.Pb.Na-Na7-885B	885	gut_naples		F		Hc	Pb	Na	Frozen
Hc.Pb.Na-Ox4-149A	149	ox_old_P190726	66	M	Positive	Hc	Pb	Na	Frozen
Hc.Pb.Na-Ox4-36A	36	ox_old_P190726	46	M	Positive	Hc	Pb	Na	Frozen
Hc.Pb.Na-Ox4-456A	456	ox_old_P190726	54	M	Positive	Hc	Pb	Na	Frozen
Hc.Pb.Na-Ox5-239A	239	ox_va_pb_sf	23	M		Hc	Pb	Na	Frozen
Hc.Pb.Na-Ox5-308A	308	ox_va_pb_sf	29	M		Hc	Pb	Na	Frozen
Hc.Pb.Na-Ox5-396A	396	ox_va_pb_sf	36	F		Hc	Pb	Na	Frozen
Hc.Pb.Na-Ox5-487A	487	ox_va_pb_sf	23	M		Hc	Pb	Na	Frozen
Hc.Pb.Na-Ox5-677A	677	ox_va_pb_sf	39	M	Negative	Hc	Pb	Na	Frozen
Hc.Pb.Na-Ox5-685A	685	ox_va_pb_sf	28	M		Hc	Pb	Na	Frozen
Hc.Pe.Na-Le10-192A	192	spine_enthesis		F		Hc	Pe	Na	Fresh
Hc.Pe.Na-Le10-458A	458	spine_enthesis		F		Hc	Pe	Na	Fresh

Hc.Pe.Na-Le10-66A	66	spine_enthesis		M		Hc	Pe	Na	Fresh
Hc.Pe.Na-Le10-838A	838	spine_enthesis		F		Hc	Pe	Na	Fresh
Ma.Pb.Bn-Be6-577A	577	berlin_pb_sf	37	F	Negative	Ma	Pb	Bn	Frozen
Ma.Sf.Bn-Be6-577B	577	berlin_pb_sf	37	F	Negative	Ma	Sf	Bn	Frozen
Pa.Pb.Bn-Be6-538A	538	berlin_pb_sf	55	M	Negative	Pa	Pb	Bn	Frozen
Pa.Pb.Bn-Be6-95A	95	berlin_pb_sf	43	M	Negative	Pa	Pb	Bn	Frozen
Pa.Pb.Bt-Be6-780A	780	berlin_pb_sf	57	M	Negative	Pa	Pb	Bt	Frozen
Pa.Sf.Bn-Be6-538B	538	berlin_pb_sf	55	M	Negative	Pa	Sf	Bn	Frozen
Pa.Sf.Bn-Be6-95B	95	berlin_pb_sf	43	M	Negative	Pa	Sf	Bn	Frozen
Pa.Sf.Bt-Be6-780B	780	berlin_pb_sf	57	M	Negative	Pa	Sf	Bt	Frozen
Ps.Pb.Bn-Be6-454A	454	berlin_pb_sf	49	M	Positive	Ps	Pb	Bn	Frozen
Ps.Pb.Bn-Be6-767A	767	berlin_pb_sf	57	M	Positive	Ps	Pb	Bn	Frozen
Ps.Pb.Bt-Be6-42A	42	berlin_pb_sf	33	M	Positive	Ps	Pb	Bt	Frozen
Ps.Sf.Bn-Be6-454B	454	berlin_pb_sf	49	M	Positive	Ps	Sf	Bn	Frozen
Ps.Sf.Bn-Be6-767B	767	berlin_pb_sf	57	M	Positive	Ps	Sf	Bn	Frozen
Ps.Sf.Bt-Be6-42B	42	berlin_pb_sf	33	M	Positive	Ps	Sf	Bt	Frozen
Ra.Pb.Bn-Ox5-572A	572	ox_va_pb_sf	64	F		Ra	Pb	Bn	Frozen
Ra.Pb.Bn-Ox5-756A	756	ox_va_pb_sf	69	M		Ra	Pb	Bn	Frozen

Ra.Pb.Bn-Ox5-951A	951	ox_va_pb_sf	54	F		Ra	Pb	Bn	Frozen
Ra.Pb.Bn-Ox5-951B	951	ox_va_pb_sf	54	F		Ra	Pb	Bn	Frozen
Ra.Pb.Bt-Ox5-742A	742	ox_va_pb_sf	53	F		Ra	Pb	Bt	Frozen
Ra.Pb.Na-Ox5-601A	601	ox_va_pb_sf	30	F		Ra	Pb	Ni	Frozen
Ra.Sf.Bn-Ox5-464A	464	ox_va_pb_sf	64	F		Ra	Sf	Bn	Frozen
Ra.Sf.Bn-Ox5-572B	572	ox_va_pb_sf	64	F		Ra	Sf	Bn	Frozen
Ra.Sf.Bn-Ox5-756B	756	ox_va_pb_sf	69	M		Ra	Sf	Bn	Frozen
Ra.Sf.Bn-Ox5-757A	757	ox_va_pb_sf	83	M		Ra	Sf	Bn	Frozen
Ra.Sf.Bt-Ox5-742B	742	ox_va_pb_sf	53	F		Ra	Sf	Bt	Frozen
Ra.Sf.Ni-Be12-332A	332	cd8_sfmc_berlin	68	F	Negative	Ra	Sf	Ni	
Ra.Sf.Ni-Be12-953A	953	cd8_sfmc_berlin	24	F	Negative	Ra	Sf	Ni	

Appendix - Chapter 3

Figure B.1 Initial clustering for cells from project P180407 for sample identity inference
(A) UMAP embeddings for cells from P180407 colored by Leiden clusters (resolution = 0.2).
(B) Dot plot showing the expression of canonical immune marker genes across clusters.
Marker profiles established annotation of the major immune lineages.



Appendix - Chapter 4

Table C.1 Antibody panel used for CITE-seq library in P190230
Details of the antibodies included in the CITE-seq panel used for P190230 project, including antibody ID, target name, read, capture pattern, and oligonucleotide sequence.

id	name	read	pattern	sequence
C005	CD80_TotalSeqC	R2	5PNNNNNNNNNN(BC)	ACGAATCAATCTGTG
C390	CD127_TotalSeqC	R2	5PNNNNNNNNNN(BC)	GTGTGTTGTCCTATG
C083	CD16_TotalSeqC	R2	5PNNNNNNNNNN(BC)	AAGTTCACTCTTTGC
C089	TIGIT_TotalSeqC	R2	5PNNNNNNNNNN(BC)	TTGCTTACCGCCAGA
C148	CD197_TotalSeqC	R2	5PNNNNNNNNNN(BC)	AGTTCAGTCAACCG A
C391	CD45_TotalSeqC	R2	5PNNNNNNNNNN(BC)	TGCAATTACCCGGAT
C050	CD19_TotalSeqC	R2	5PNNNNNNNNNN(BC)	CTGGGCAATTACTCG
C161	CD11b_TotalSeqC	R2	5PNNNNNNNNNN(BC)	GACAAGTGATCTGC A
C006	CD86_TotalSeqC	R2	5PNNNNNNNNNN(BC)	GTCTTTGTCAGTGCA
C159	HLA-DR_TotalSeqC	R2	5PNNNNNNNNNN(BC)	AATAGCGAGCAAGTA
C081	CD14_TotalSeqC	R2	5PNNNNNNNNNN(BC)	TCTCAGACCTCCGTA
C084	CD56_TotalSeqC	R2	5PNNNNNNNNNN(BC)	TTCGCCGCATTGAGT
C072	CD4_TotalSeqC	R2	5PNNNNNNNNNN(BC)	TGTTCCCGCTCAACT
C080	CD8a_TotalSeqC	R2	5PNNNNNNNNNN(BC)	GCTGCGCTTTCCATT
C085	CD25_TotalSeqC	R2	5PNNNNNNNNNN(BC)	TTTGTCCTGTACGCC
C147	CD62L_TotalSeqC	R2	5PNNNNNNNNNN(BC)	GTCCCTGCAACTTG A
C088	CD279_TotalSeqC	R2	5PNNNNNNNNNN(BC)	ACAGCGCCGTATTTA
C087	CD45RO_TotalSeqC	R2	5PNNNNNNNNNN(BC)	CTCCGAATCATGTTG
C154	CD27_TotalSeqC	R2	5PNNNNNNNNNN(BC)	GCACTCCTGCATGTA
C034	CD3_TotalSeqC	R2	5PNNNNNNNNNN(BC)	CTCATTGTAACTCCT
C171	CD278_TotalSeqC	R2	5PNNNNNNNNNN(BC)	CGCGCACCCATTAAA
C386	CD28_TotalSeqC	R2	5PNNNNNNNNNN(BC)	TGAGAACGACCCTA A
C063	CD45RA_TotalSeqC	R2	5PNNNNNNNNNN(BC)	TCAATCCTTCCGCTT
C251	Hashtag1_TotalSeq C	R2	5PNNNNNNNNNN(BC)	GTCAACTCTTTAGCG
C252	Hashtag2_TotalSeq C	R2	5PNNNNNNNNNN(BC)	TGATGGCCTATTGGG
C253	Hashtag3_TotalSeq C	R2	5PNNNNNNNNNN(BC)	TTCCGCCTCTCTTTG
C254	Hashtag4_TotalSeq C	R2	5PNNNNNNNNNN(BC)	AGTAAGTTCAGCGTA

Table C.2 Antibody panel used for CITE-seq library in P190726
Details of the antibodies included in the CITE-seq panel used for P190726 project, including antibody ID, target name, read, capture pattern, and oligonucleotide sequence.

id	name	read	pattern	sequence
C001	CD11c_TotalSeqC	R2	5PNNNNNNNNNN(BC)	GTACTTGATTAGCCT
C002	CD14_TotalSeqC	R2	5PNNNNNNNNNN(BC)	TCCGAGTCCGTCGCG
C003	CD16_TotalSeqC	R2	5PNNNNNNNNNN(BC)	GAGTTGCGAAGTTCT
C004	CD19_TotalSeqC	R2	5PNNNNNNNNNN(BC)	TGCTAACACAACGAG
C005	CD3_TotalSeqC	R2	5PNNNNNNNNNN(BC)	CAAGCATGTAGGAGT
C006	CD34_TotalSeqC	R2	5PNNNNNNNNNN(BC)	CCGCGAATCAGCCGC
C007	CD4_TotalSeqC	R2	5PNNNNNNNNNN(BC)	CTTCTACAACAATGG
C008	CD56_TotalSeqC	R2	5PNNNNNNNNNN(BC)	CCTAATGGTCCAGAC
C009	CD8a_TotalSeqC	R2	5PNNNNNNNNNN(BC)	GTGGTAAGCAGACGC
C010	CD45RA_TotalSeqC	R2	5PNNNNNNNNNN(BC)	CCGGTTCTGGCACAG
C011	HLADR_TotalSeqC	R2	5PNNNNNNNNNN(BC)	ATGTTATGCGTCGTG
C012	CD11b_TotalSeqC	R2	5PNNNNNNNNNN(BC)	GGTGATTACTGGAGA
C013	CCR7_TotalSeqC	R2	5PNNNNNNNNNN(BC)	GCGGCGAAGAAGCTA
C014	TCRgd_TotalSeqC	R2	5PNNNNNNNNNN(BC)	ATAGCTCTGGCAACG
C015	CCR2_TotalSeqC	R2	5PNNNNNNNNNN(BC)	AAGAACCTCTCACAT
C016	CX3CR1_TotalSeqC	R2	5PNNNNNNNNNN(BC)	TTCATTCGCATCATC
C017	CD45_hash17_TotalSeqC	R2	5PNNNNNNNNNN(BC)	TATTACAAGCGCAAT
C018	CD45_hash18_TotalSeqC	R2	5PNNNNNNNNNN(BC)	CATTGTCGACCGCGA
C019	CD45_hash19_TotalSeqC	R2	5PNNNNNNNNNN(BC)	GCACAGTCCGCAATC
C020	CD45_hash20_TotalSeqC	R2	5PNNNNNNNNNN(BC)	TAATACCGGAGCCGA
C021	CD45_hash21_TotalSeqC	R2	5PNNNNNNNNNN(BC)	AGGAACCGACACCTA
C022	CD45_hash22_TotalSeqC	R2	5PNNNNNNNNNN(BC)	TCTGCACCTTGCACG
C023	HC10_TotalSeqC	R2	5PNNNNNNNNNN(BC)	ACATGATATATTCAC

C024	KIR3DL2_TotalSeqC	R2	5PNNNNNNNNNN(BC)	TTAGCCTACGATACT
C025	W6_32_TotalSeqC	R2	5PNNNNNNNNNN(BC)	GCAGAATGAGCGTCA
C026	ME1_TotalSeqC	R2	5PNNNNNNNNNN(BC)	ACCTGGCAAGCTAGT

Table C.3 Antibody panel TotalSeq-C Human Universal Cocktail
Details of the antibody panel TotalSeq-C Human Universal Cocktail, including antibody ID, name, read, capture pattern, and oligonucleotide sequence.

id	name	read	pattern	sequence
ADT_C0944	Hu.CD101	R2	5PNNNNNNNNNN(BC)	CTACTTCCCTGTCAA
ADT_C0145	Hu.CD103	R2	5PNNNNNNNNNN(BC)	GACCTCATTGTGAAT
ADT_C0068	Hu.CD105_43A3	R2	5PNNNNNNNNNN(BC)	ATCGTCGAGAGCTAG
ADT_C0155	Hu.CD107a	R2	5PNNNNNNNNNN(BC)	CAGCCCACTGCAATA
ADT_C0024	Hu.CD112	R2	5PNNNNNNNNNN(BC)	AACCTTCCGTCTAAG
ADT_C0219	Hu.CD119	R2	5PNNNNNNNNNN(BC)	TGTGTATTCCCTTGT
ADT_C0185	Hu.CD11a	R2	5PNNNNNNNNNN(BC)	TATATCCTTGTGAGC
ADT_C0161	Hu.CD11b	R2	5PNNNNNNNNNN(BC)	GACAAGTGATCTGCA
ADT_C0053	Hu.CD11c	R2	5PNNNNNNNNNN(BC)	TACGCCTATAACTTG
ADT_C0246	Hu.CD122	R2	5PNNNNNNNNNN(BC)	TCATTTCCTCCGATT
ADT_C0064	Hu.CD123	R2	5PNNNNNNNNNN(BC)	CTTCACTCTGTCAGG
ADT_C0363	Hu.CD124	R2	5PNNNNNNNNNN(BC)	CCGTCCTGATAGATG
ADT_C0390	Hu.CD127	R2	5PNNNNNNNNNN(BC)	GTGTGTTGTCCTATG
ADT_C0364	Hu.CD13	R2	5PNNNNNNNNNN(BC)	TTTCAACGCCCTTTC
ADT_C0158	Hu.CD134	R2	5PNNNNNNNNNN(BC)	AACCCACCGTTGTTA
ADT_C0355	Hu.CD137	R2	5PNNNNNNNNNN(BC)	CAGTAAGTTCGGGAC
ADT_C0163	Hu.CD141	R2	5PNNNNNNNNNN(BC)	GGATAACCGCGCTTT
ADT_C0134	Hu.CD146	R2	5PNNNNNNNNNN(BC)	CCTTGGATAACATCA
ADT_C0081	Hu.CD14_M5E2	R2	5PNNNNNNNNNN(BC)	TCTCAGACCTCCGTA
ADT_C0151	Hu.CD152	R2	5PNNNNNNNNNN(BC)	ATGGTTCACGTAATC
ADT_C0032	Hu.CD154	R2	5PNNNNNNNNNN(BC)	GCTAGATAGATGCAA
ADT_C0023	Hu.CD155	R2	5PNNNNNNNNNN(BC)	ATCACATCGTTGCCA
ADT_C0420	Hu.CD158	R2	5PNNNNNNNNNN(BC)	TATCAACCAACGCTT
ADT_C0592	Hu.CD158b	R2	5PNNNNNNNNNN(BC)	GACCCGTAGTTTGAT
ADT_C0599	Hu.CD158e1	R2	5PNNNNNNNNNN(BC)	GGACGCTTTCCTTGA
ADT_C0083	Hu.CD16	R2	5PNNNNNNNNNN(BC)	AAGTTCACTCTTTGC
ADT_C0149	Hu.CD161	R2	5PNNNNNNNNNN(BC)	GTACGCAGTCCTTCT
ADT_C0358	Hu.CD163	R2	5PNNNNNNNNNN(BC)	GCTTCTCCTTCCTTA
ADT_C0206	Hu.CD169	R2	5PNNNNNNNNNN(BC)	TACTCAGCGTGTTTG
ADT_C0385	Hu.CD18	R2	5PNNNNNNNNNN(BC)	TATTGGGACACTTCT
ADT_C0140	Hu.CD183	R2	5PNNNNNNNNNN(BC)	GCGATGGTAGATTAT
ADT_C0144	Hu.CD185	R2	5PNNNNNNNNNN(BC)	AATTCAACCGTCGCC
ADT_C0050	Hu.CD19	R2	5PNNNNNNNNNN(BC)	CTGGGCAATTACTCG
ADT_C0071	Hu.CD194	R2	5PNNNNNNNNNN(BC)	AGCTTACCTGCACGA
ADT_C0141	Hu.CD195	R2	5PNNNNNNNNNN(BC)	CCAAAGTAAGAGCCA
ADT_C0143	Hu.CD196	R2	5PNNNNNNNNNN(BC)	GATCCCTTTGTCACT

ADT_C0160	Hu.CD1c	R2	5PNNNNNNNNNN(BC)	GAGCTACTTCACTCG
ADT_C0164	Hu.CD1d	R2	5PNNNNNNNNNN(BC)	TCGAGTCGCTTATCA
ADT_C0367	Hu.CD2	R2	5PNNNNNNNNNN(BC)	TACGATTTGTCAGGG
ADT_C0100	Hu.CD20_2H7	R2	5PNNNNNNNNNN(BC)	TTCTGGGTCCCTAGA
ADT_C0181	Hu.CD21	R2	5PNNNNNNNNNN(BC)	AACCTAGTAGTTCGG
ADT_C0393	Hu.CD22	R2	5PNNNNNNNNNN(BC)	GGGTTGTTGTCTTTG
ADT_C0152	Hu.CD223	R2	5PNNNNNNNNNN(BC)	CATTTGTCTGCCGGT
ADT_C1052	Hu.CD224	R2	5PNNNNNNNNNN(BC)	CTGATGAGATGTCAG
ADT_C0368	Hu.CD226_11A8	R2	5PNNNNNNNNNN(BC)	TCTCAGTGTTTGTGG
ADT_C0897	Hu.CD23	R2	5PNNNNNNNNNN(BC)	TCTGTATAACCGTCT
ADT_C0180	Hu.CD24	R2	5PNNNNNNNNNN(BC)	AGATTCCTTCGTGTT
ADT_C0189	Hu.CD244	R2	5PNNNNNNNNNN(BC)	TCGCTTGGATGGTAG
ADT_C0085	Hu.CD25	R2	5PNNNNNNNNNN(BC)	TTTGTCCTGTACGCC
ADT_C0396	Hu.CD26	R2	5PNNNNNNNNNN(BC)	GGTGGCTAGATAATG
ADT_C0247	Hu.CD267	R2	5PNNNNNNNNNN(BC)	AGTGATGGAGCGAAC
ADT_C0215	Hu.CD268	R2	5PNNNNNNNNNN(BC)	CGAAGTCGATCCGTA
ADT_C0154	Hu.CD27	R2	5PNNNNNNNNNN(BC)	GCACTCCTGCATGTA
ADT_C0020	Hu.CD270	R2	5PNNNNNNNNNN(BC)	TGATAGAAACAGACC
ADT_C0170	Hu.CD272	R2	5PNNNNNNNNNN(BC)	GTTATTGGACTAAGG
ADT_C0007	Hu.CD274	R2	5PNNNNNNNNNN(BC)	GTTGTCCGACAATAC
ADT_C0088	Hu.CD279	R2	5PNNNNNNNNNN(BC)	ACAGCGCCGTATTTA
ADT_C0386	Hu.CD28	R2	5PNNNNNNNNNN(BC)	TGAGAACGACCCTAA
ADT_C0369	Hu.CD29	R2	5PNNNNNNNNNN(BC)	GTATTCCCTCAGTCA
ADT_C0370	Hu.CD303	R2	5PNNNNNNNNNN(BC)	GAGATGTCCGAATTT
ADT_C0124	Hu.CD31	R2	5PNNNNNNNNNN(BC)	ACCTTTATGCCACGG
ADT_C0165	Hu.CD314	R2	5PNNNNNNNNNN(BC)	CGTGTTTGTTCCTCA
ADT_C0830	Hu.CD319	R2	5PNNNNNNNNNN(BC)	AGTATGCCATGTCTT
ADT_C0142	Hu.CD32	R2	5PNNNNNNNNNN(BC)	GCTTCCGAATTACCG
ADT_C0902	Hu.CD328	R2	5PNNNNNNNNNN(BC)	CTTAGCATTTCACTG
ADT_C0052	Hu.CD33	R2	5PNNNNNNNNNN(BC)	TAACTCAGGGCCTAT
ADT_C0101	Hu.CD335	R2	5PNNNNNNNNNN(BC)	ACAATTTGAACAGCG
ADT_C0167	Hu.CD35	R2	5PNNNNNNNNNN(BC)	ACTTCCGTCGATCTT
ADT_C0864	Hu.CD352	R2	5PNNNNNNNNNN(BC)	AGTTTCCACTCAGGC
ADT_C0407	Hu.CD36	R2	5PNNNNNNNNNN(BC)	TTCTTTGCCTTGCCA
ADT_C0389	Hu.CD38_HIT2	R2	5PNNNNNNNNNN(BC)	TGTACCCGCTTGTGA
ADT_C0176	Hu.CD39	R2	5PNNNNNNNNNN(BC)	TTACCTGGTATCCGT
ADT_C0034	Hu.CD3_UCHT1	R2	5PNNNNNNNNNN(BC)	CTCATTGTAACTCCT
ADT_C0031	Hu.CD40	R2	5PNNNNNNNNNN(BC)	CTCAGATGGAGTATG
ADT_C0353	Hu.CD41	R2	5PNNNNNNNNNN(BC)	ACGTTGTGGCCTTGT
ADT_C0216	Hu.CD42b	R2	5PNNNNNNNNNN(BC)	TCCTAGTACCGAAGT

ADT_C0063	Hu.CD45RA	R2	5PNNNNNNNNNN(BC)	TCAATCCTTCCGCTT
ADT_C0087	Hu.CD45RO	R2	5PNNNNNNNNNN(BC)	CTCCGAATCATGTTG
ADT_C0391	Hu.CD45_HI30	R2	5PNNNNNNNNNN(BC)	TGCAATTACCCGGAT
ADT_C0026	Hu.CD47	R2	5PNNNNNNNNNN(BC)	GCATTCTGTCACCTA
ADT_C0029	Hu.CD48	R2	5PNNNNNNNNNN(BC)	CTACGACGTAGAAG A
ADT_C0575	Hu.CD49a	R2	5PNNNNNNNNNN(BC)	ACTGATGGACTCAGA
ADT_C0371	Hu.CD49b	R2	5PNNNNNNNNNN(BC)	GCTTTCTTCAGTATG
ADT_C0576	Hu.CD49d	R2	5PNNNNNNNNNN(BC)	CCATTCAACTTCCGG
ADT_C0072	Hu.CD4_RPA.T4	R2	5PNNNNNNNNNN(BC)	TGTTCCCGCTCAACT
ADT_C0138	Hu.CD5	R2	5PNNNNNNNNNN(BC)	CATTAACGGGATGCC
ADT_C0033	Hu.CD52	R2	5PNNNNNNNNNN(BC)	CTTTGTACGAGCAAA
ADT_C0217	Hu.CD54	R2	5PNNNNNNNNNN(BC)	CTGATAGACTTGAGT
ADT_C0047	Hu.CD56	R2	5PNNNNNNNNNN(BC)	TCCTTTCCTGATAGG
ADT_C0168	Hu.CD57	R2	5PNNNNNNNNNN(BC)	AACTCCCTATGGAGG
ADT_C0174	Hu.CD58	R2	5PNNNNNNNNNN(BC)	GTTCCTATGGACGAC
ADT_C0147	Hu.CD62L	R2	5PNNNNNNNNNN(BC)	GTCCCTGCAACTTGA
ADT_C0218	Hu.CD62P	R2	5PNNNNNNNNNN(BC)	CCTTCCGTATCCCTT
ADT_C0162	Hu.CD64	R2	5PNNNNNNNNNN(BC)	AAGTATGCCCTACGA
ADT_C0146	Hu.CD69	R2	5PNNNNNNNNNN(BC)	GTCTCTTGGCTTAAA
ADT_C0066	Hu.CD7	R2	5PNNNNNNNNNN(BC)	TGGATTCCCGGACTT
ADT_C0394	Hu.CD71	R2	5PNNNNNNNNNN(BC)	CCGTGTTCCTCATTA
ADT_C0577	Hu.CD73	R2	5PNNNNNNNNNN(BC)	CAGTTCCTCAGTTCG
ADT_C0187	Hu.CD79b	R2	5PNNNNNNNNNN(BC)	ATTCTTCAACCGAAG
ADT_C0046	Hu.CD8	R2	5PNNNNNNNNNN(BC)	GCGCAACTTGATGAT
ADT_C0373	Hu.CD81	R2	5PNNNNNNNNNN(BC)	GTATCCTTCCTTGGC
ADT_C0920	Hu.CD82	R2	5PNNNNNNNNNN(BC)	TCCCACTTCCGCTTT
ADT_C0359	Hu.CD83	R2	5PNNNNNNNNNN(BC)	CCACTCATTTCCGGT
ADT_C0896	Hu.CD85j	R2	5PNNNNNNNNNN(BC)	CCTTGTGAGGCTATG
ADT_C0006	Hu.CD86	R2	5PNNNNNNNNNN(BC)	GTCTTTGTCAGTGCA
ADT_C1046	Hu.CD88	R2	5PNNNNNNNNNN(BC)	GCCGCATGAGAAAC A
ADT_C0867	Hu.CD94	R2	5PNNNNNNNNNN(BC)	CTTTCCGGTCCTACA
ADT_C0156	Hu.CD95	R2	5PNNNNNNNNNN(BC)	CCAGCTCATTAGAGC
ADT_C0845	Hu.CD99	R2	5PNNNNNNNNNN(BC)	ACCCGTCCCTAAGAA
ADT_C0853	Hu.CLEC12A	R2	5PNNNNNNNNNN(BC)	CATTAGAGTCTGCCA
ADT_C0179	Hu.CX3CR1	R2	5PNNNNNNNNNN(BC)	AGTATCGTCTCTGGG
ADT_C0352	Hu.FceRIa	R2	5PNNNNNNNNNN(BC)	CTCGTTTCCGTATCG
ADT_C0912	Hu.GPR56	R2	5PNNNNNNNNNN(BC)	GCCTAGTTTCCGTTT
ADT_C0058	Hu.HLA.ABC	R2	5PNNNNNNNNNN(BC)	TATGCGAGGCTTATC
ADT_C0159	Hu.HLA.DR	R2	5PNNNNNNNNNN(BC)	AATAGCGAGCAAGT A

ADT_C0918	Hu.HLA.E	R2	5PNNNNNNNNNN(BC)	GAGTCGAGAAATCAT
ADT_C0894	Hu.Ig.LightChain.k	R2	5PNNNNNNNNNN(BC)	AGCTCAGCCAGTATG
ADT_C0898	Hu.Ig.LightChain.l	R2	5PNNNNNNNNNN(BC)	CAGCCAGTAAGTCAC
ADT_C0384	Hu.IgD	R2	5PNNNNNNNNNN(BC)	CAGTCTCCGTAGAGT
ADT_C0136	Hu.IgM	R2	5PNNNNNNNNNN(BC)	TAGCGAGCCCGTATA
ADT_C0153	Hu.KLRG1	R2	5PNNNNNNNNNN(BC)	CTTATTTCCTGCCCT
ADT_C0591	Hu.LOX.1	R2	5PNNNNNNNNNN(BC)	ACCCTTTACCGAATA
ADT_C0224	Hu.TCR.AB	R2	5PNNNNNNNNNN(BC)	CGTAACGTAGAGCG A
ADT_C0581	Hu.TCR.Va7.2	R2	5PNNNNNNNNNN(BC)	TACGAGCAGTATTCA
ADT_C0582	Hu.TCR.Vd2	R2	5PNNNNNNNNNN(BC)	TCAGTCAGATGGTAT
ADT_C0089	Hu.TIGIT	R2	5PNNNNNNNNNN(BC)	TTGCTTACCGCCAGA
ADT_C0073	HuMs.CD44	R2	5PNNNNNNNNNN(BC)	TGGCTTCAGGTCCTA
ADT_C0070	HuMs.CD49f	R2	5PNNNNNNNNNN(BC)	TTCCGAGGATGATCT
ADT_C0214	HuMs.integrin.b7	R2	5PNNNNNNNNNN(BC)	TCCTTGGATGTACCG
ADT_C0171	HuMsRt.CD278	R2	5PNNNNNNNNNN(BC)	CGCGCACCCATTAAA
ADT_C0241	Isotype_HTK888	R2	5PNNNNNNNNNN(BC)	CCTGTCATTAAGACT
ADT_C0091	Isotype_MOPC.17 3	R2	5PNNNNNNNNNN(BC)	CTCCTACCTAAACTG
ADT_C0090	Isotype_MOPC.21	R2	5PNNNNNNNNNN(BC)	GCCGGACGACATTAA
ADT_C0092	Isotype_MPC.11	R2	5PNNNNNNNNNN(BC)	ATATGTATCACGCGA
ADT_C0236	Isotype_RTK2071	R2	5PNNNNNNNNNN(BC)	ATCAGATGCCCTCAT
ADT_C0238	Isotype_RTK2758	R2	5PNNNNNNNNNN(BC)	AAGTCAGGTTCGTTT
ADT_C0095	Isotype_RTK4530	R2	5PNNNNNNNNNN(BC)	GATTCTTGACGACCT

Table C.4 Resolutions and source clusters for defined cell populations
This table summarizes how each cell population was derived during the clustering process combining multiple resolution. The “source resolution” and “source cluster” columns indicate the Leiden clustering resolution and corresponding cluster from which each population originated. If the “Parent cluster” column is empty, the population was taken directly from the full region. If a parent cluster is listed, the source cluster represents a subdivision of that parent cluster from the base resolution. The “region” column denotes the UMAP-defined subregion in which Leiden clustering was applied independently. The regions and their corresponding base resolutions are as follows: Region A (0) naïve CD8 region; Region B (0.5) CD4 region; Region C (0.8) other CD8 region; Region D (0.6) NK region; Region E (1.6) B cell region; Region F (0.7) myeloid region; and Region G (0.5) other remaining cells. Each row represents a distinct cell population that subsequently underwent separate annotation and filtering.

Region	Cell lineage	Source resolution	Source cluster	Parent cluster
A	T	0	0	
B	T	0.5	0	
B	T	0.5	1	
B	T	1.6	5	1
B	T	0.5	2	
B	T	1.3	10	2
B	T	0.5	3	
B	T	0.5	4	
B	T	1.1	10	4
B	T	0.5	5	
B	T	1.8	19	5
B	T	1.8	14	5
B	T	0.5	6	
B	T	1.8	21	6
B	T	0.5	7	
B	T	0.5	8	
C	T	0.8	0	
C	T	0.8	1	
C	T	0.8	2	
C	T	2	20	2
C	T	1.2	14	2
C	T	0.8	3	
C	T	1.1	11	3
C	T	0.8	4	
C	T	1.5	11	4
C	T	1.7	16	4
C	T	0.8	5	
C	T	1.4	19	5
C	T	0.8	6	

C	T	0.8	7	
C	T	0.8	8	
C	NK	2.5	35	8
C	T	2.5	36	8
C	T	0.8	9	
C	T	2.8	24	9
C	T	2.8	32	9
C	T	0.8	10	
C	T	0.8	11	
C	T	0.8	12	
C	T	0.8	13	
C	T	0.8	14	
D	NK	0.6	0	
D	NK	0.6	1	
D	NK	0.6	2	
D	NK	0.6	3	
D	NK	1.2	9	3
D	NK	0.6	4	
D	NK	0.7	4	4
D	NK	0.6	5	
D	NK	0.6	6	
D	NK	0.6	7	
E	B	1.6	0	
E	B	1.6	1	
E	B	1.6	2,3,4,11,15,23	
E	B	1.6	5	
E	B	1.6	6	
E	B	1.6	7,16	
E	PC	1.6	8	
E	PC	2.5	30	8
E	B	1.6	9	
E	B	1.6	10	
E	B	1.6	12	
E	B	1.6	13	
E	B	1.6	14	
E	B	2.3	24	14
E	B	1.6	17	
E	B	1.6	18	
E	PC	1.6	19	
E	B	1.6	20	
E	B	1.6	21	
E	B	1.6	22	

F	Myeloid	0.7	0	
F	Myeloid	0.7	1	
F	Myeloid	1.4	15	1
F	Myeloid	1.4	17	1
F	Myeloid	0.7	2	
F	Myeloid	1.4	26	2
F	Myeloid	0.7	3	
F	Myeloid	0.7	4	
F	Myeloid	0.7	5	
F	Myeloid	0.7	6	
F	Myeloid	0.7	7	
F	Myeloid	2	20	7
F	Myeloid	0.7	8	
F	Myeloid	0.7	9	
F	Myeloid	3.6	53	9
F	Myeloid	0.7	10	
F	Myeloid	0.7	11	
F	Myeloid	0.7	12	
F	Myeloid	0.7	13	
F	Myeloid	0.7	14	
F	Myeloid	1.4	11	14
F	Myeloid	0.7	15	
G	Myeloid	0.5	0,20	
G	Myeloid	0.5	1	
G	Myeloid	0.5	2	
G	Myeloid	0.5	3	
G	Myeloid	0.5	4	
G	T	0.5	5	
G	Myeloid	0.5	6	
G	Myeloid	1.6	12	6
G	Fibroblast	0.5	7	
G	Fibroblast	1.6	19	7
G	Myeloid	0.5	8	
G	Myeloid	0.5	9	
G	Myeloid	0.5	10	
G	Myeloid	0.5	11	
G	Myeloid	0.5	12	
G	Myeloid	0.5	13	
G	Myeloid	0.5	14	
G	Fibroblast	0.5	15	
G	Myeloid	0.5	16	
G	Myeloid	0.5	17	

G	Myeloid	0.5	18	
G	T	0.5	19	
G	B	0.5	21	

Appendix - Chapter 5

Table D.1 Sample allocation to analytical cohorts in compositional analysis
Overview of sample assignments to the analytical cohorts used in the compositional analysis. Columns indicate inclusion in the core and expanded cohorts for the AS vs HC and AS vs RA comparisons. UID refers to the unique sample identifier.

UID	Project name	Core cohort (AS vs HC)	Expanded cohort (AS vs HC)	Core cohort (AS vs RA)	Expanded cohort (AS vs RA)
As.Pb.Bt-Ox1-7A	P170676		Y		Y
As.Pb.Bn-Ox1-925A	P170676		Y		Y
As.Pb.Bt-Ox1-346A	P170676		Y		Y
As.Pb.Pb-Ox1-143A	P170676		Y		Y
As.Pb.Bt-Ox1-473A	P170676		Y		Y
As.Pb.Bt-Ox1-319A	P170676		Y		Y
As.Pb.Bn-Ox1-134A	P170676		Y		Y
As.Pb.Bn-Ox1-503A	P170676		Y		Y
As.Pb.Bn-Ox2-681A	P180407		Y		Y
As.Pb.Bt-Ox2-681B	P180407		Y		Y
As.Pb.Bn-Ox2-598A	P180407		Y		Y
As.Pb.Bt-Ox2-598B	P180407		Y		Y
As.Pb.Bt-Ox3-598C	P190230		Y		Y
As.Pb.Bt-Ox3-598D	P190230		Y		Y
As.Pb.Bn-Ox4-810A	P190726		Y		Y
As.Pb.Bn-Ox4-580A	P190726		Y		Y
As.Pb.Bn-Ox4-600A	P190726		Y		Y
Hc.Pb.Na-Ox4-36A	P190726		Y		
Hc.Pb.Na-Ox4-149A	P190726		Y		
Hc.Pb.Na-Ox4-456A	P190726		Y		
Hc.Pb.Na-Ox5-685A	ox_va_pb_sf	Y	Y		
Hc.Pb.Na-Ox5-396A	ox_va_pb_sf	Y	Y		
Ra.Pb.Bt-Ox5-742A	ox_va_pb_sf			Y	Y
Ra.Pb.Bn-Ox5-951A	ox_va_pb_sf			Y	Y
As.Pb.Bn-Ox5-800A	ox_va_pb_sf	Y	Y	Y	Y
As.Pb.Bt-Ox5-50A	ox_va_pb_sf	Y	Y	Y	Y
As.Pb.Bt-Ox5-109A	ox_va_pb_sf	Y	Y	Y	Y
As.Pb.Bn-Ox5-585A	ox_va_pb_sf	Y	Y	Y	Y
Hc.Pb.Na-Ox5-677A	ox_va_pb_sf	Y	Y		
Hc.Pb.Na-Ox5-487A	ox_va_pb_sf	Y	Y		
Ra.Pb.Bn-Ox5-756A	ox_va_pb_sf			Y	Y

Ra.Pb.Na-Ox5-601A	ox_va_pb_sf			Y	Y
As.Pb.Bt-Ox5-744A	ox_va_pb_sf	Y	Y	Y	Y
As.Pb.Bn-Ox5-874A	ox_va_pb_sf	Y	Y	Y	Y
As.Pb.Bt-Ox5-497A	ox_va_pb_sf	Y	Y	Y	Y
Hc.Pb.Na-Ox5-239A	ox_va_pb_sf	Y	Y		
Hc.Pb.Na-Ox5-308A	ox_va_pb_sf	Y	Y		
Ra.Pb.Bn-Ox5-572A	ox_va_pb_sf			Y	Y
Ra.Pb.Bn-Ox5-951B	ox_va_pb_sf			Y	Y
As.Pb.Bt-Ox5-447A	ox_va_pb_sf	Y	Y	Y	Y
As.Pb.Bn-Ox5-105A	ox_va_pb_sf	Y	Y	Y	Y
As.Pb.Bt-Ox5-120A	ox_va_pb_sf	Y	Y	Y	Y
As.Pb.Bn-Ox5-434A	ox_va_pb_sf	Y	Y	Y	Y
As.Sf.Bn-Ox5-800B	ox_va_pb_sf	Y	Y	Y	Y
As.Sf.Bt-Ox5-744B	ox_va_pb_sf	Y	Y	Y	Y
As.Sf.Bt-Ox5-447B	ox_va_pb_sf	Y	Y	Y	Y
Ra.Sf.Bn-Ox5-756B	ox_va_pb_sf			Y	Y
Ra.Sf.Bt-Ox5-742B	ox_va_pb_sf			Y	Y
Ra.Sf.Bn-Ox5-464A	ox_va_pb_sf			Y	Y
As.Sf.Bn-Be5-102A	ox_va_pb_sf			Y	Y
Ra.Sf.Bn-Ox5-572B	ox_va_pb_sf			Y	Y
Ra.Sf.Bn-Ox5-757A	ox_va_pb_sf			Y	Y
As.Pb.Bn-Be6-508A	berlin_pb_sf		Y		Y
As.Pb.Bt-Be6-609A	berlin_pb_sf		Y		Y
As.Pb.Bn-Be6-453A	berlin_pb_sf		Y		Y
As.Pb.Bn-Be6-369A	berlin_pb_sf		Y		Y
As.Pb.Pb-Be6-243A	berlin_pb_sf		Y		Y
As.Pb.Pb-Be6-929A	berlin_pb_sf		Y		Y
As.Sf.Bn-Be6-369B	berlin_pb_sf				Y
As.Sf.Pb-Be6-243B	berlin_pb_sf				Y
As.Sf.Pb-Be6-929B	berlin_pb_sf				Y
As.Sf.Bn-Be6-508B	berlin_pb_sf				Y
As.Sf.Bt-Be6-609B	berlin_pb_sf				Y
As.Sf.Bn-Be6-453B	berlin_pb_sf				Y
As.Sf.Pb-Be6-243C	berlin_pb_sf				Y
Hc.Im.Na-Na7-568A	gut_naples	Y	Y		
Hc.Im.Na-Na7-630A	gut_naples	Y	Y		
Hc.Pb.Na-Na7-568B	gut_naples	Y	Y		
Hc.Pb.Na-Na7-630B	gut_naples	Y	Y		
As.Im.Bn-Na7-263A	gut_naples	Y	Y		
Hc.Im.Na-Na7-885A	gut_naples	Y	Y		
As.Im.Bn-Na7-614A	gut_naples	Y	Y		
Hc.Im.Na-Na7-606A	gut_naples	Y	Y		

As.Im.Bn-Na7-910A	gut_naples	Y	Y		
Hc.Im.Na-Na7-734A	gut_naples	Y	Y		
As.Pb.Bn-Na7-263B	gut_naples	Y	Y		
Hc.Pb.Na-Na7-885B	gut_naples	Y	Y		
As.Pb.Bn-Na7-614B	gut_naples	Y	Y		
Hc.Pb.Na-Na7-606B	gut_naples	Y	Y		
As.Pb.Bn-Na7-910B	gut_naples	Y	Y		
Hc.Pb.Na-Na7-734B	gut_naples	Y	Y		
As.Im.Bn-Ox8-275A	gut_tgu		Y		
As.Im.Bn-Ox8-275B	gut_tgu		Y		
Hc.Pe.Na-Le10-458A	spine_enthesis		Y		
Hc.Et.Na-Le10-458B	spine_enthesis		Y		
Hc.Pe.Na-Le10-66A	spine_enthesis		Y		
Hc.Et.Na-Le10-66B	spine_enthesis		Y		
Hc.Pe.Na-Le10-192A	spine_enthesis		Y		
Hc.Et.Na-Le10-192B	spine_enthesis		Y		
Hc.Pe.Na-Le10-838A	spine_enthesis		Y		
Hc.Et.Na-Le10-838B	spine_enthesis		Y		
As.Pe.Na-Le10-843A	spine_enthesis		Y		
As.Et.Na-Le10-843B	spine_enthesis		Y		
Ra.Sf.Ni-Be12-332A	cd8_sfmc_berlin				Y
Ra.Sf.Ni-Be12-953A	cd8_sfmc_berlin				Y
Ra.Sf.Ni-Be12-256A	cd8_sfmc_berlin				Y
As.Sf.Ni-Be12-528A	cd8_sfmc_berlin				Y
As.Sf.Ni-Be12-948A	cd8_sfmc_berlin				Y
As.Sf.Ni-Be12-190A	cd8_sfmc_berlin				Y
As.Sf.Ni-Be12-518A	cd8_sfmc_berlin				Y
As.Sf.Ni-Be12-956A	cd8_sfmc_berlin				Y
As.Sf.Ni-Be12-415A	cd8_sfmc_berlin				Y
As.Sf.Ni-Be12-714A	cd8_sfmc_berlin				Y
As.Sf.Ni-Be12-560A	cd8_sfmc_berlin				Y
As.Sf.Ni-Be12-593A	cd8_sfmc_berlin				Y
As.Sf.Ni-Be12-155A	cd8_sfmc_berlin				Y
As.Pe.Ni-Le10-834A	spine_enthesis		Y		
As.Pe.Ni-Le10-91A	spine_enthesis		Y		
As.Et.Ni-Le10-91B	spine_enthesis		Y		
As.Pe.Ni-Le10-706A	spine_enthesis		Y		
As.Pe.Ni-Le10-706B	spine_enthesis		Y		
As.Pb.Ni-Ox8-35A	gut_tgu		Y		
As.Im.Ni-Ox8-35B	gut_tgu		Y		
As.Sf.Ni-Ox5-644A	ox_va_pb_sf				Y
As.Sf.Ni-Ox5-644B	ox_va_pb_sf				Y

As.Sf.Ni-Ox5-721A	ox_va_pb_sf				Y

Figure D.2 Relationship between age and naïve T cell proportion in blood
Scatter plot showing the correlation between donor age and the relative proportion of naïve cells within (A) CD4-positive T cell compartment and (B) CD8-positive t cell compartment from PBMC samples. Each point represents one individual sample, and the red line indicates the fitted linear regression. Pearson's correlation coefficient (r) and corresponding p-value are shown in the plot.

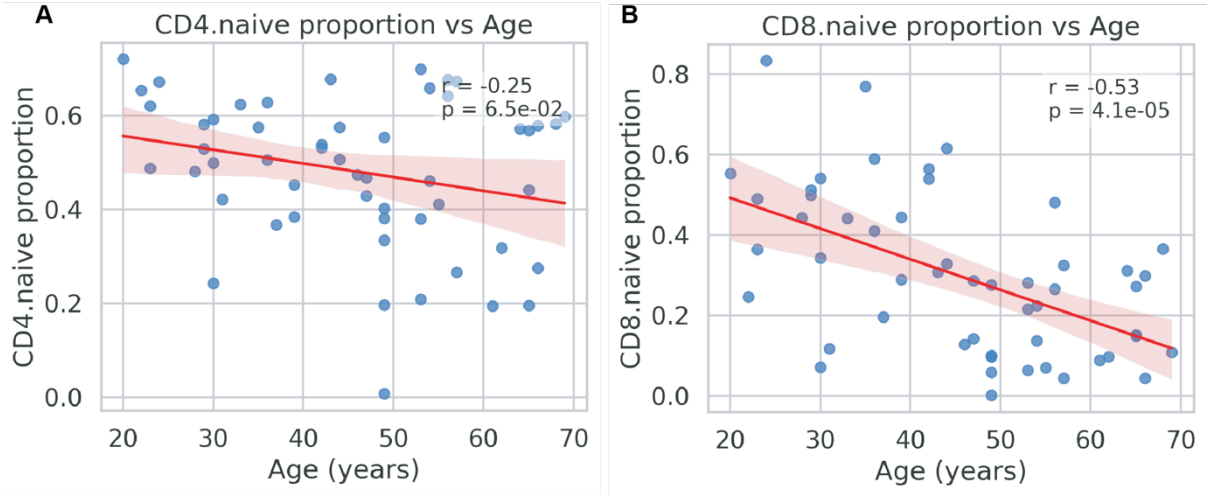


Figure D.3 Differential abundance of CD4-positive T-cell subsets across tissues and patient groups at cell type level in the core cohort
Heatmap showing differential abundance analysis of CD4-positive T cell subsets in the core cohort using edgeR with TMM-normalized cell type counts. Colour indicates logFC of each subset in AxSpA relative to the comparison group. Statistical significance was determined by edgeR with symbols indicating adjusted p-value thresholds: *** < 0.001, ** < 0.01, * < 0.05, + < 0.1, . < 0.2, and no label for non-significant results.

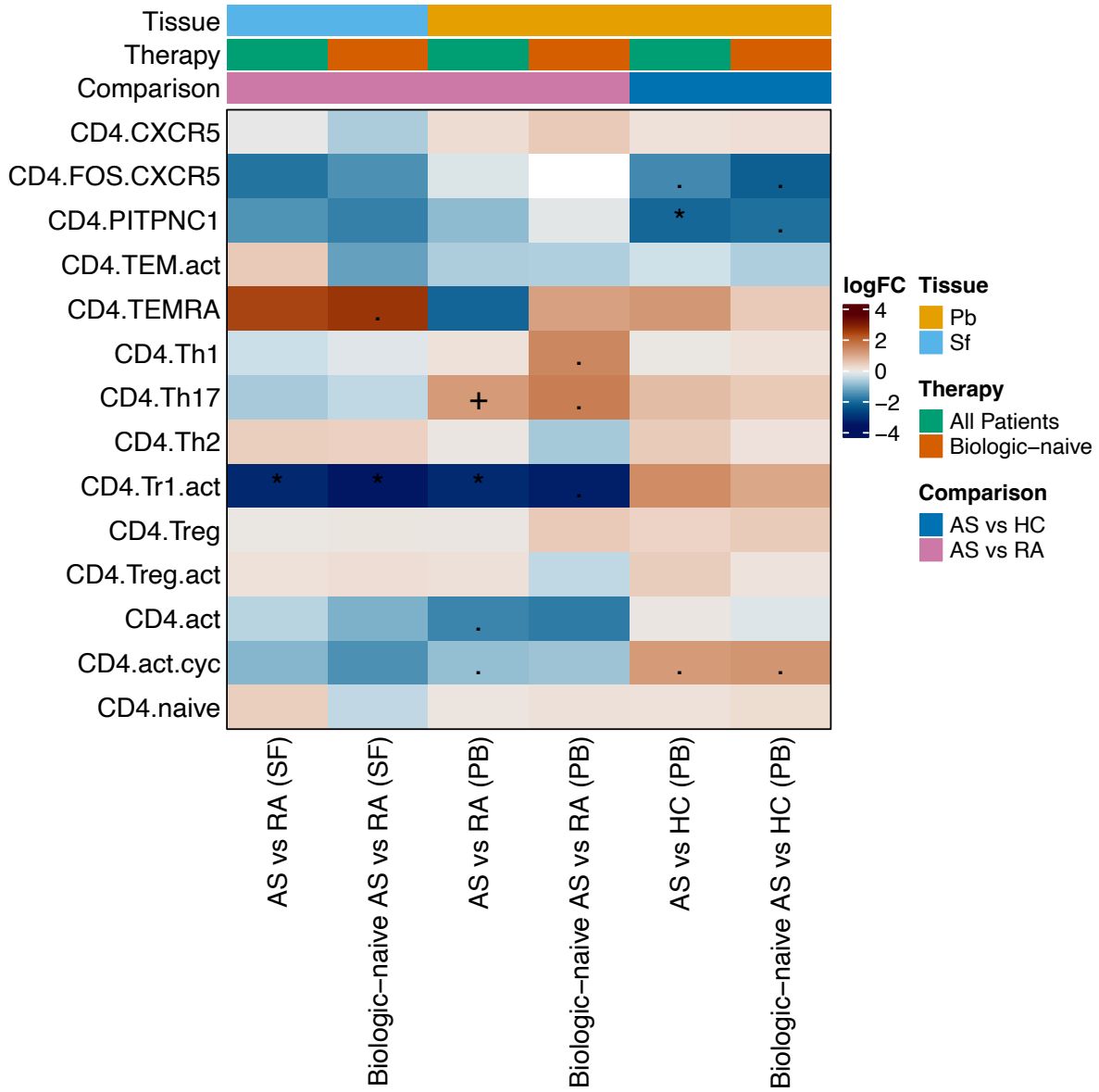


Figure D.4 Differential abundance of CD4-positive T-cell subsets across tissues and patient groups at cell type level in the expanded cohort.
Heatmap showing differential abundance analysis of CD4-positive T cell subsets in the expanded cohort using edgeR with TMM-normalized cell type counts. Colour indicates logFC of each subset in AxSpA relative to the comparison group. Statistical significance was determined by edgeR with symbols indicating adjusted p-value thresholds: *** < 0.001, ** < 0.01, * < 0.05, + < 0.1, . < 0.2, and no label for non-significant results.

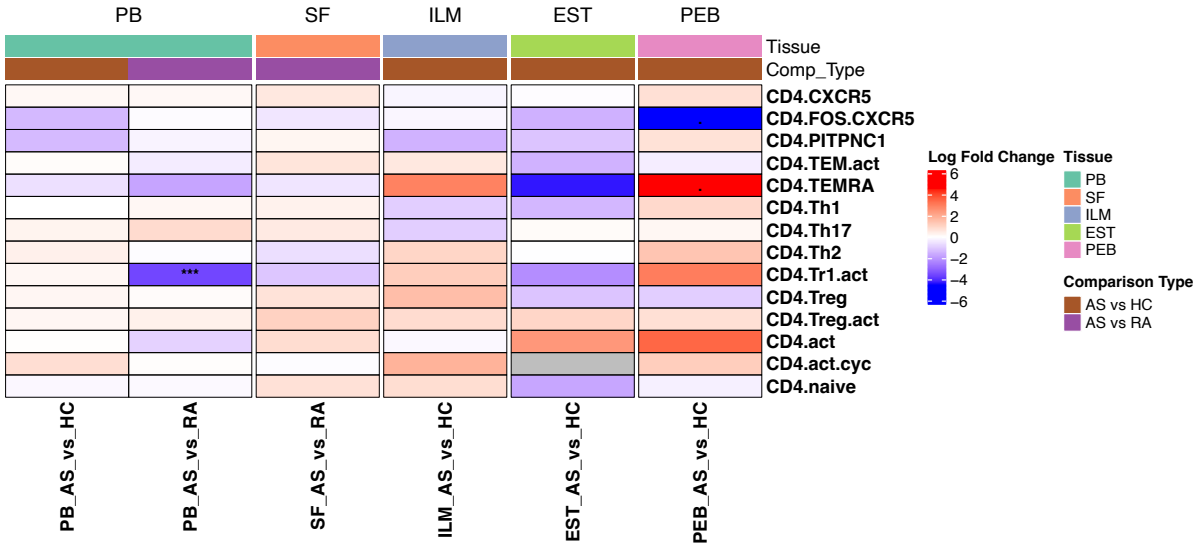


Figure D.5 Compositional differences of CD4⁺ T-cell subsets between AxSpA and RA in PBMC at the cell-type level

Boxplots illustrating differences in the relative abundance of CD4⁺ T-cell subsets between AxSpA and RA patient groups in PBMC. Each dot represents an individual sample from the expanded cohort; red dots indicate samples also included in the core cohort.

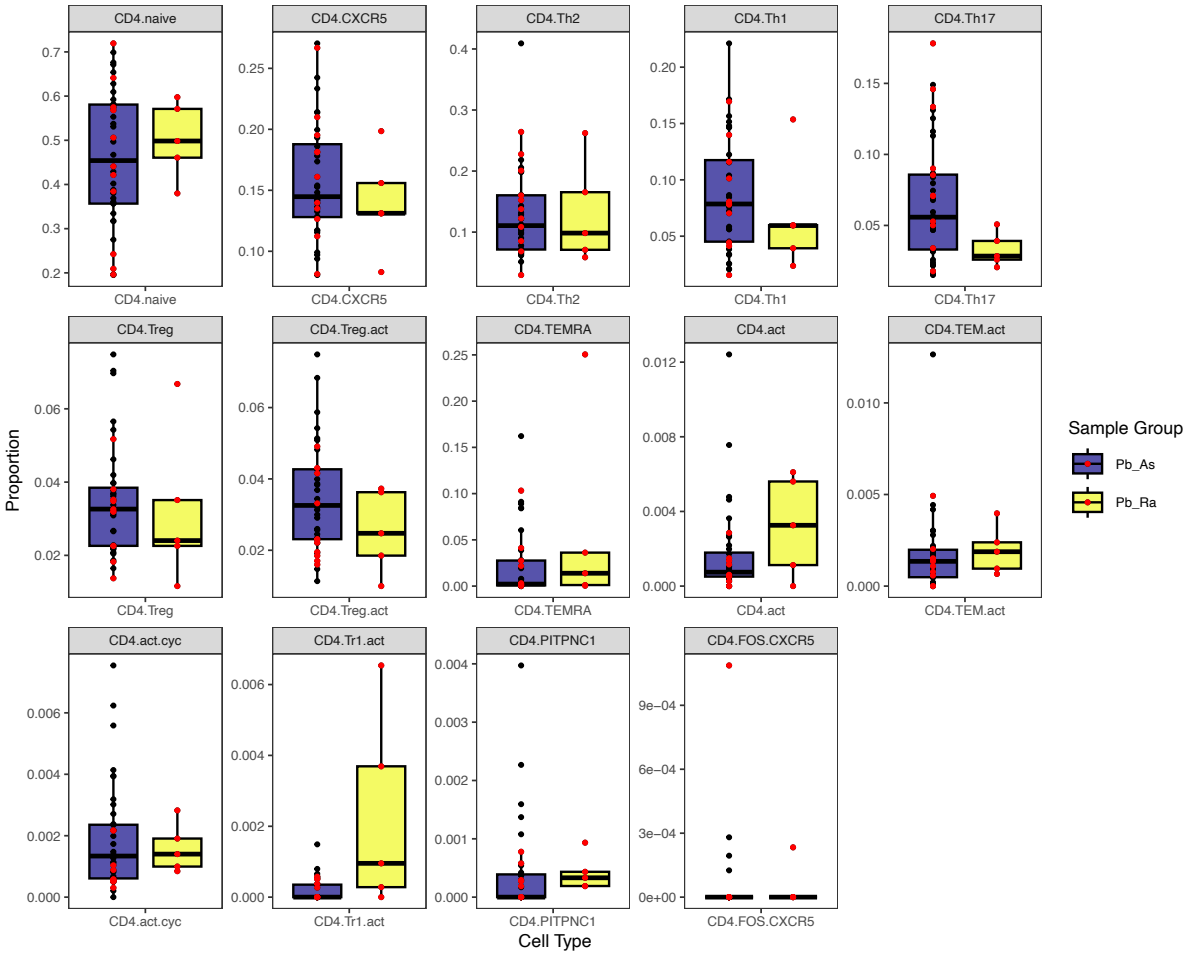


Figure D.6 Compositional differences of CD4⁺ T-cell subsets between AxSpA and HC in PBMC at the cell-type level

Boxplots illustrating differences in the relative abundance of CD4⁺ T-cell subsets between AxSpA and HC groups in PBMC. Each dot represents an individual sample from the expanded cohort; red dots indicate samples also included in the core cohort.

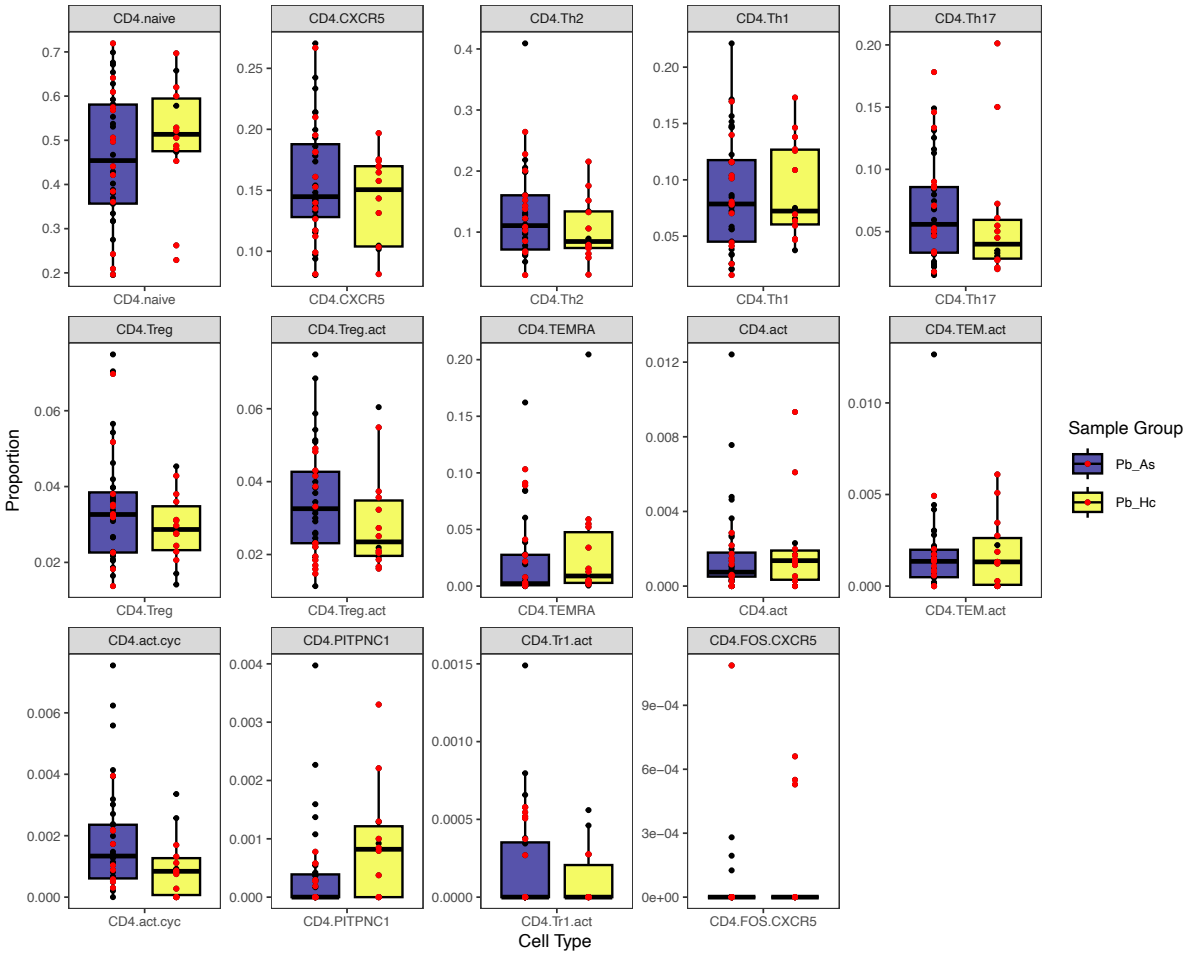


Figure D.7 Compositional differences of CD4⁺ T-cell subsets between AxSpA and RA in SFMC at the cell-type level

Boxplots illustrating differences in the relative abundance of CD4⁺ T-cell subsets between AxSpA and RA patient groups in SFMC. Each dot represents an individual sample from the expanded cohort; red dots indicate samples also included in the core cohort.

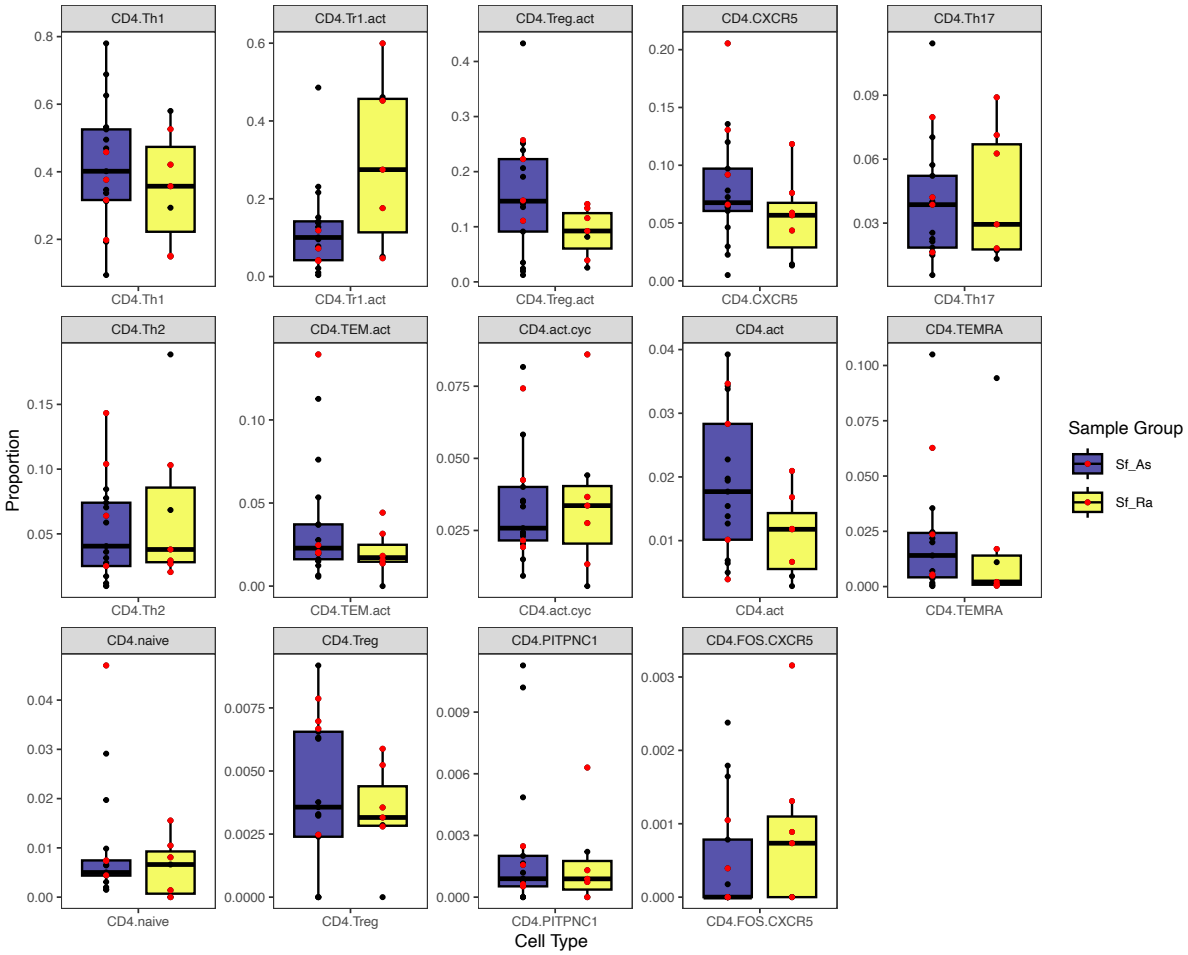


Figure D.8 Compositional differences of CD4⁺ T-cell subsets between AxSpA and HC in ILM at the cell-type level

Boxplots illustrating differences in the relative abundance of CD4⁺ T-cell subsets between AxSpA and HC groups in ILM. Each dot represents an individual sample from the expanded cohort; red dots indicate samples also included in the core cohort.

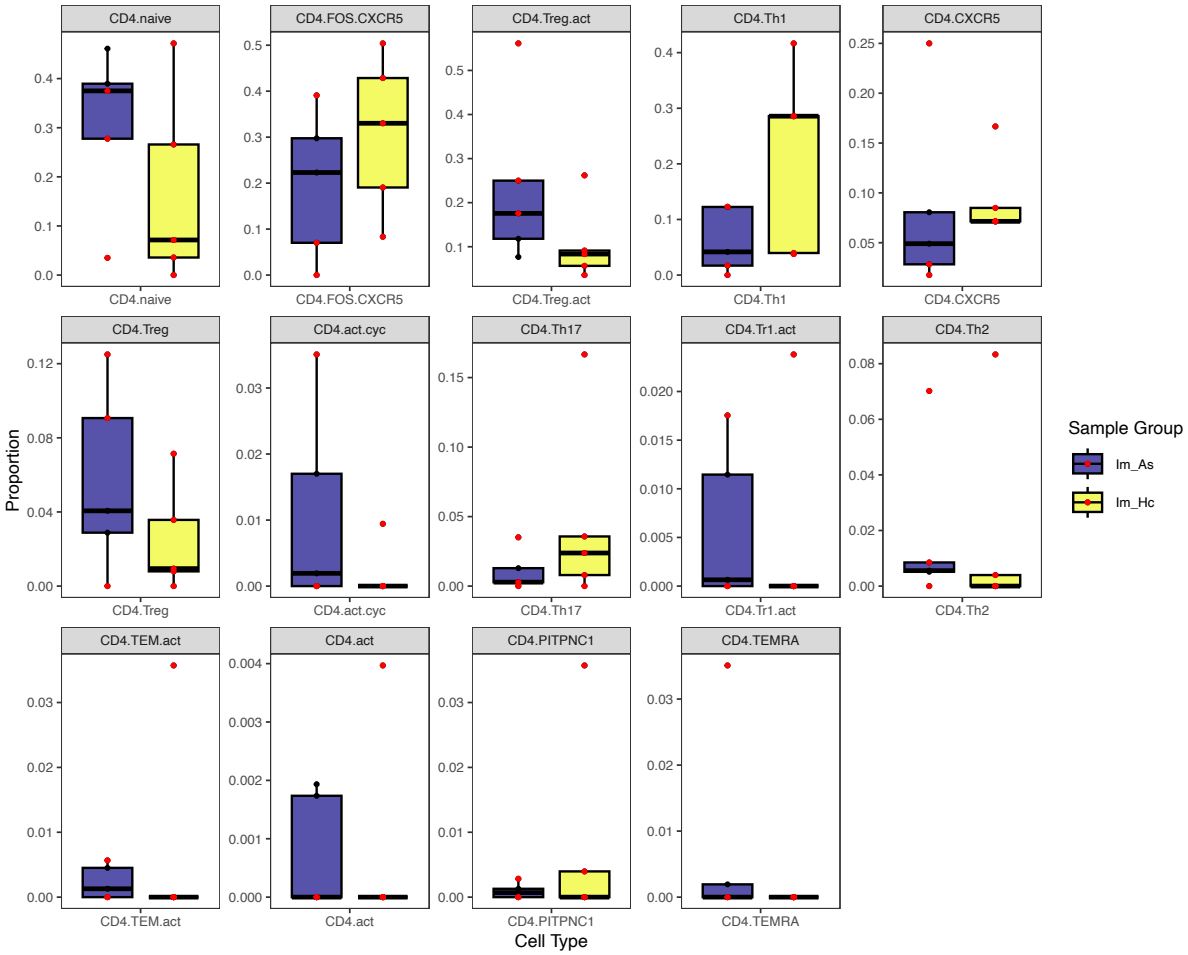


Figure D.9 Compositional differences of CD4⁺ T-cell subsets between AxSpA and HC in PEB at the cell-type level

Boxplots illustrating differences in the relative abundance of CD4⁺ T-cell subsets between AxSpA and HC groups in PEB. Each dot represents an individual sample from the expanded cohort; red dots indicate samples also included in the core cohort.

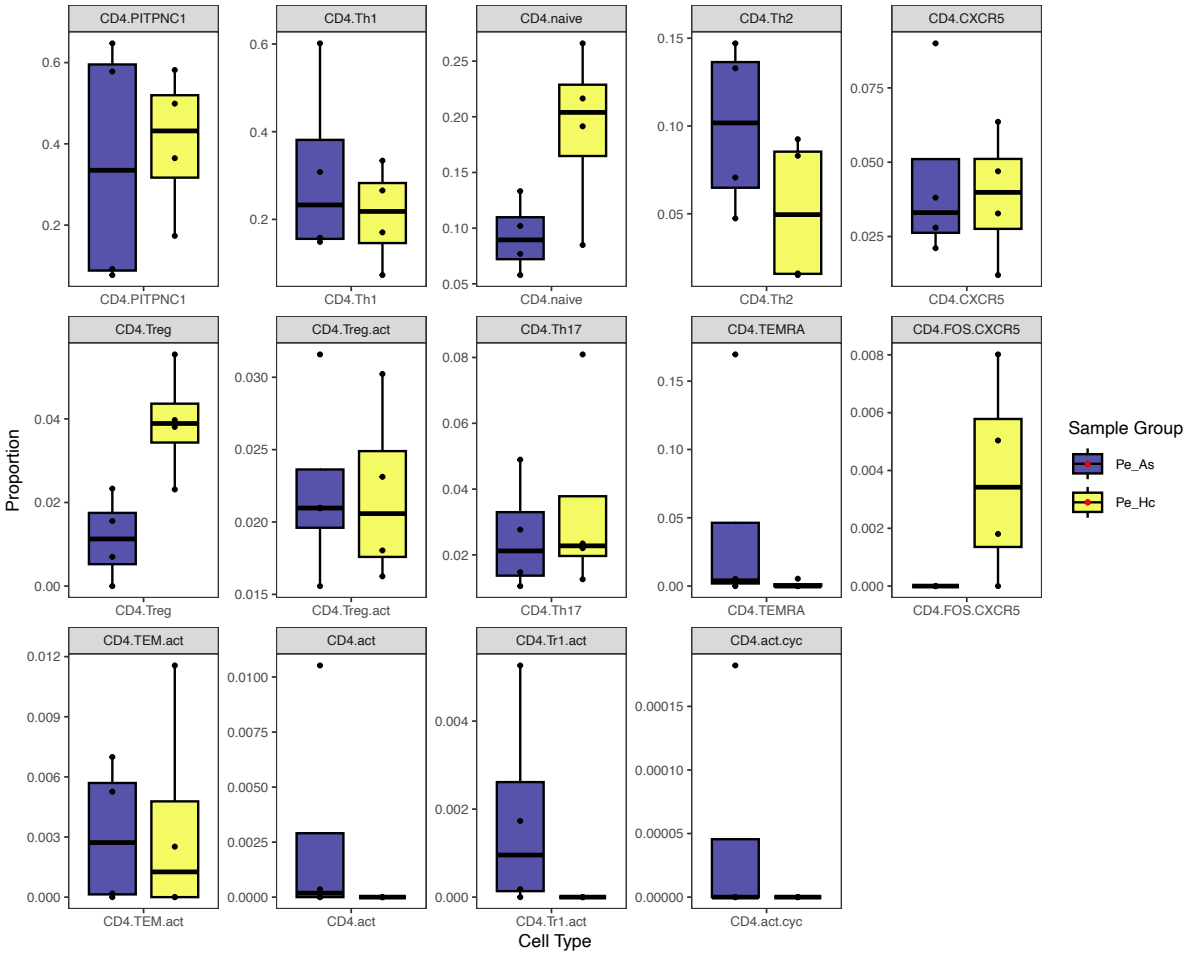


Figure D.10 Compositional differences of CD4⁺ T-cell subsets between AxSpA and HC in EST at the cell-type level

Boxplots illustrating differences in the relative abundance of CD4⁺ T-cell subsets between AxSpA and HC groups in PEB. Each dot represents an individual sample from the expanded cohort; red dots indicate samples also included in the core cohort.

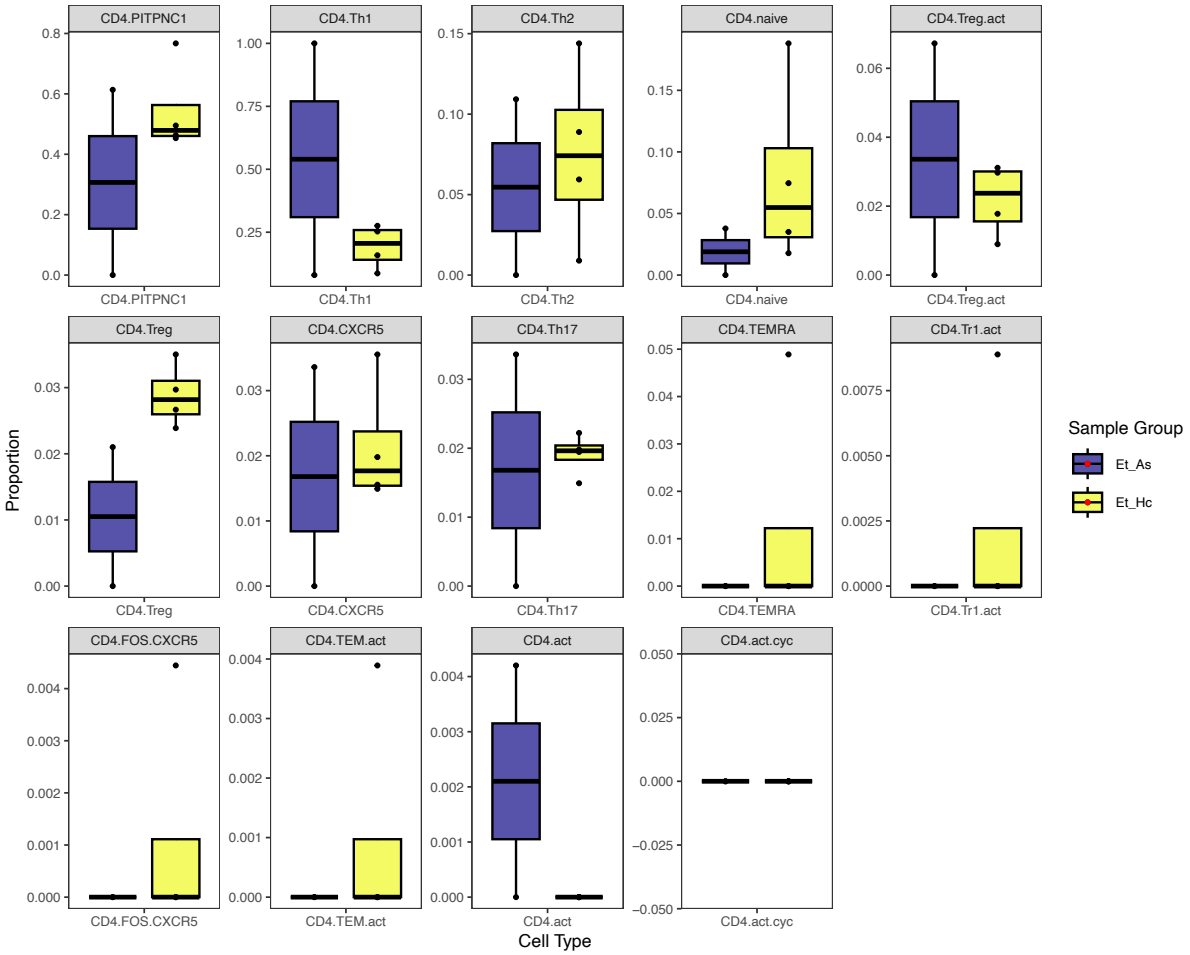


Figure D.11 Differential abundance of CD8-positive T-cell subsets across tissues and patient groups at cell type level in the core cohort.
Heatmap showing differential abundance analysis of CD8-positive T cell subsets in the core cohort using edgeR with TMM-normalized cell type counts. Colour indicates logFC of each subset in AxSpA relative to the comparison group. Statistical labels: *** < 0.001, ** < 0.01, * < 0.05, + < 0.1, . < 0.2, and no label for non-significant results.

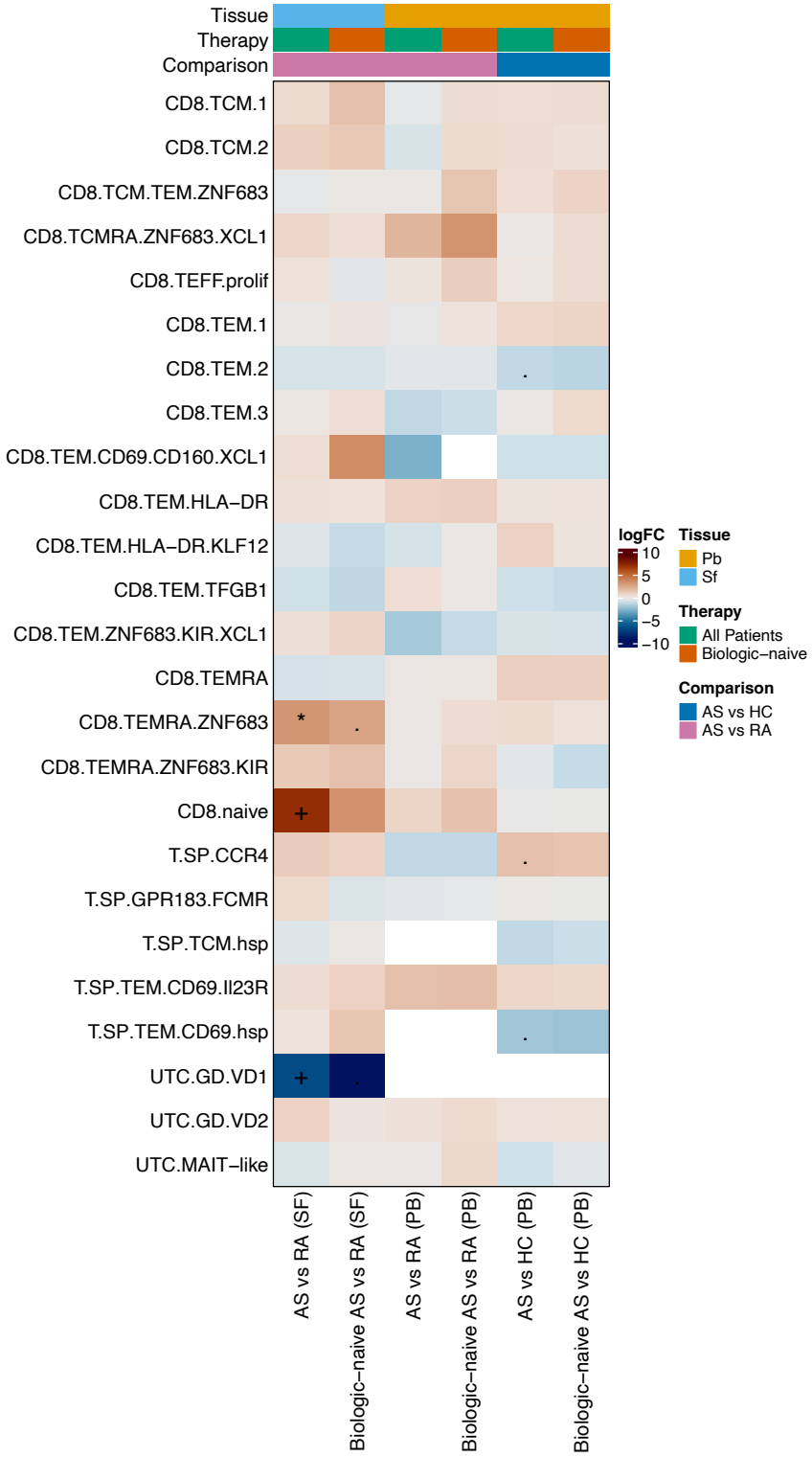


Figure D.12 Differential abundance of CD8-positive T-cell subsets across tissues and patient groups at cell type level in the expanded cohort

Heatmap showing differential abundance analysis of CD8-positive T cell subsets in the expanded cohort using edgeR with TMM-normalized cell type counts. Colour indicates logFC of each subset in AxSpA relative to the comparison group. Significance label: *** < 0.001, ** < 0.01, * < 0.05, + < 0.1, . < 0.2, and no label for non-significant results.

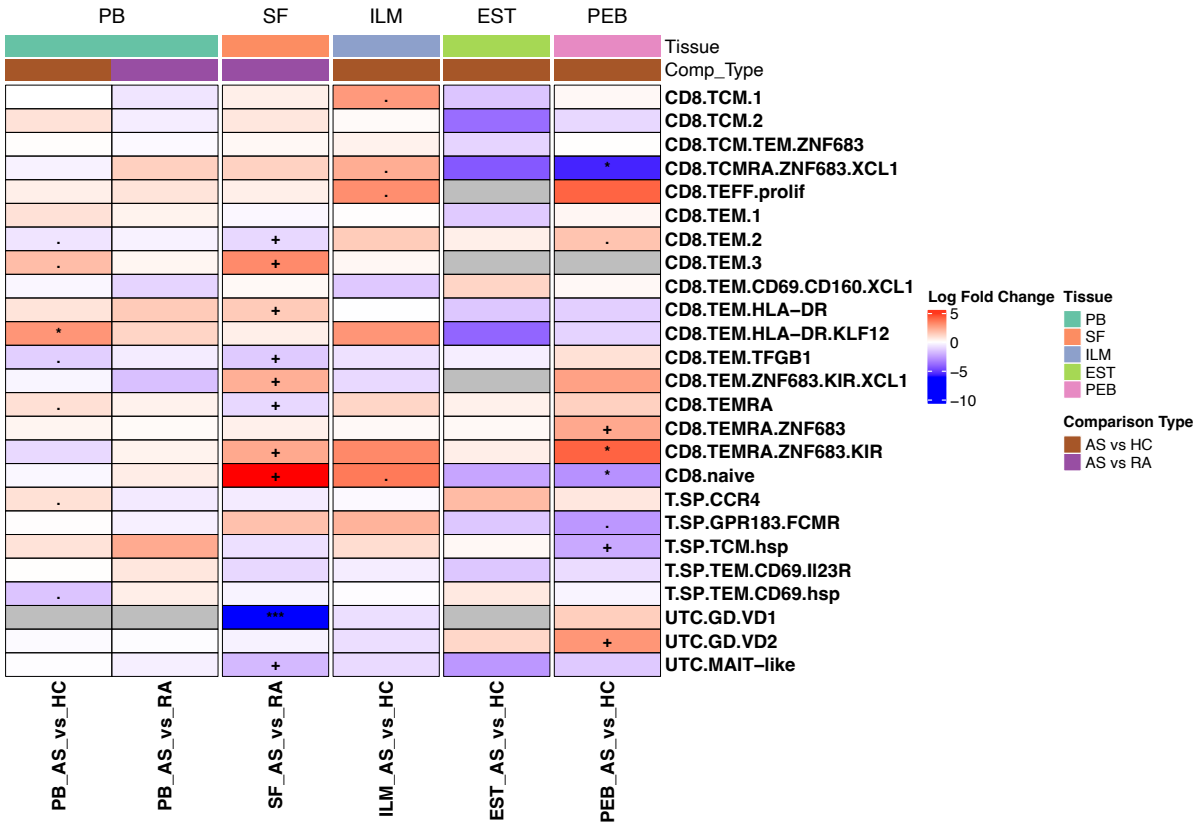


Figure D.13 Differential abundance of CD8-positive T-cell subsets across tissues and patient groups at minor subset level in the expanded cohort
Heatmap showing differential abundance analysis of CD8-positive T cell subsets in the expanded cohort using edgeR with TMM-normalized cell type counts. Colour indicates logFC of each subset in AxSpA relative to the comparison group. Significance label: *** < 0.001, ** < 0.01, * < 0.05, + < 0.1, . < 0.2, and no label for non-significant results.

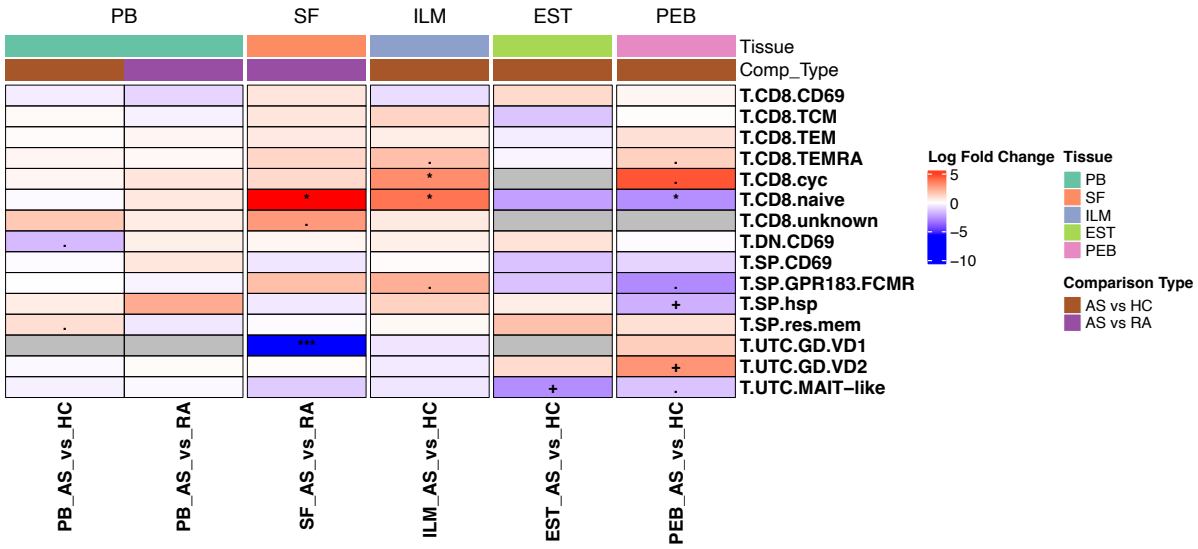


Figure D.14 Compositional differences of CD8⁺ T-cell subsets between AxSpA and RA in PBMC at the cell-type level

Boxplots illustrating differences in the relative abundance of CD8⁺ T-cell subsets between AxSpA and RA patient groups in PBMC. Each dot represents an individual sample from the expanded cohort; red dots indicate samples also included in the core cohort.

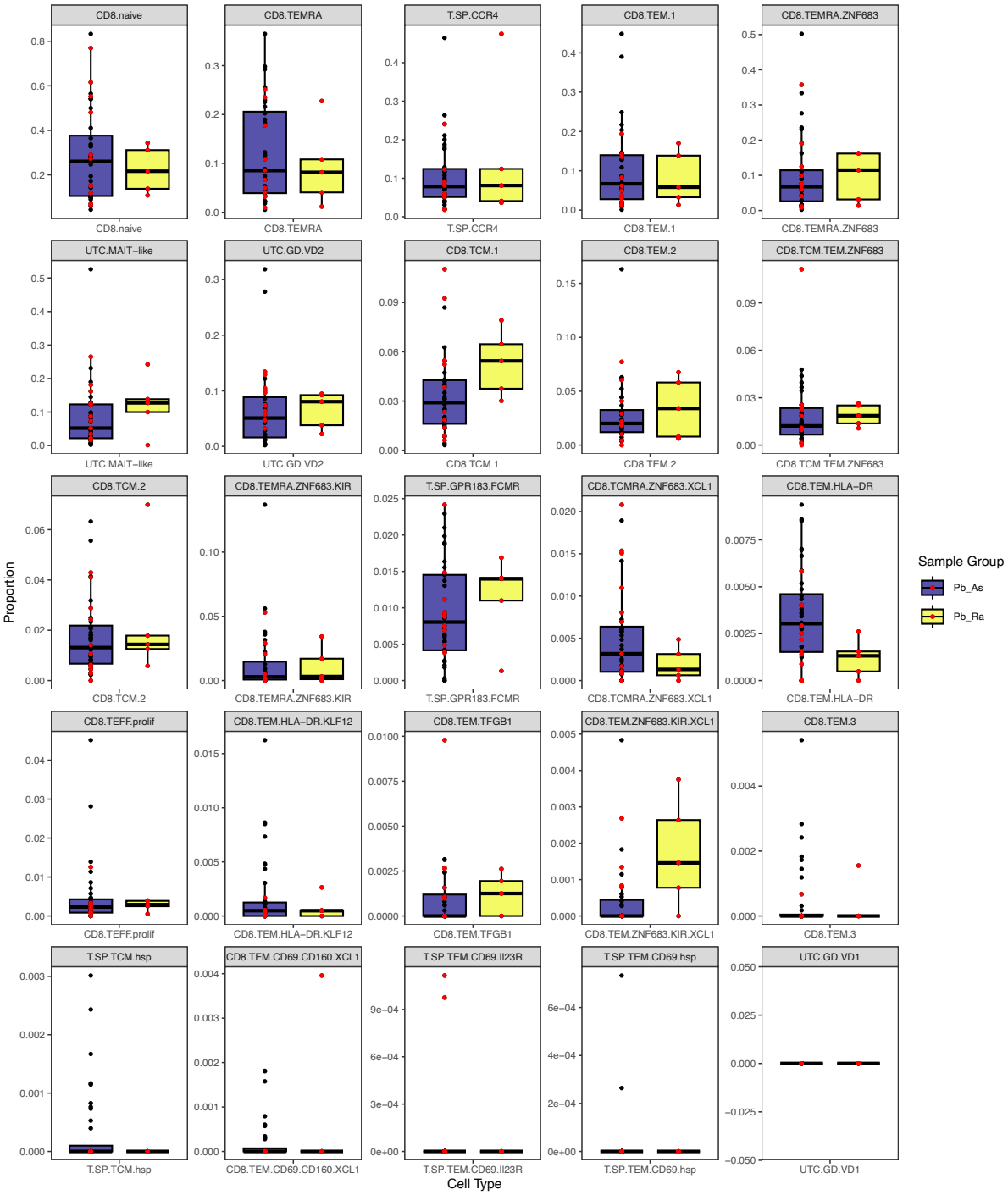


Figure D.15 Compositional differences of CD8⁺ T-cell subsets between AxSpA and HC in PBMC at the cell-type level

Boxplots illustrating differences in the relative abundance of CD8⁺ T-cell subsets between AxSpA and HC groups in PBMC. Each dot represents an individual sample from the expanded cohort; red dots indicate samples also included in the core cohort.

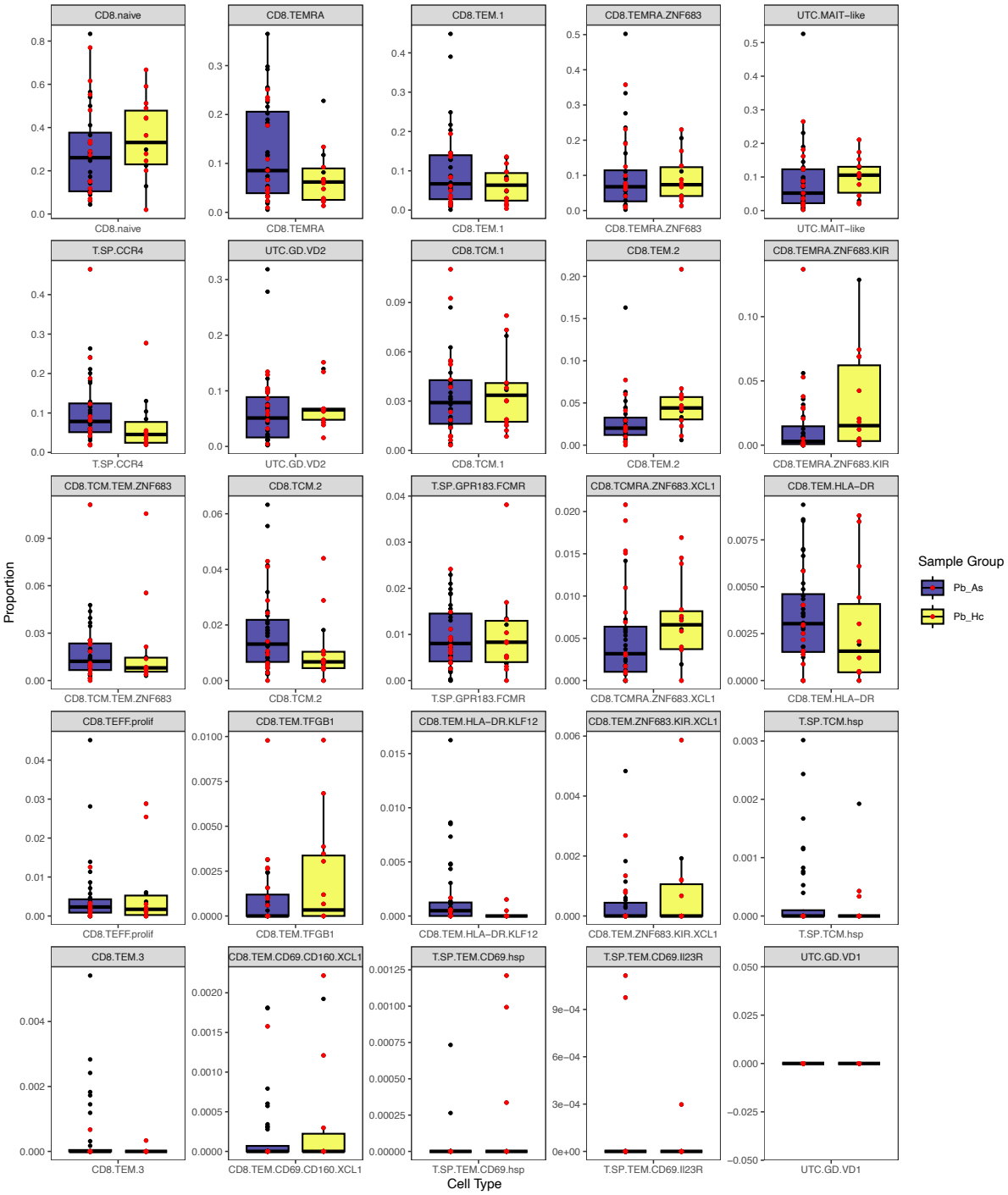


Figure D.16 Compositional differences of CD8⁺ T-cell subsets between AxSpA and RA in SFMC at the cell-type level

Boxplots illustrating differences in the relative abundance of CD8⁺ T-cell subsets between AxSpA and RA patient groups in SFMC. Each dot represents an individual sample from the expanded cohort; red dots indicate samples also included in the core cohort.

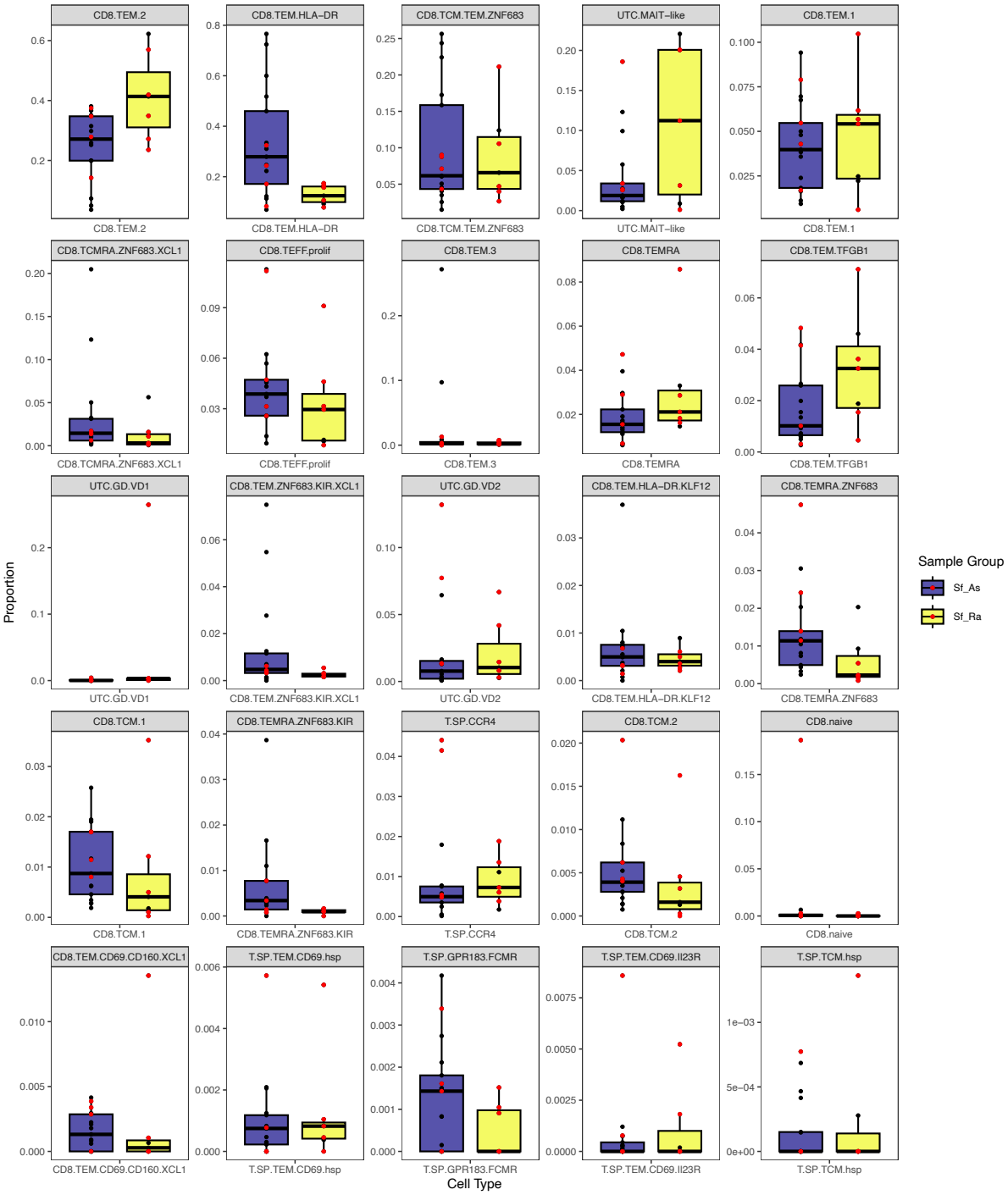


Figure D.17 Compositional differences of CD8⁺ T-cell subsets between AxSpA and HC in ILM at the cell-type level

Boxplots illustrating differences in the relative abundance of CD8⁺ T-cell subsets between AxSpA and HC groups in ILM. Each dot represents an individual sample from the expanded cohort; red dots indicate samples also included in the core cohort.

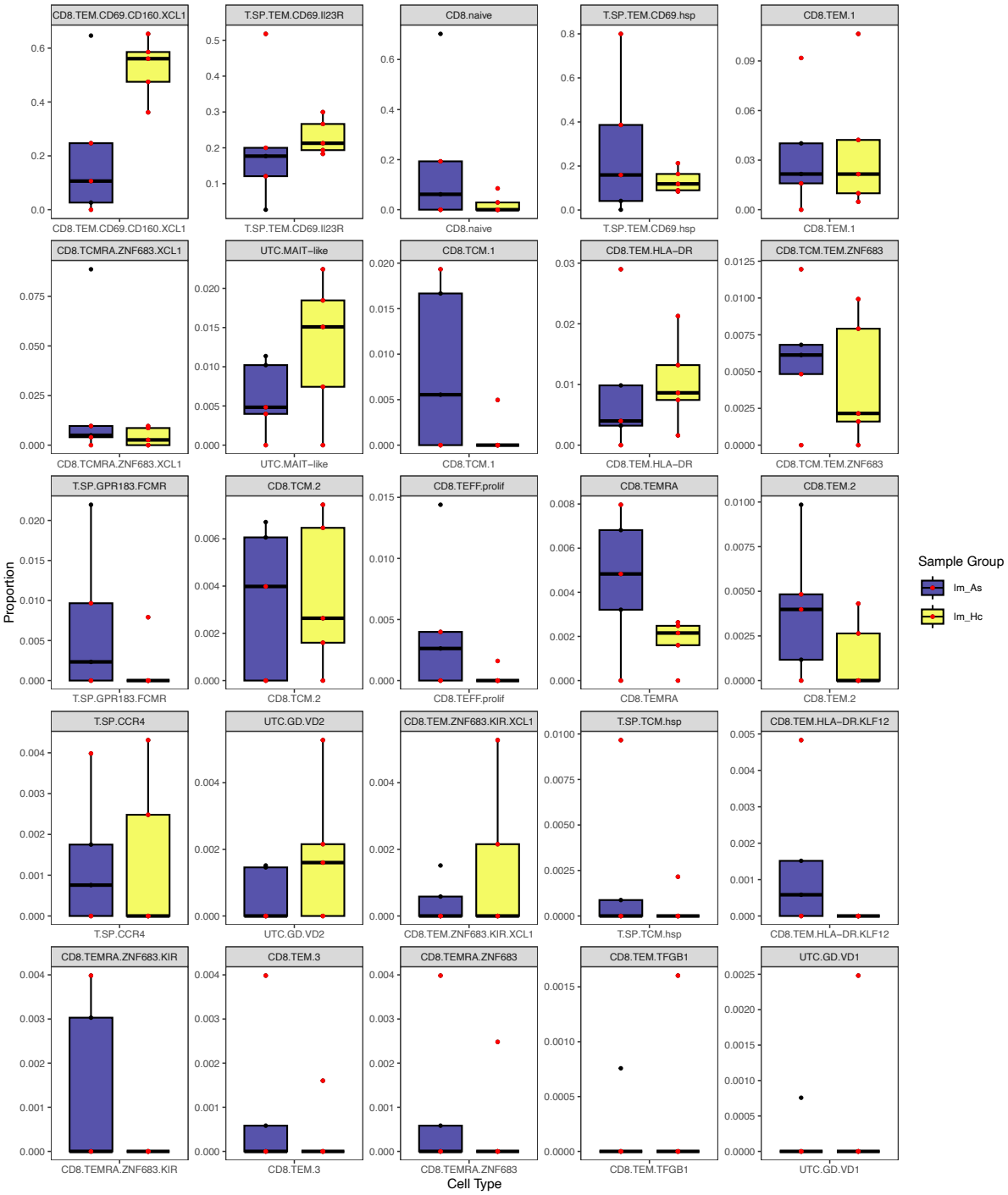


Figure D.18 Compositional differences of CD8⁺ T-cell subsets between AxSpA and HC in PEB at the cell-type level

Boxplots illustrating differences in the relative abundance of CD8⁺ T-cell subsets between AxSpA and HC groups in PEB. Each dot represents an individual sample from the expanded cohort; red dots indicate samples also included in the core cohort.

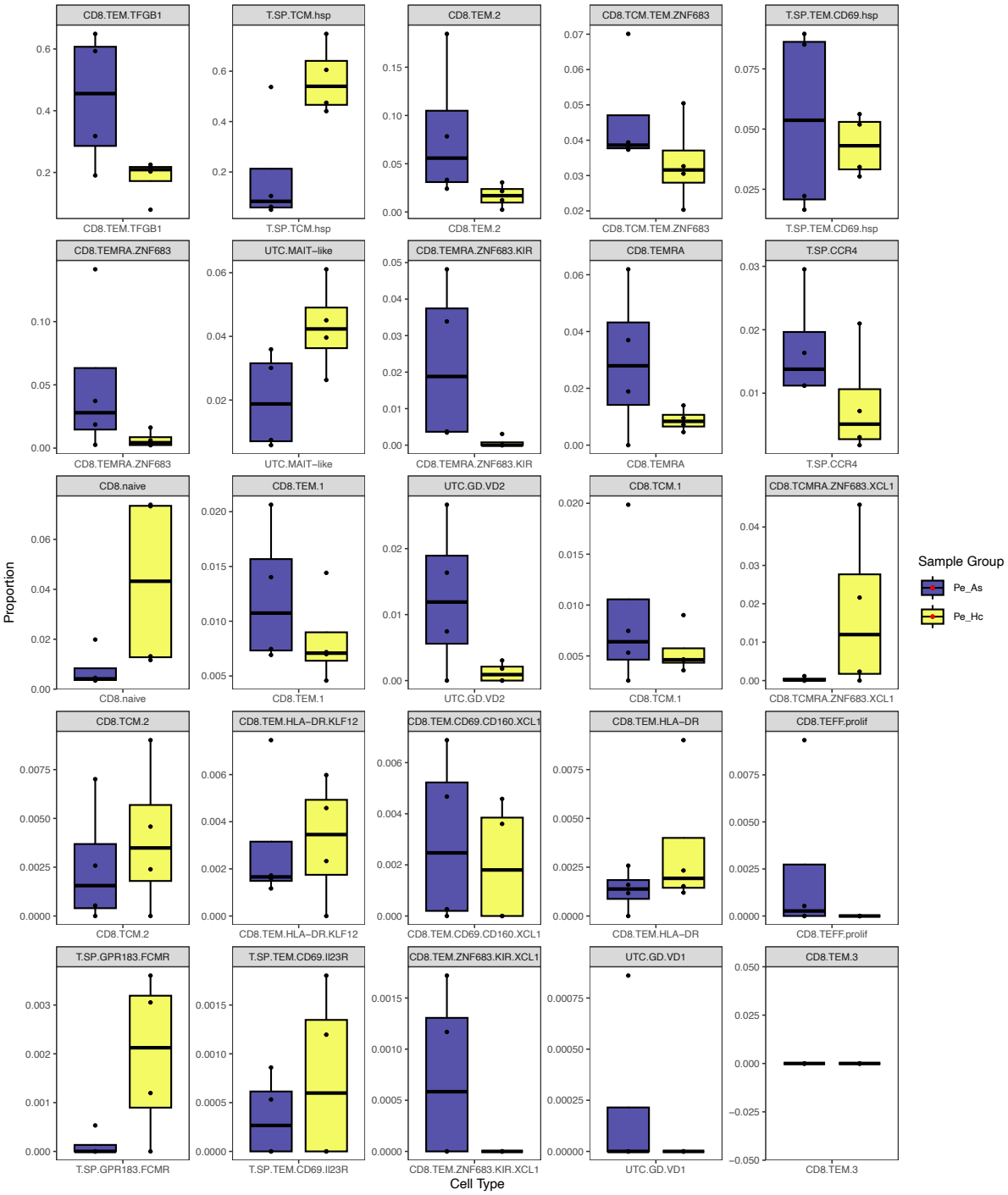


Figure D.19 Compositional differences of CD8⁺ T-cell subsets between AxSpA and HC in EST at the cell-type level

Boxplots illustrating differences in the relative abundance of CD8⁺ T-cell subsets between AxSpA and HC groups in PEB. Each dot represents an individual sample from the expanded cohort; red dots indicate samples also included in the core cohort.

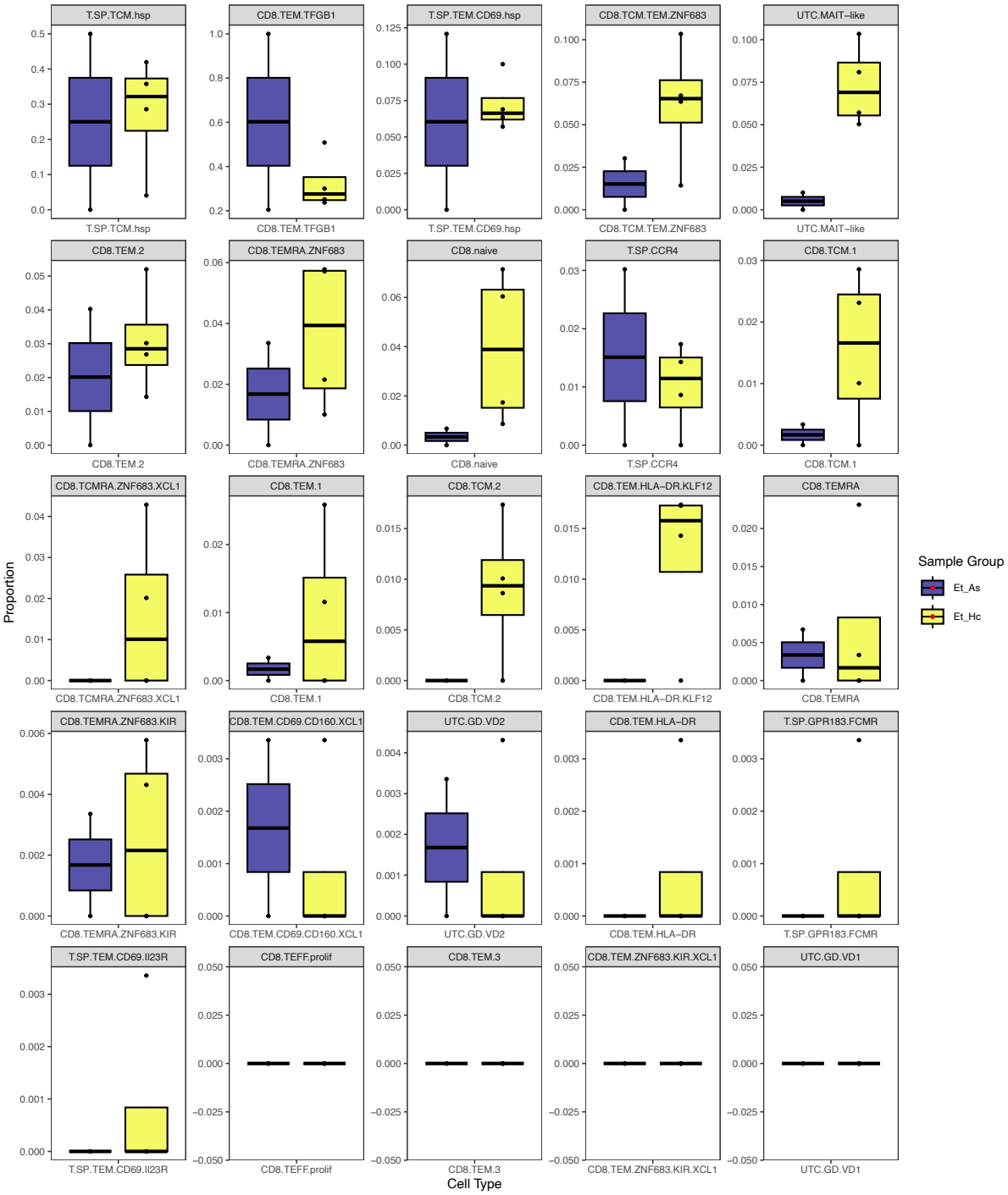


Figure D.20 Compositional differences of NK subsets between AxSpA and RA in PBMC at the cell-type level

Boxplots illustrating differences in the relative abundance of NK cell subsets between AxSpA and RA patient groups in PBMC. Each dot represents an individual sample from the expanded cohort; red dots indicate samples also included in the core cohort.

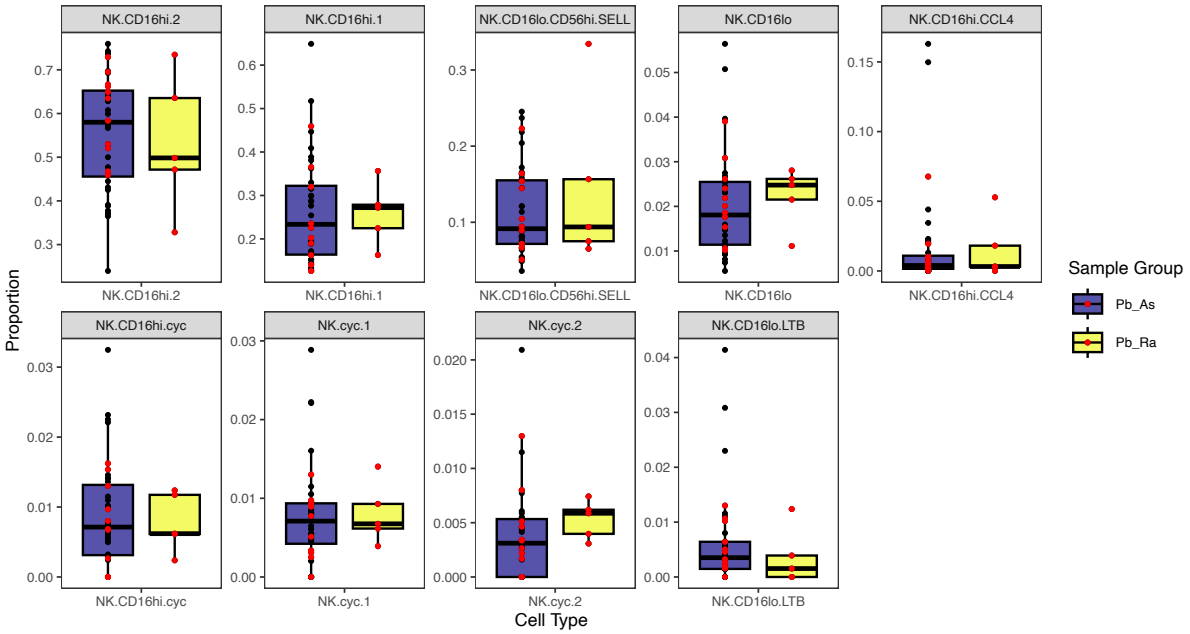


Figure D.21 Compositional differences of NK cell subsets between AxSpA and HC in PBMC at the cell-type level

Boxplots illustrating differences in the relative abundance of NK cell subsets between AxSpA and HC groups in PBMC. Each dot represents an individual sample from the expanded cohort; red dots indicate samples also included in the core cohort.

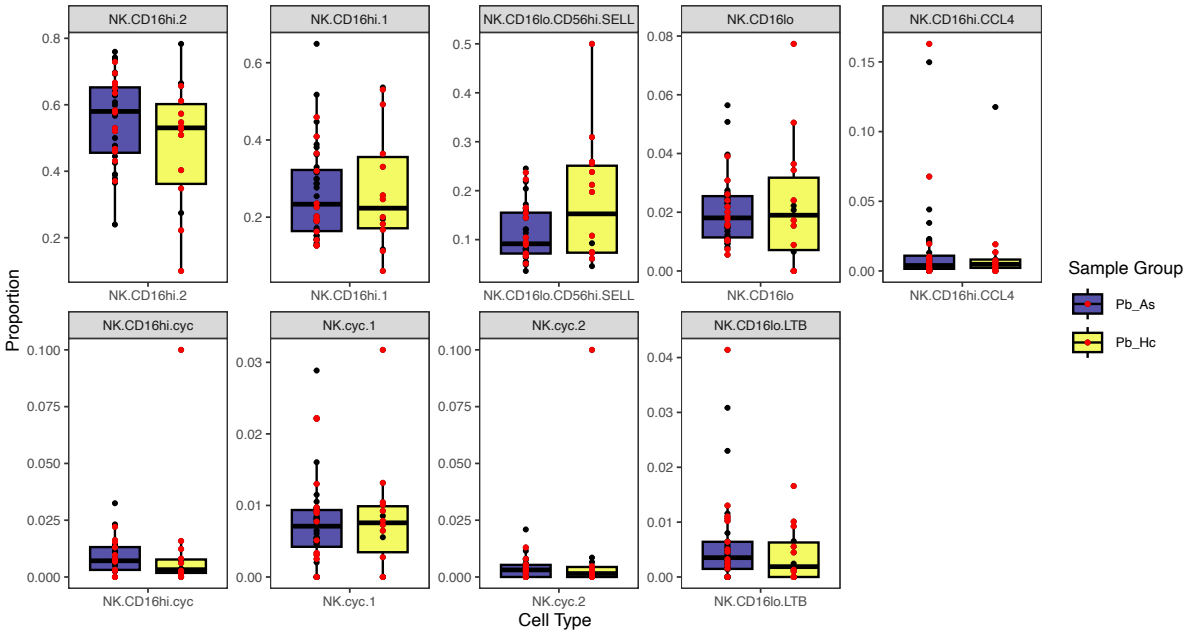


Figure D.22 Compositional differences of NK cell subsets between AxSpA and RA in SFMC at the cell-type level

Boxplots illustrating differences in the relative abundance of NK cell subsets between AxSpA and RA patient groups in SFMC. Each dot represents an individual sample from the expanded cohort; red dots indicate samples also included in the core cohort.

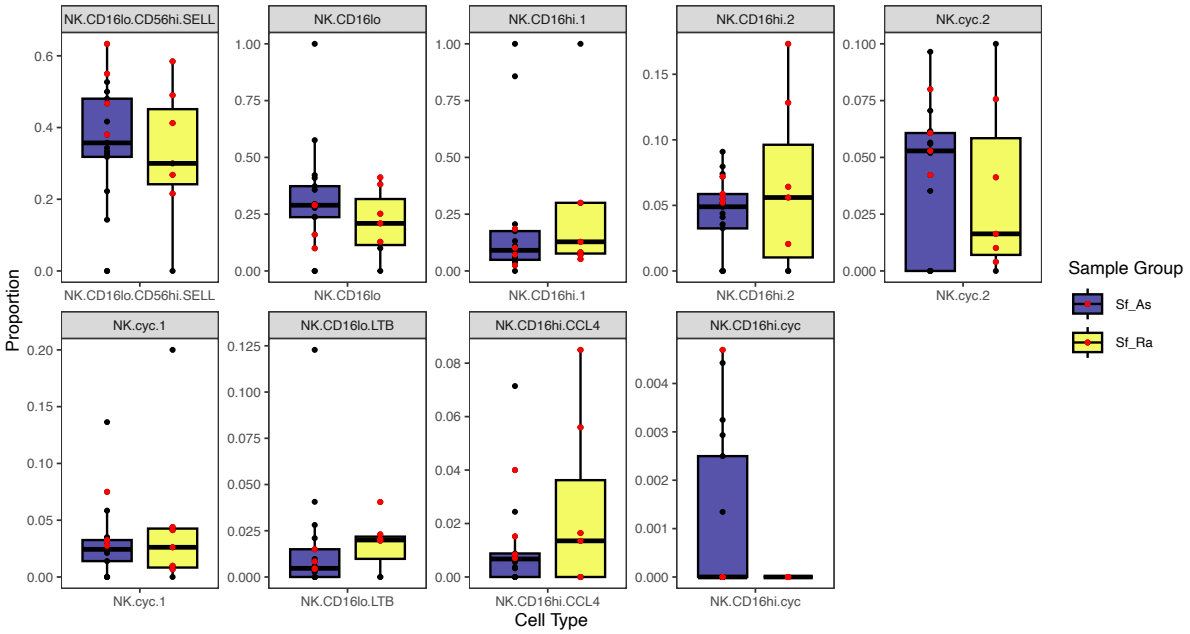


Figure D.23 Compositional differences of NK cell subsets between AxSpA and HC in ILM at the cell-type level

Boxplots illustrating differences in the relative abundance of NK cell subsets between AxSpA and HC groups in ILM. Each dot represents an individual sample from the expanded cohort; red dots indicate samples also included in the core cohort.

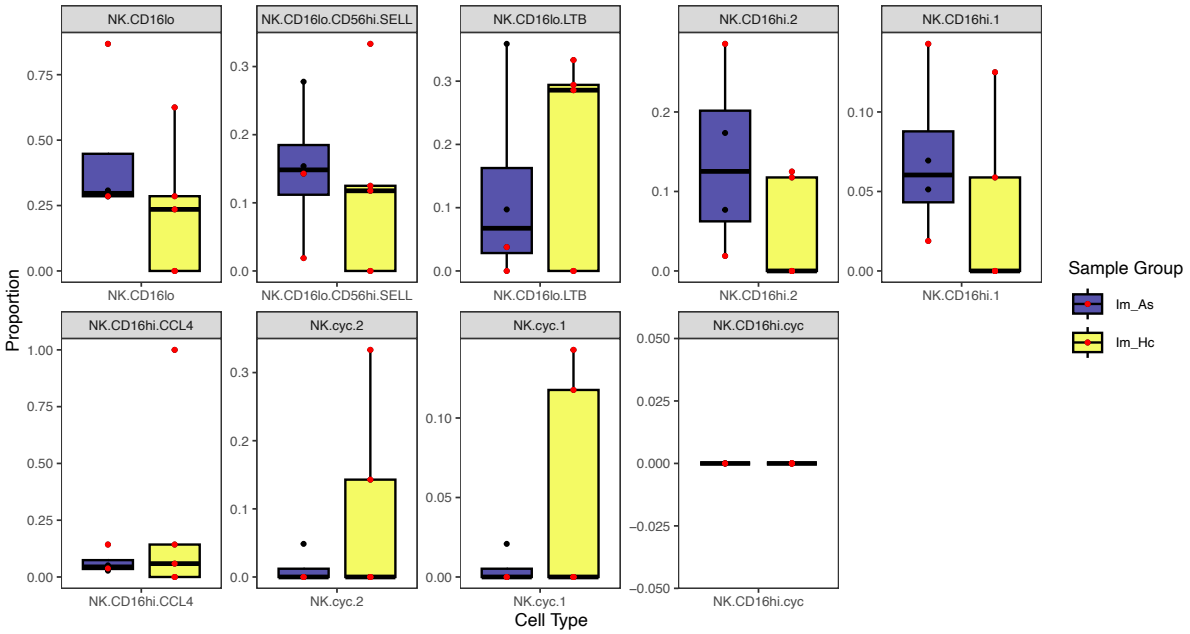


Figure D.24 Compositional differences of NK cell subsets between AxSpA and HC in PEB at the cell-type level

Boxplots illustrating differences in the relative abundance of NK cell subsets between AxSpA and HC groups in PEB. Each dot represents an individual sample from the expanded cohort; red dots indicate samples also included in the core cohort.

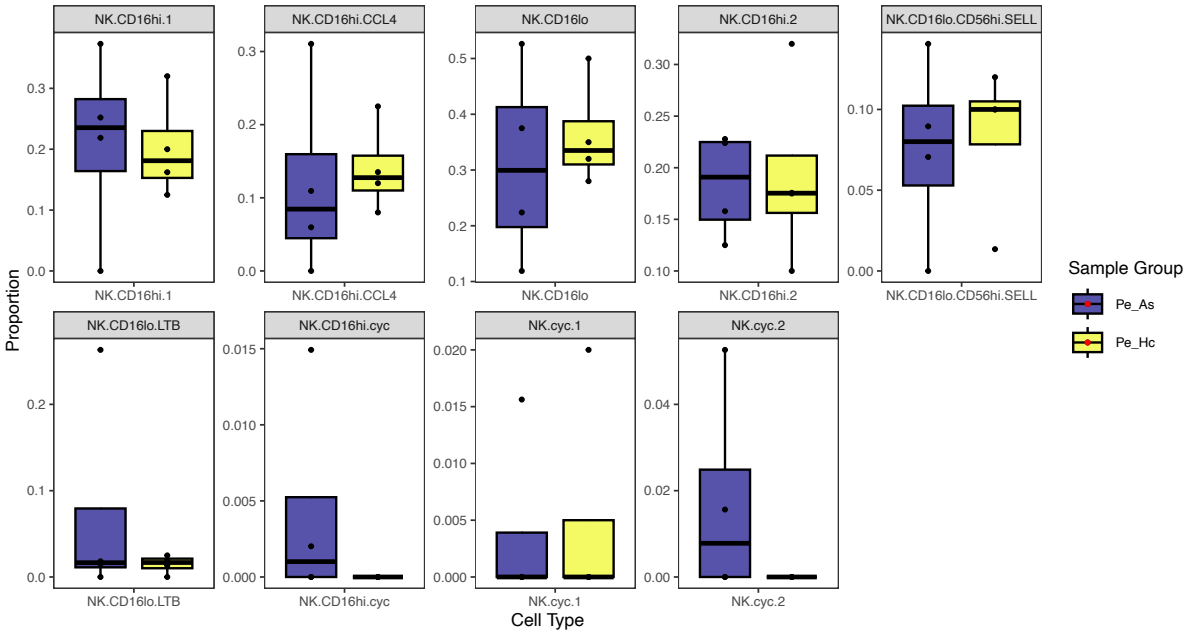


Figure D.25 Compositional differences of NK cell subsets between AxSpA and HC in EST at the cell-type level

Boxplots illustrating differences in the relative abundance of NK cell subsets between AxSpA and HC groups in PEB. Each dot represents an individual sample from the expanded cohort; red dots indicate samples also included in the core cohort.

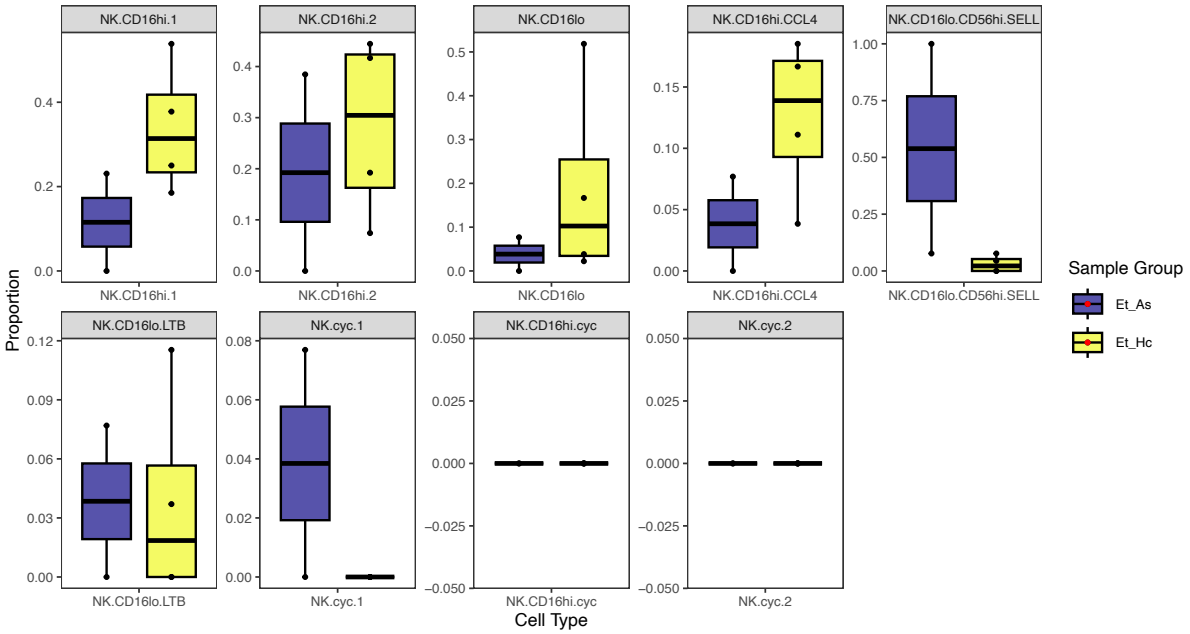


Figure D.26 Compositional differences of myeloid subsets between AxSpA and RA in PBMC at the cell-type level

Boxplots illustrating differences in the relative abundance of myeloid cell subsets between AxSpA and RA patient groups in PBMC. Each dot represents an individual sample from the expanded cohort; red dots indicate samples also included in the core cohort.

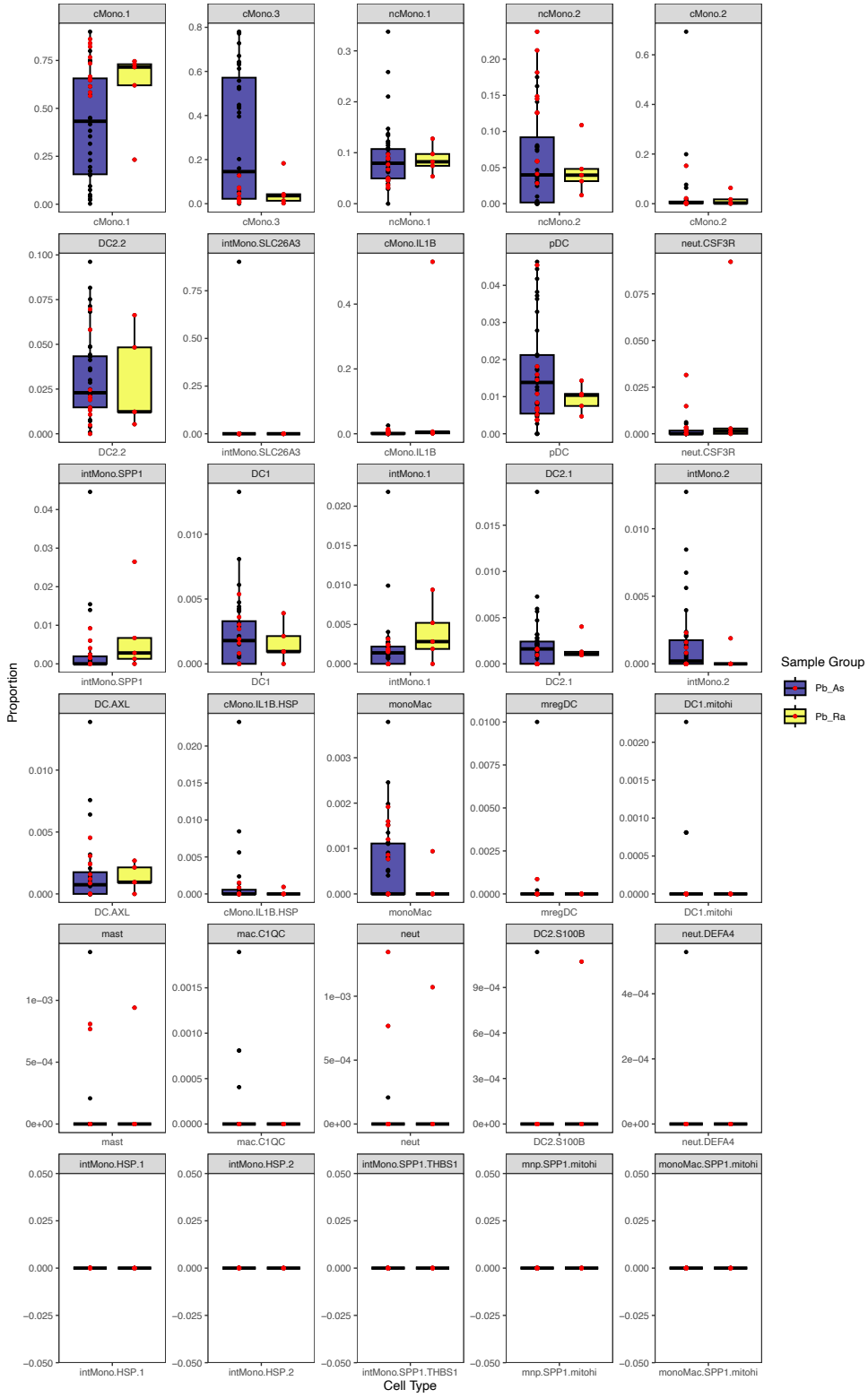


Figure D.27 Compositional differences of myeloid cell subsets between AxSpA and HC in PBMC at the cell-type level

Boxplots illustrating differences in the relative abundance of myeloid cell subsets between AxSpA and HC groups in PBMC. Each dot represents an individual sample from the expanded cohort; red dots indicate samples also included in the core cohort.

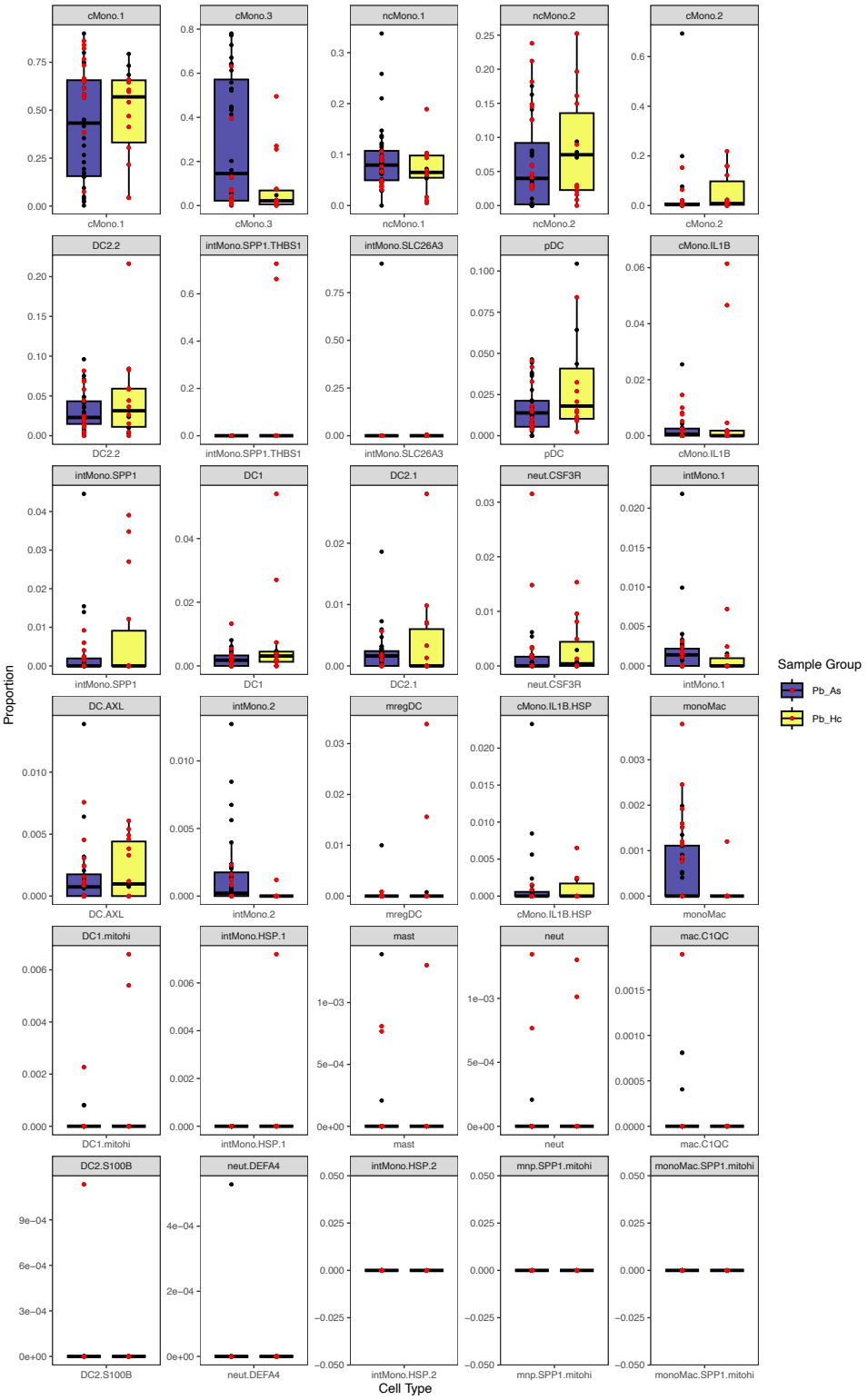


Figure D.28 Compositional differences of myeloid cell subsets between AxSpA and RA in SFMC at the cell-type level

Boxplots illustrating differences in the relative abundance of myeloid cell subsets between AxSpA and RA patient groups in SFMC. Each dot represents an individual sample from the expanded cohort; red dots indicate samples also included in the core cohort.

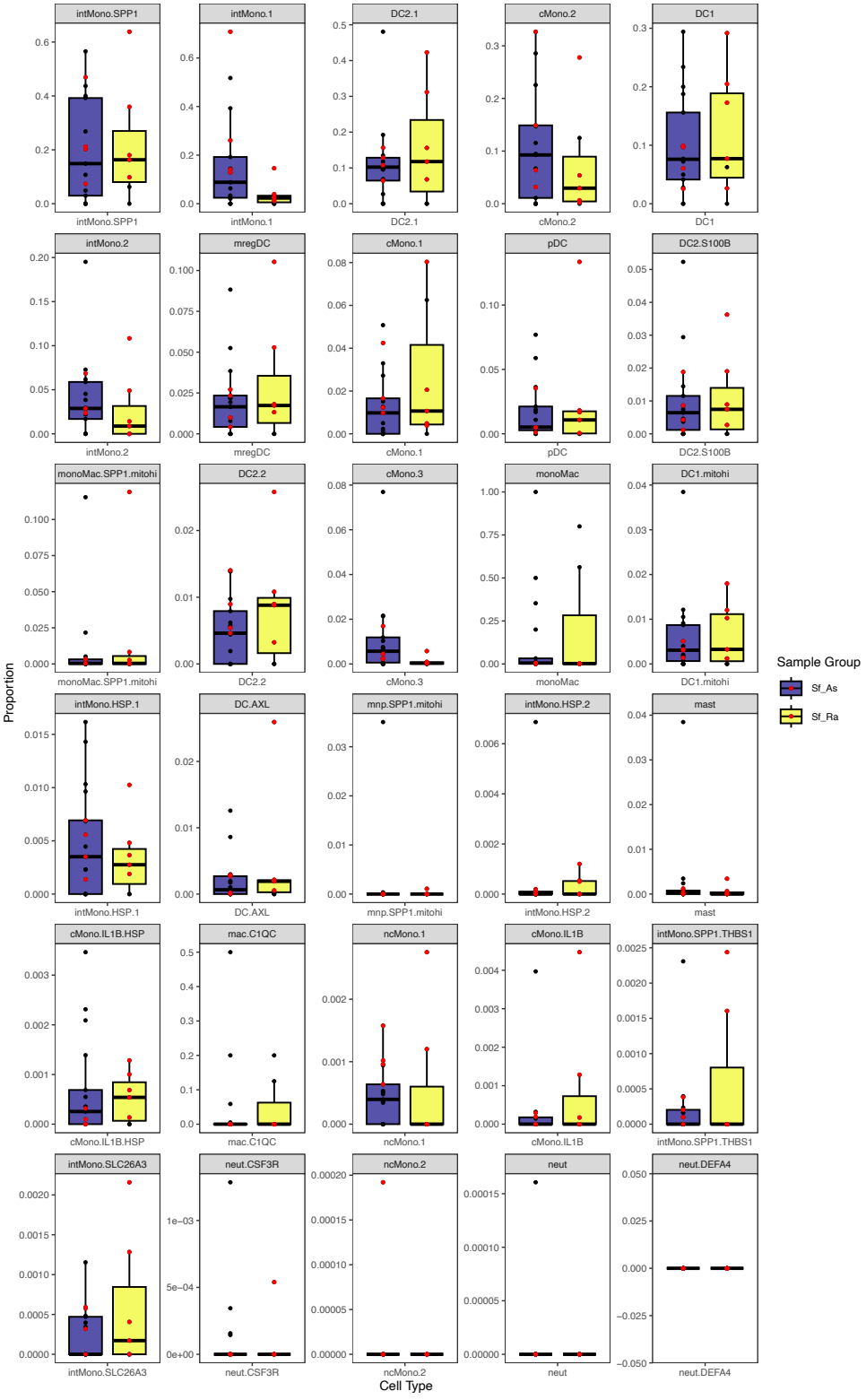


Figure D.29 Compositional differences of myeloid cell subsets between AxSpA and HC in ILM at the cell-type level

Boxplots illustrating differences in the relative abundance of myeloid cell subsets between AxSpA and HC groups in ILM. Each dot represents an individual sample from the expanded cohort; red dots indicate samples also included in the core cohort.

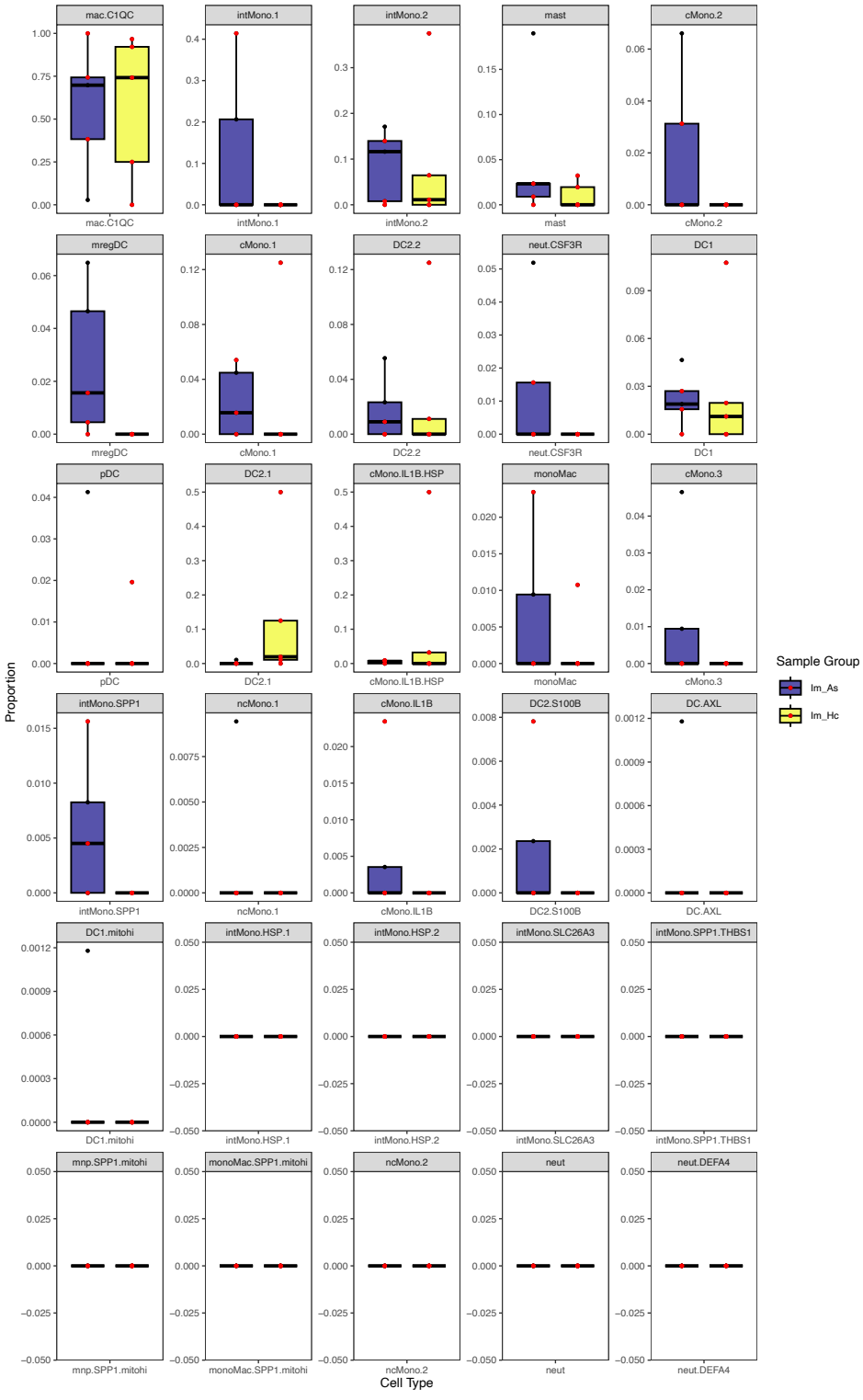


Figure D.30 Compositional differences of myeloid cell subsets between AxSpA and HC in PEB at the cell-type level

Boxplots illustrating differences in the relative abundance of myeloid cell subsets between AxSpA and HC groups in PEB. Each dot represents an individual sample from the expanded cohort; red dots indicate samples also included in the core cohort.

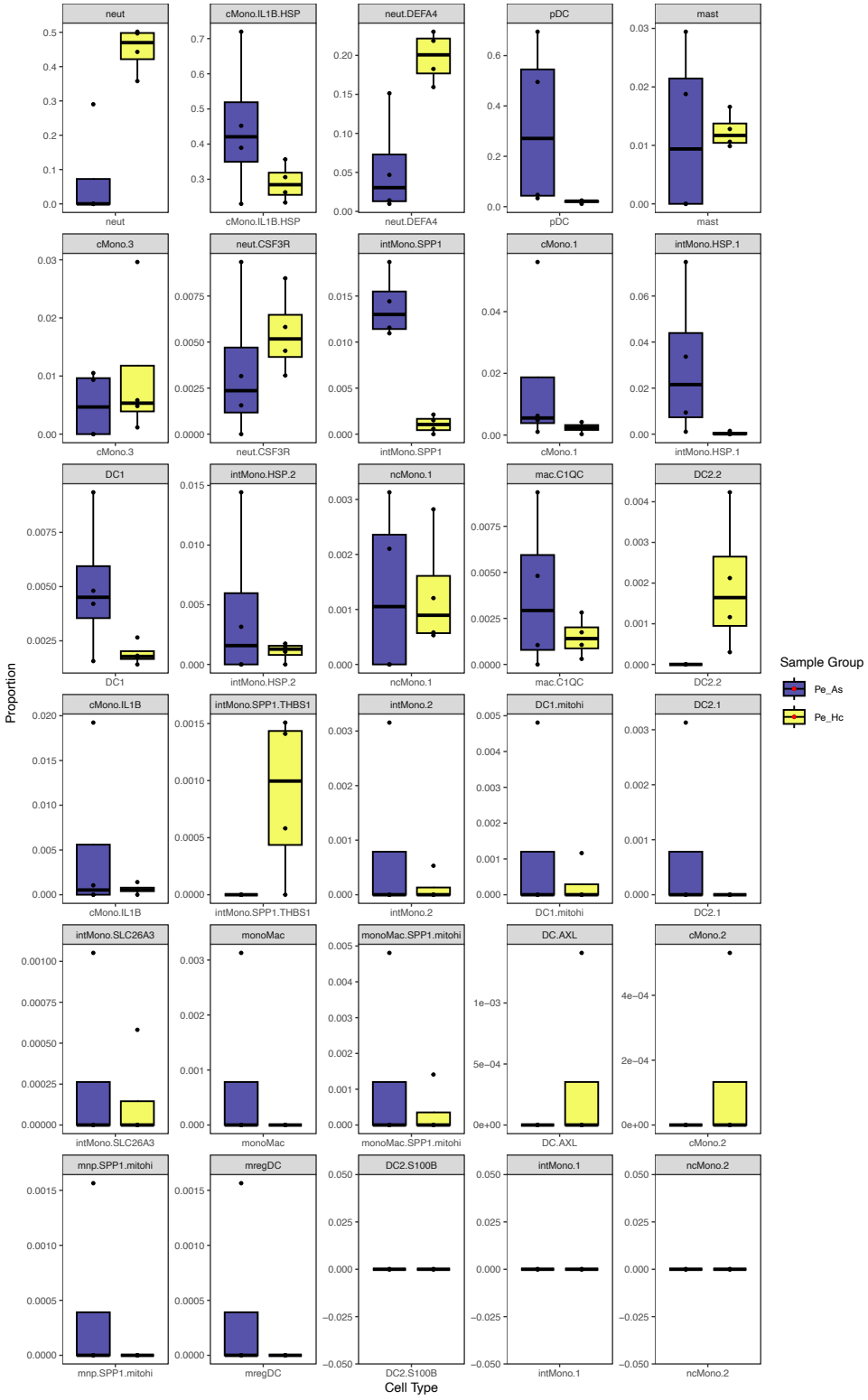


Figure D.31 Compositional differences of myeloid cell subsets between AxSpA and HC in EST at the cell-type level

Boxplots illustrating differences in the relative abundance of myeloid cell subsets between AxSpA and HC groups in EST. Each dot represents an individual sample from the expanded cohort; red dots indicate samples also included in the core cohort.

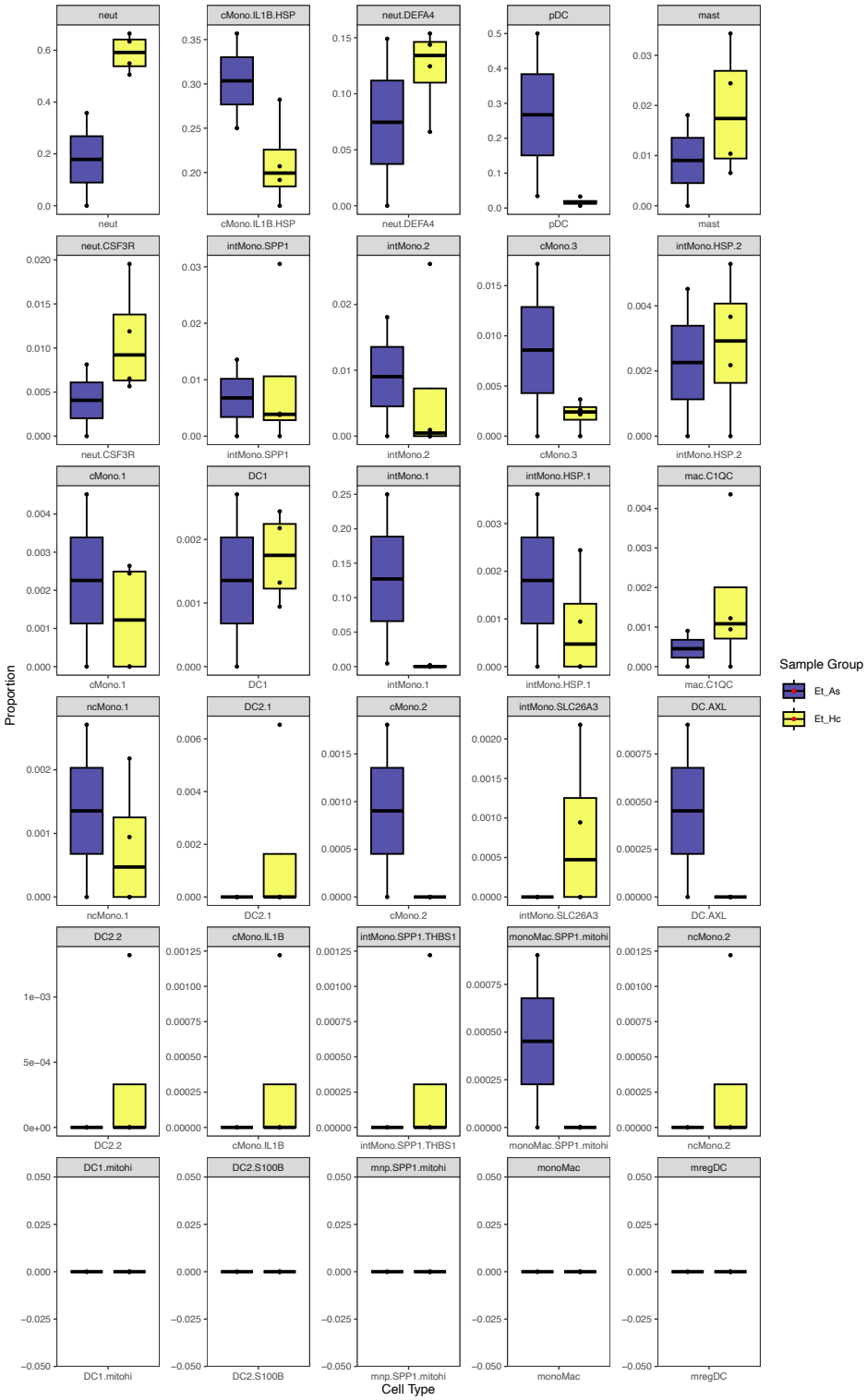


Figure D.32 Compositional differences of B and plasma subsets between AxSpA and RA in PBMC at the cell-type level

Boxplots illustrating differences in the relative abundance of B and plasma subsets between AxSpA and RA patient groups in PBMC. Each dot represents an individual sample from the expanded cohort; red dots indicate samples also included in the core cohort.

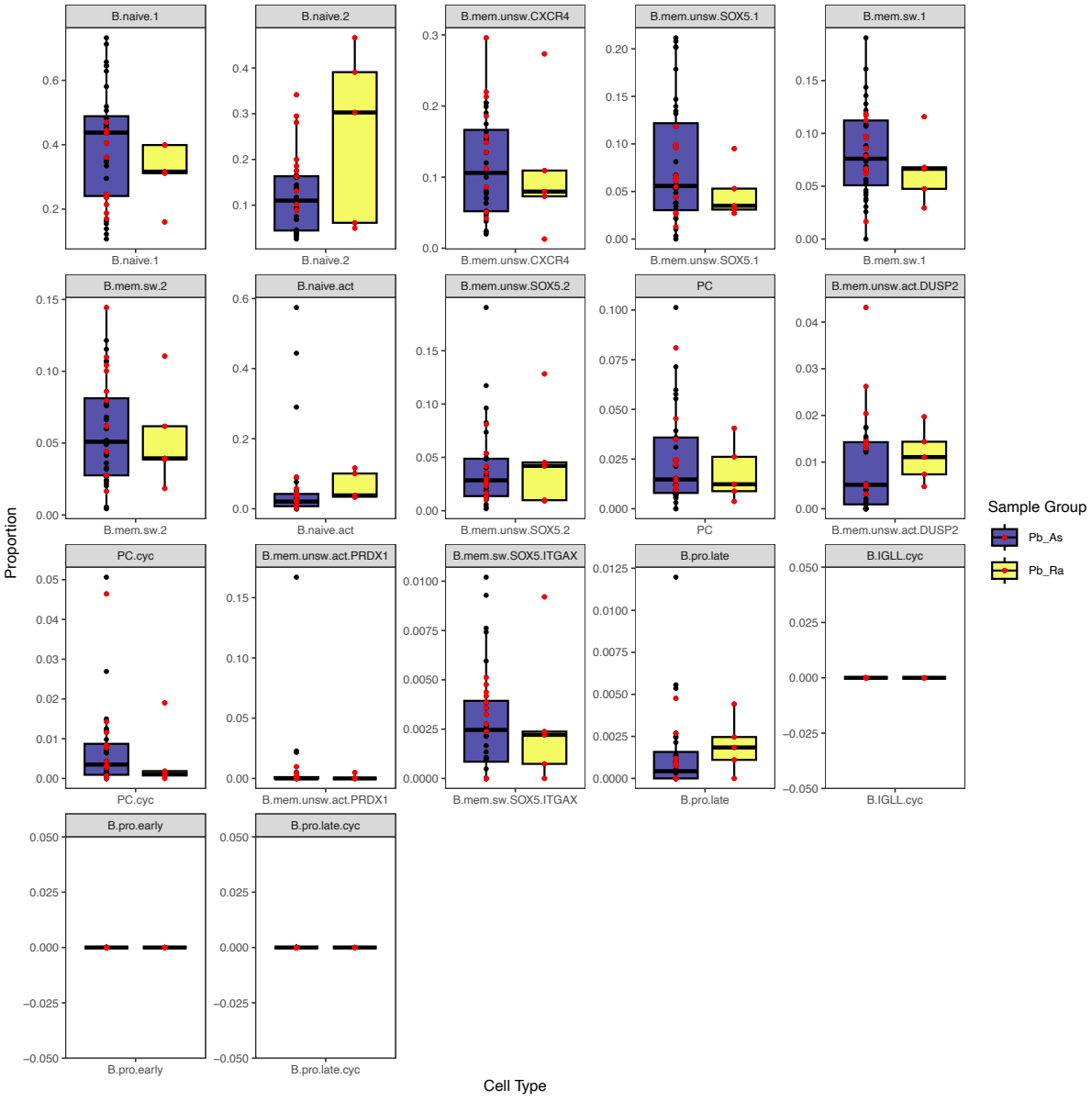


Figure D.33 Compositional differences of B and plasma subsets between AxSpA and HC in PBMC at the cell-type level

Boxplots illustrating differences in the relative abundance of B and plasma subsets between AxSpA and HC groups in PBMC. Each dot represents an individual sample from the expanded cohort; red dots indicate samples also included in the core cohort.

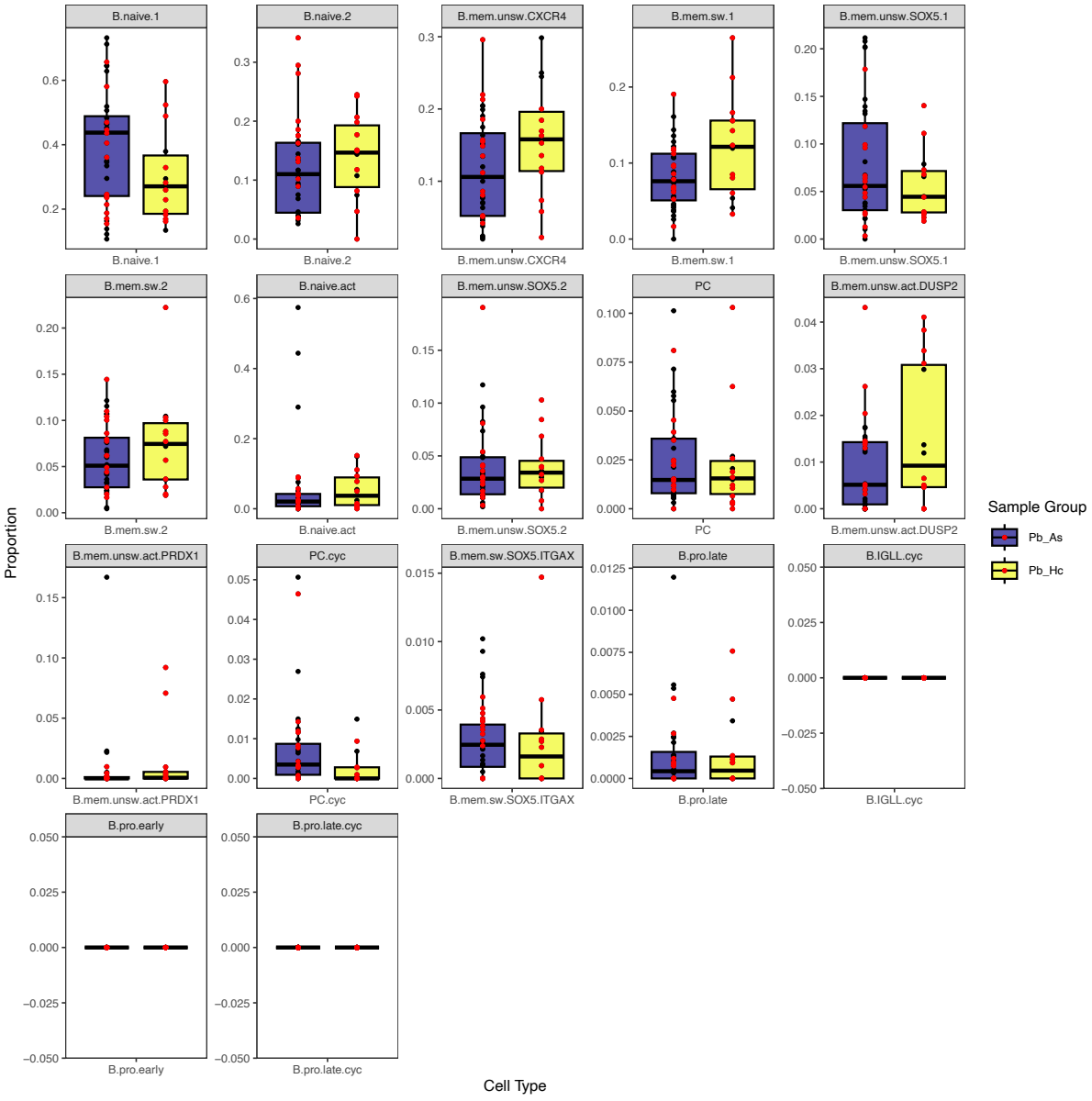


Figure D.34 Compositional differences of B and plasma subsets between AxSpA and RA in SFMC at the cell-type level

Boxplots illustrating differences in the relative abundance of B and plasma cell subsets between AxSpA and RA patient groups in SFMC. Each dot represents an individual sample from the expanded cohort; red dots indicate samples also included in the core cohort.

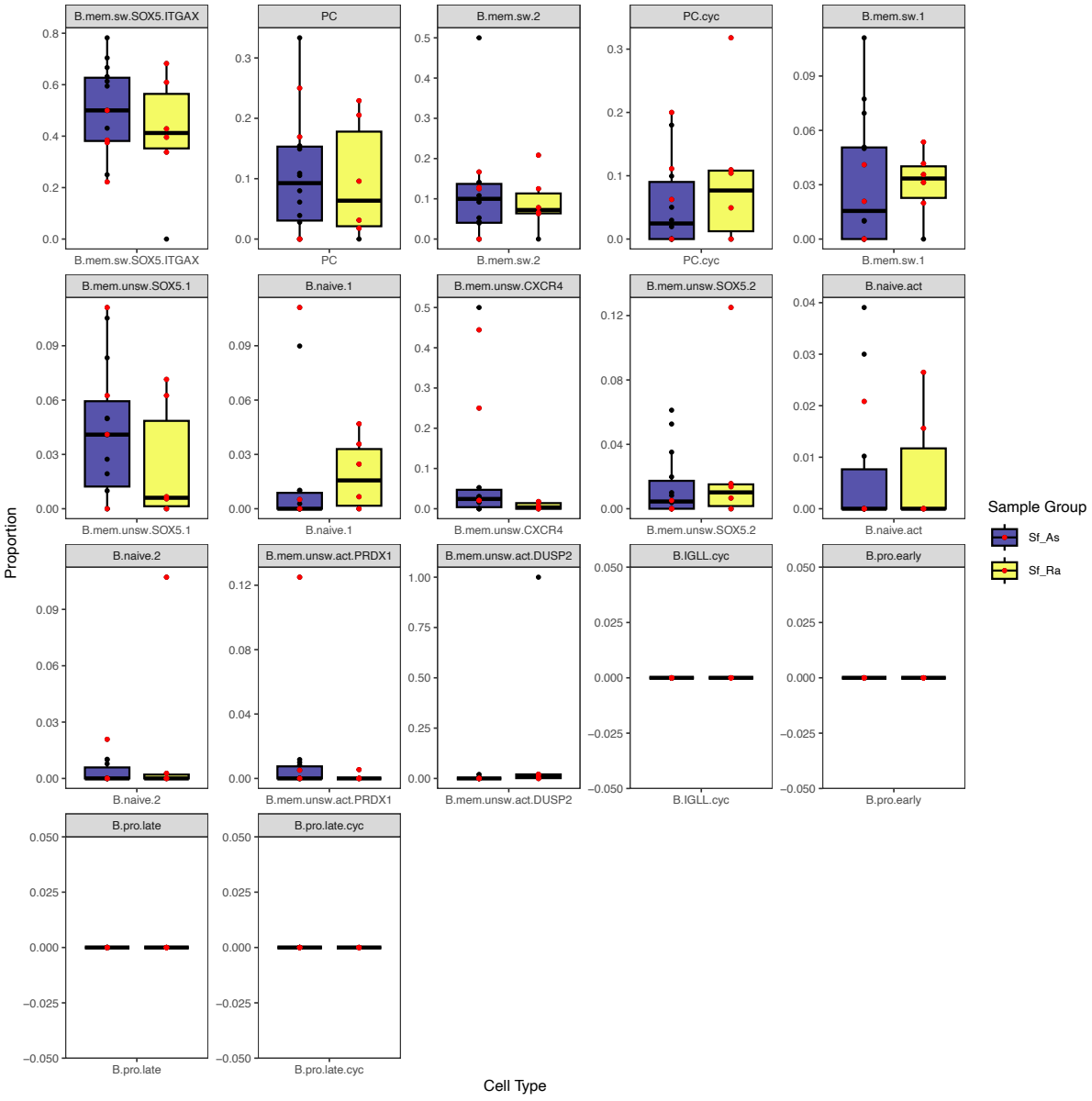


Figure D.35 Compositional differences of B and plasma cell subsets between AxSpA and HC in ILM at the cell-type level

Boxplots illustrating differences in the relative abundance of B and plasma cell subsets between AxSpA and HC groups in ILM. Each dot represents an individual sample from the expanded cohort; red dots indicate samples also included in the core cohort.

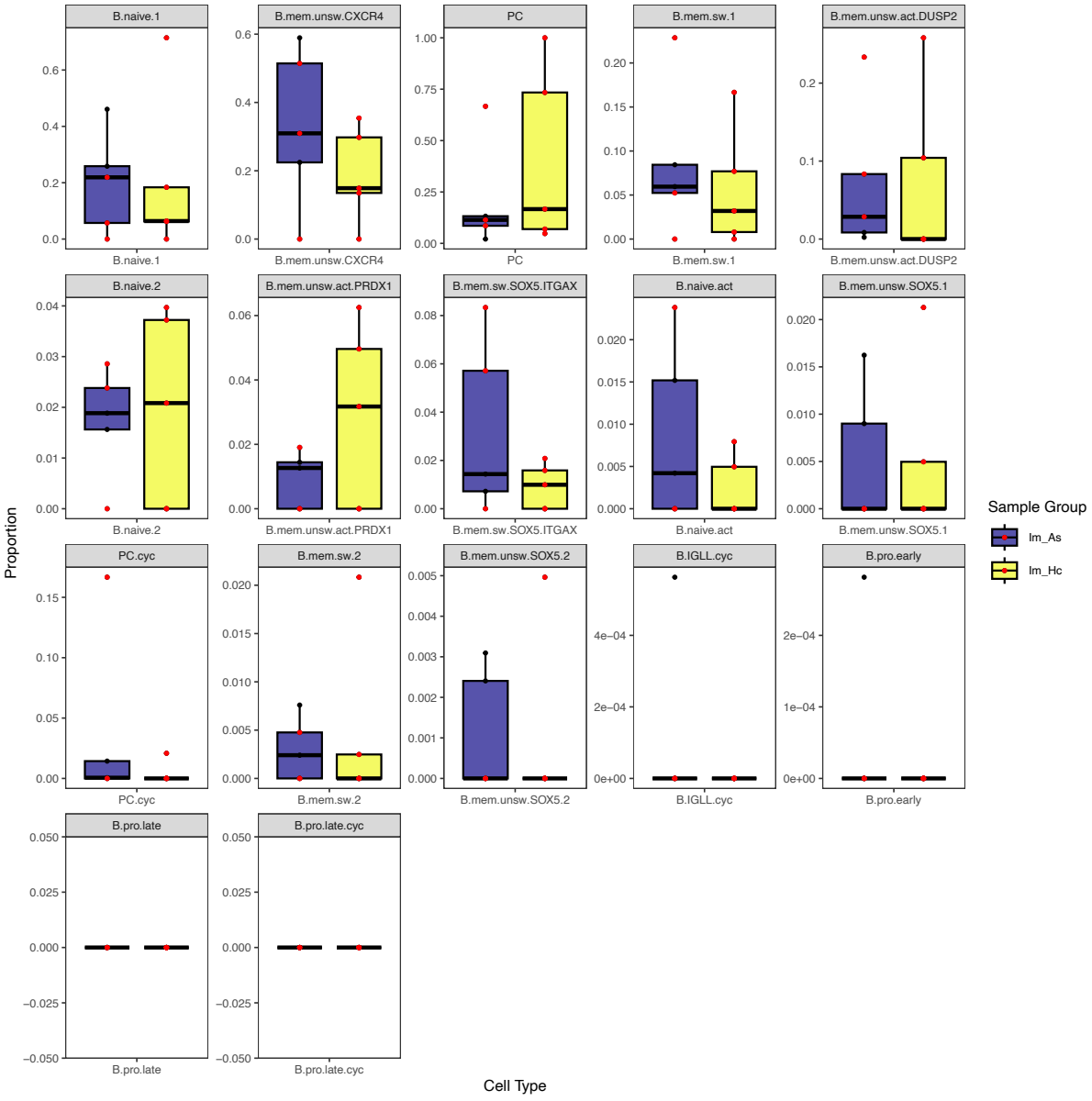


Figure D.36 Compositional differences of B and plasma subsets between AxSpA and HC in PEB at the cell-type level

Boxplots illustrating differences in the relative abundance of B and plasma subsets between AxSpA and HC groups in PEB. Each dot represents an individual sample from the expanded cohort; red dots indicate samples also included in the core cohort.

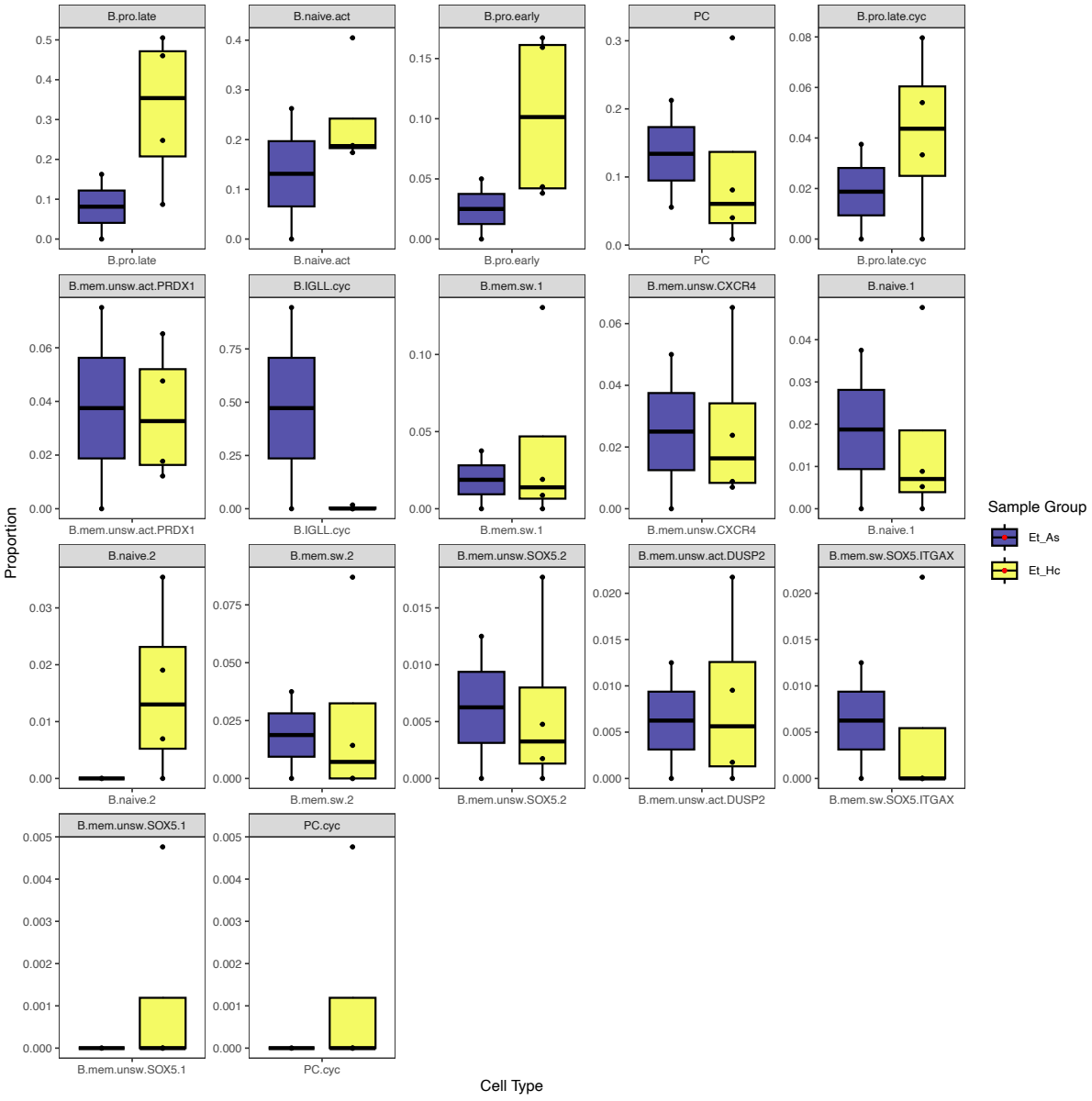


Figure D.37 Compositional differences of B and plasma subsets between AxSpA and HC in EST at the cell-type level

Boxplots illustrating differences in the relative abundance of B and plasma cell subsets between AxSpA and HC groups in EST. Each dot represents an individual sample from the expanded cohort; red dots indicate samples also included in the core cohort.

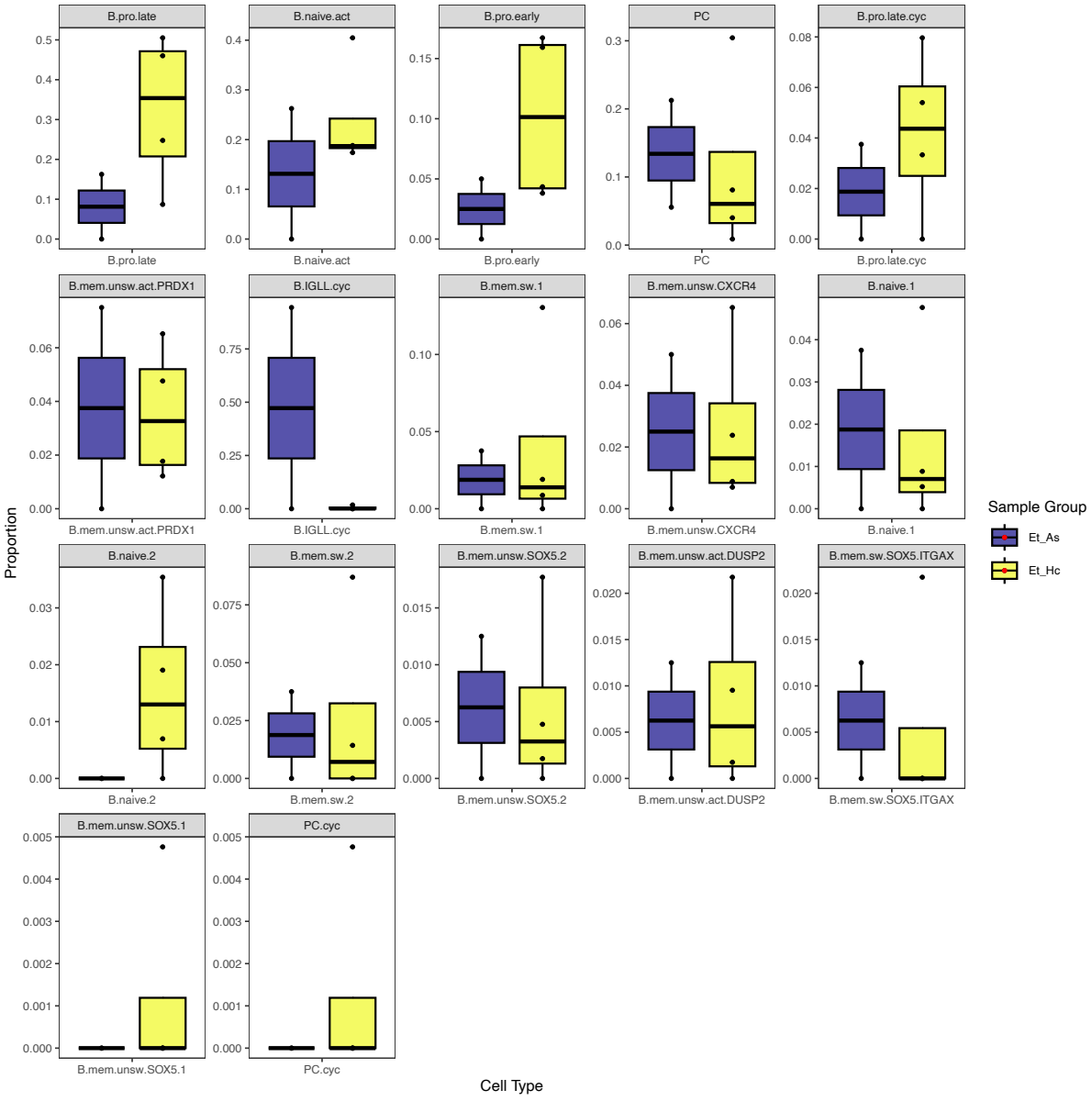


Figure D.38 Tissue-associated compositional differences in the CD4⁺ T-cell compartment
Heatmap showing tissue-associated enrichment of CD8⁺ T-cell subsets across AxSpA tissues. Significance determined by Poisson regression (adjusted $p < 0.05$).

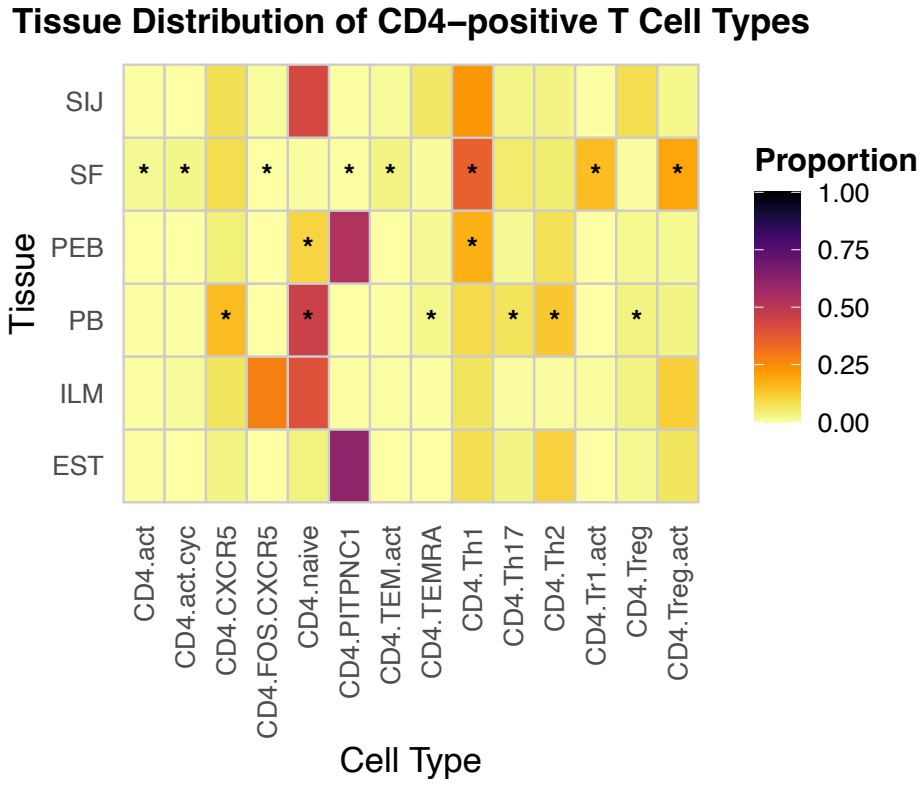


Figure D.39 Tissue-associated compositional differences in the NK cell compartment
Heatmap showing tissue-associated enrichment of NK cell subsets across AxSpA tissues. Significance determined by Poisson regression (adjusted p < 0.05).

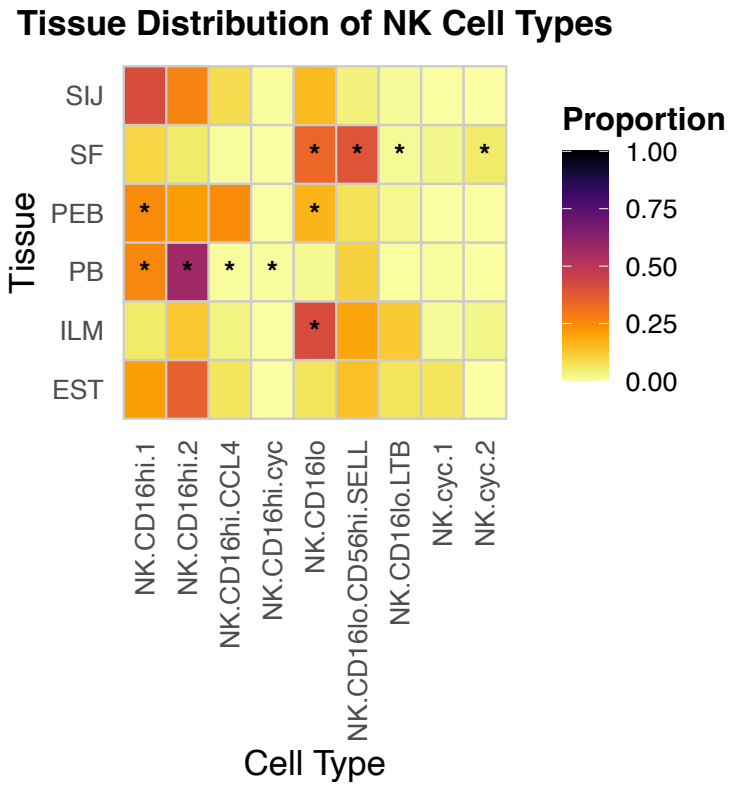


Figure D.40 Tissue-associated compositional differences in the other cell compartment
Heatmap showing tissue-associated enrichment of other cell subsets across AxSpA tissues. Significance determined by Poisson regression (adjusted p < 0.05).

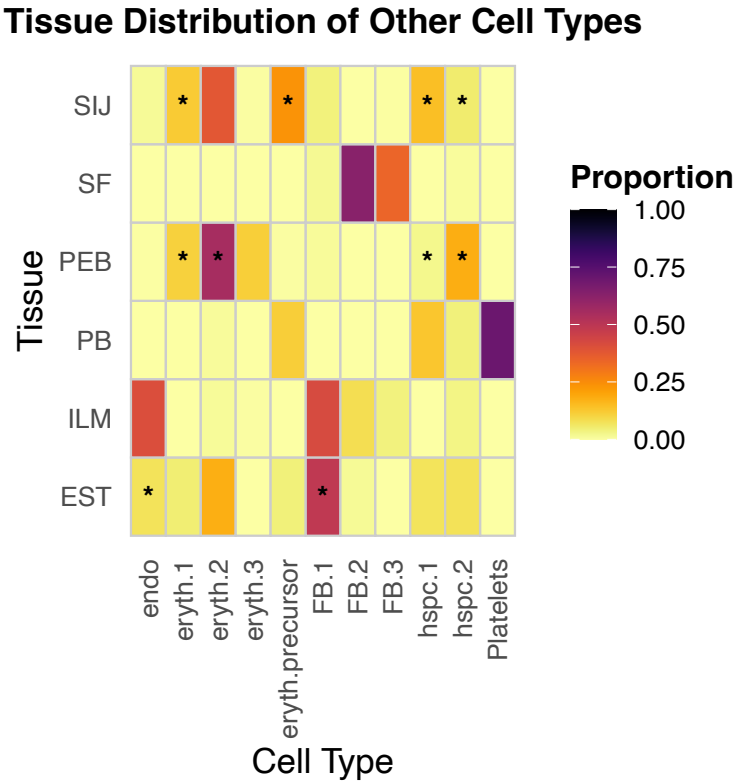
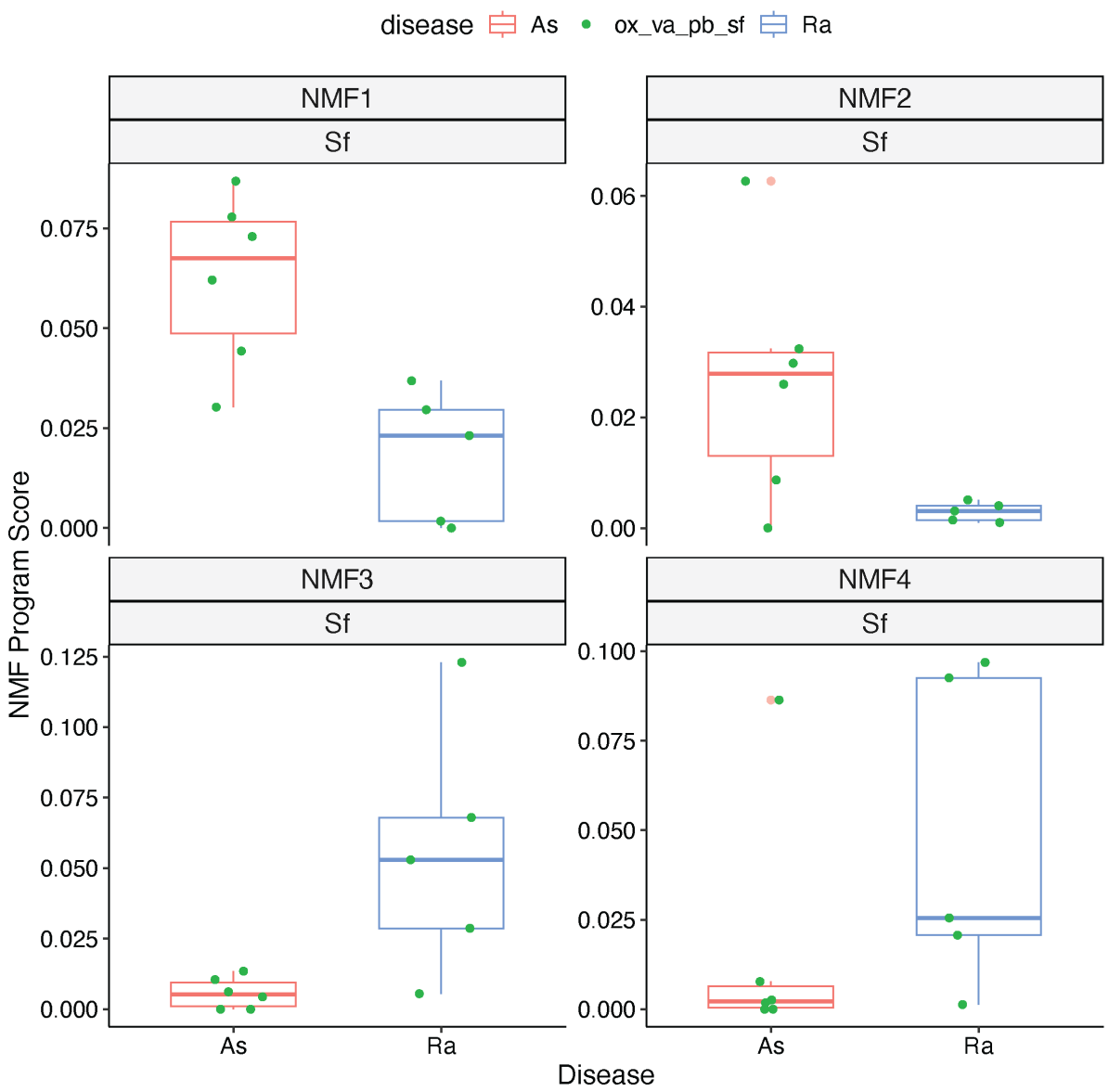


Figure D.41 NMF program scores in synovial fluid T cells of the core cohort
Boxplots showing NMF1-NMF4 program scores derived from NMF of synovial fluid T cells in the core cohort, comparing AxSpA and RA samples.



Appendix - Chapter 6

Table E.1 Manually curated pathway list used for scDRS pathway-level analysis
List of manually curated pathways included in the scDRS pathway-level analysis, with corresponding pathway names and genes included. These pathways were selected based on prior literature and relevance to AxSpA pathogenesis, covering major immune and inflammatory processes such as IL-23/IL-17 signaling, TNF and IFN pathways, antigen presentation, and cellular stress responses.

TRAIT	GENESET
REACTOME_INTERLEUKIN_17_SIGNALING	ATF1,ATF2,BTRC,CHUK,CREB1,CUL1,DUSP3,DUSP4,DUSP6,DUSP7,ELK1,FBXW11,FOS,IKBKB,IKBKG,IL17A,IL17C,IL17F,IL17RA,IL17RB,IL17RC,IL17RE,IL25,IRAK1,IRAK2,JUN,MAP2K1,MAP2K3,MAP2K4,MAP2K6,MAP2K7,MAP3K7,MAP3K8,MAPK1,MAPK10,MAPK11,MAPK14,MAPK3,MAPK7,MAPK8,MAPK9,MAPKAPK2,MAPKAPK3,MEF2A,MEF2C,NFKB1,NOD1,NOD2,PPP2CA,PPP2CB,PPP2R1A,PPP2R1B,PPP2R5D,RIPK2,RPS27A,RPS6KA1,RPS6KA2,RPS6KA3,RPS6KA5,SKP1,TAB1,TAB2,TAB3,TNIP2,TRAF6,UBA52,UBB,UBC,UBE2N,UBE2V1,VRK3
REACTOME_INTERLEUKIN_23_SIGNALING	IL12B,IL12RB1,IL23A,IL23R,JAK2,P4HB,STAT3,STAT4,TYK2
REACTOME_TNF_SIGNALING	ADAM17,BAG4,BIRC2,BIRC3,CASP8,CFLAR,CHUK,CLIP3,CYLD,FADD,IKBKB,IKBKE,IKBKG,MADD,MAP3K7,MAPKAPK2,MIB2,NSMAF,OPTN,OTUD1,OTUD7B,OTULIN,RACK1,RBCK1,RIPK1,RNF31,RPS27A,SHARPIN,SMPD2,SMPD3,SPATA2,SPPL2A,SPPL2B,STUB1,TAB1,TAB2,TAB3,TAX1BP1,TBK1,TNF,TNFAIP3,TNFRSF1A,TRADD,TRAF1,TRAF2,UBA52,UBB,UBC,UBE2D1,UBE2D2,UBE2D3,UBE2L3,ULK1,USP2,USP21,USP4,XIAP
REACTOME_JAK_STAT_SIGNALING_AFTER_INTERLEUKIN_12_STIMULATION	AIP,ANXA2,ARF1,BOLA2,BOLA2B,CA1,CAPZA1,CDC42,CFL1,CNN2,GSTA2,GSTO1,HNRNPA2B1,HNRNPDL,HNRNPF,HSPA9,IFNG,IL10,LCP1,LMNB1,MIF,MSN,MTAP,PAK2,PDCD4,PITPNA,PPIA,PSME2,RALA,RAP1B,RPLP0,SERPINB2,SNRPA1,SOD1,SOD2,STAT4,TALDO1,TCP1
REACTOME_ANTIGEN_PRESENTATION_FOLDING_ASSEMBLY_AND_PEPTIDE_LOADING_OF_CLASS_I_MHC	ATG14,B2M,BCAP31,BECN1,CALR,CANX,ERAP1,ERAP2,HLA-A,HLA-B,HLA-C,HLA-E,HLA-F,HLA-G,HSPA5,PDIA3,PIK3C3,PIK3R4,SAR1B,SEC13,SEC23A,SEC24A,SEC24B,SEC24C,SEC24D,SEC31A,TAP1,TAP2,TAPBP

REACTOME_MHC_CLASS_II_ANTIGEN_PRESENTATION	ACTR10,ACTR1A,ACTR1B,AP1B1,AP1G1,AP1M1,AP1M2,AP1S1,AP1S2,AP1S3,AP2A1,AP2A2,AP2B1,AP2M1,AP2S1,ARF1,CANX,CAPZA1,CAPZA2,CAPZA3,CAPZB,CD74,CENPE,CLTA,CLTC,CTSA,CTSB,CTSC,CTSD,CTSE,CTSF,CTSH,CTSK,CTSL,CTSO,CTSS,CTSV,DCTN1,DCTN2,DCTN3,DCTN4,DCTN5,DCTN6,DNM1,DNM2,DNM3,DYNC1H1,DYNC1I1,DYNC1I2,DYNC1LI1,DYNC1LI2,DYNLL1,DYNLL2,HLA-DMA,HLA-DMB,HLA-DOA,HLA-DOB,HLA-DPA1,HLA-DPB1,HLA-DQA1,HLA-DQA2,HLA-DQB1,HLA-DQB2,HLA-DRA,HLA-DRB1,HLA-DRB3,HLA-DRB4,HLA-DRB5,IFI30,KIF11,KIF15,KIF18A,KIF20A,KIF22,KIF23,KIF26A,KIF2A,KIF2B,KIF2C,KIF3A,KIF3B,KIF3C,KIF4A,KIF4B,KIF5A,KIF5B,KIFAP3,KLC1,KLC2,KLC3,KLC4,LAG3,LGMN,OSBPL1A,RAB7A,RACGAP1,RILP,SAR1B,SEC13,SEC23A,SEC24A,SEC24B,SEC24C,SEC24D,SEC31A,SH3GL2,SPTBN2,TUBA1A,TUBA1B,TUBA1C,TUBA3C,TUBA3D,TUBA3E,TUBA4A,TUBA4B,TUBA8,TUBAL3,TUBB1,TUBB2A,TUBB2B,TUBB3,TUBB4A,TUBB4B,TUBB6,TUBB8,TUBB8B
REACTOME_ANTIGEN_PROCESSING_CROSS_PRESENTATION	B2M,BTK,CALR,CD14,CD207,CD36,CHUK,CTSL,CTSS,CTSV,CYBA,CYBB,FCGR1A,FCGR1BP,FGA,FGB,FGG,HLA-A,HLA-B,HLA-C,HLA-E,HLA-F,HLA-G,HMGB1,IKBKB,IKBKG,ITGAV,ITGB5,LNPEP,LY96,MRC1,MRC2,MYD88,NCF1,NCF2,NCF4,PDIA3,PSMA1,PSMA2,PSMA3,PSMA4,PSMA5,PSMA6,PSMA7,PSMA8,PSMB1,PSMB10,PSMB11,PSMB2,PSMB3,PSMB4,PSMB5,PSMB6,PSMB7,PSMB8,PSMB9,PSMC1,PSMC2,PSMC3,PSMC4,PSMC5,PSMC6,PSMD1,PSMD10,PSMD11,PSMD12,PSMD13,PSMD14,PSMD2,PSMD3,PSMD4,PSMD5,PSMD6,PSMD7,PSMD8,PSMD9,PSME1,PSME2,PSME3,PSME4,PSMF1,RPS27A,S100A1,S100A8,S100A9,SEC22B,SEC61A1,SEC61A2,SEC61B,SEC61G,SEM1,SNAP23,STX4,TAP1,TAP2,TAPBP,TIRAP,TLR1,TLR2,TLR4,TLR6,UBA52,UBB,UBC,VAMP3,VAMP8
REACTOME_ANTIGEN_PROCESSING_UBIQUITINATION_PROTEASOME_DEGRADATION	ANAPC1,ANAPC10,ANAPC11,ANAPC13,ANAPC2,ANAPC4,ANAPC5,ANAPC7,AREL1,ARIH2,ASB1,ASB10,ASB11,ASB12,ASB13,ASB14,ASB15,ASB16,ASB17,ASB18,ASB2,ASB3,ASB4,ASB5,ASB6,ASB7,ASB8,ASB9,ATG7,BLMH,BTBD1,BTBD6,BTRC,CBLB,CBLL2,CCNF,CDC16,CDC20,CDC23,CDC26,CDC27,CDC34,CUL1,CUL2,CUL3,CUL5,CUL7,DCAF1,DET1,DTX3L,DZIP3,ELOB,ELOC,FBXL12,FBXL13,FBXL14,FBXL15,FBXL16,FBXL18,FBXL19,FBXL20,FBXL22,FBXL3,FBXL4,FBXL5,FBXL7,FBXL8,FBXO10,FBXO11,FBXO15,FBXO17,FBXO2,FBXO21,FBXO22,FBXO27,FBXO30,FBXO31,FBXO32,FBXO4,FBXO40,FBXO41,FBXO44,FBXO6,FBXO7,FBXO9,FBXW10,FBXW11,FBXW12,FBXW2,FBXW4,FBXW5,FBXW7,FBXW8,FBXW9,FZR1,GAN,GLMN,HACE1,HECTD1,HECTD2,HECTD3,HECW2,HERC1,HERC2,HERC3,HERC4,HERC5,HERC6,HUWE1,ITCH,KBTBD13,KBTBD6,KBTBD7,KBTBD8,KCTD6,KCTD7,KEAP1,KLHL11,KLHL13,KLHL2,KLHL20,KLHL21,KLHL22,KLHL25,KLHL3,KLHL41,KLHL42,KLHL5,KLHL9,LMO7,LNPEP,LNX1,LONRF1,LRR1,LRRC41,LRSAM1,LTN1,MEX3C,MGRN1,MIB2,MKRN1,MYLIP,NEDD4,NEDD4L,NPEPPS,PJA1,PJA2,PRKN,PSMA1,PSMA2,PSMA3,PSMA4,PSMA5,PSMA6,PSMA7

	,PSMA8,PSMB1,PSMB10,PSMB11,PSMB2,PSMB3,PSMB4,PSMB5,PSMB6,PSMB7,PSMB8,PSMB9,PSMC1,PSMC2,PSMC3,PSMC4,PSMC5,PSMC6,PSMD1,PSMD10,PSMD11,PSMD12,PSMD13,PSMD14,PSMD2,PSMD3,PSMD4,PSMD5,PSMD6,PSMD7,PSMD8,PSMD9,PSME1,PSME2,PSME3,PSME4,PSMF1,RBBP6,RBCK1,RBX1,RCHY1,RLIM,RNF111,RNF114,RNF115,RNF123,RNF126,RNF130,RNF138,RNF14,RNF144B,RNF182,RNF19A,RNF19B,RNF213,RNF217,RNF220,RNF25,RNF34,RNF4,RNF41,RNF6,RNF7,RPS27A,SEM1,SH3RF1,SIAH1,SIAH2,SKP1,SKP2,SMURF1,SMURF2,SOCS1,SOCS3,SPSB1,SPSB2,SPSB4,STUB1,THOP1,TPP2,TRAF7,TRAIP,TRIM11,TRIM21,TRIM32,TRIM36,TRIM37,TRIM39,TRIM4,TRIM41,TRIM50,TRIM63,TRIM69,TRIM71,TRIM9,TRIP12,UBA1,UBA3,UBA5,UBA52,UBA6,UBA7,UBAC1,UBB,UBC,UBE2A,UBE2B,UBE2C,UBE2D1,UBE2D2,UBE2D3,UBE2D4,UBE2E1,UBE2E2,UBE2E3,UBE2F,UBE2G1,UBE2G2,UBE2H,UBE2J1,UBE2J2,UBE2K,UBE2L3,UBE2L6,UBE2M,UBE2N,UBE2O,UBE2Q1,UBE2Q2,UBE2R2,UBE2S,UBE2U,UBE2V1,UBE2V2,UBE2W,UBE2Z,UBE3A,UBE3B,UBE3C,UBE3D,UBE4A,UBOX5,UBR1,UBR2,UBR4,UFL1,UNKL,VHL,WSB1,WWP1,ZBTB16,ZNRF1,ZNRF2
REACTOME_CLASS_I_MHC_MEDIATED_ANTIGEN_PROCESSING_PRESENTATION	ANAPC1,ANAPC10,ANAPC11,ANAPC13,ANAPC2,ANAPC4,ANAPC5,ANAPC7,AREL1,ARIH2,ASB1,ASB10,ASB11,ASB12,ASB13,ASB14,ASB15,ASB16,ASB17,ASB18,ASB2,ASB3,ASB4,ASB5,ASB6,ASB7,ASB8,ASB9,ATG14,ATG7,B2M,BCAP31,BECN1,BLMH,BTBD1,BTBD6,BTK,BTRC,CALR,CANX,CBLB,CBLL2,CCNF,CD14,CD207,CD36,CDC16,CDC20,CDC23,CDC26,CDC27,CDC34,CHUK,CTSL,CTSS,CTSV,CUL1,CUL2,CUL3,CUL5,CUL7,CYBA,CYBB,DCAF1,DET1,DTX3L,DZIP3,ELOB,ELOC,ERAP1,ERAP2,FBXL12,FBXL13,FBXL14,FBXL15,FBXL16,FBXL18,FBXL19,FBXL20,FBXL22,FBXL3,FBXL4,FBXL5,FBXL7,FBXL8,FBXO10,FBXO11,FBXO15,FBXO17,FBXO2,FBXO21,FBXO22,FBXO27,FBXO30,FBXO31,FBXO32,FBXO4,FBXO40,FBXO41,FBXO44,FBXO6,FBXO7,FBXO9,FBXW10,FBXW11,FBXW12,FBXW2,FBXW4,FBXW5,FBXW7,FBXW8,FBXW9,FCGR1A,FCGR1BP,FGA,FGB,FGG,FZR1,GAN,GLMN,HACE1,HECTD1,HECTD2,HECTD3,HECW2,HERC1,HERC2,HERC3,HERC4,HERC5,HERC6,HLA-A,HLA-B,HLA-C,HLA-E,HLA-F,HLA-G,HMGB1,HSPA5,HUWE1,IKBKB,IKBKG,ITCH,ITGAV,ITGB5,KBTBD13,KBTBD6,KBTBD7,KBTBD8,KCTD6,KCTD7,KEAP1,KLHL11,KLHL13,KLHL2,KLHL20,KLHL21,KLHL22,KLHL25,KLHL3,KLHL41,KLHL42,KLHL5,KLHL9,LMO7,LNPEP,LNX1,LONRF1,LRR1,LRRC41,LRSAM1,LTN1,LY96,MEX3C,MGRN1,MIB2,MKRN1,MRC1,MRC2,MYD88,MYLIP,NCF1,NCF2,NCF4,NEDD4,NEDD4L,NPEPPS,PDIA3,PIK3C3,PIK3R4,PJA1,PJA2,PRKN,PSMA1,PSMA2,PSMA3,PSMA4,PSMA5,PSMA6,PSMA7,PSMA8,PSMB1,PSMB10,PSMB11,PSMB2,PSMB3,PSMB4,PSMB5,PSMB6,PSMB7,PSMB8,PSMB9,PSMC1,PSMC2,PSMC3,PSMC4,PSMC5,PSMC6,PSMD1,PSMD10,PSMD11,PSMD12,PSMD13,PSMD14,PSMD2,PSMD3,PSMD4,PSMD5,PSMD6,PSMD7,PSMD8,PSMD9,PSME1,PSME2,PSME3,PSME4,PSMF1,RBBP6,RBCK1,RBX1,RCHY1,RLIM,RNF111,RNF114,RNF115,RNF123,RNF12

	6,RNF130,RNF138,RNF14,RNF144B,RNF182,RNF19A,RNF19B,RNF213,RNF217,RNF220,RNF25,RNF34,RNF4,RNF41,RNF6,RNF7,RPS27A,S100A1,S100A8,S100A9,SAR1B,SEC13,SEC22B,SEC23A,SEC24A,SEC24B,SEC24C,SEC24D,SEC31A,SEC61A1,SEC61A2,SEC61B,SEC61G,SEM1,SH3RF1,SIAH1,SIAH2,SKP1,SKP2,SMURF1,SMURF2,SNAP23,SOCS1,SOCS3,SPSB1,SPSB2,SPSB4,STUB1,STX4,TAP1,TAP2,TAPBP,THOP1,TIRAP,TLR1,TLR2,TLR4,TLR6,TPP2,TRAF7,TRAIP,TRIM11,TRIM21,TRIM32,TRIM36,TRIM37,TRIM39,TRIM4,TRIM41,TRIM50,TRIM63,TRIM69,TRIM71,TRIM9,TRIP12,UBA1,UBA3,UBA5,UBA52,UBA6,UBA7,UBAC1,UBB,UBC,UBE2A,UBE2B,UBE2C,UBE2D1,UBE2D2,UBE2D3,UBE2D4,UBE2E1,UBE2E2,UBE2E3,UBE2F,UBE2G1,UBE2G2,UBE2H,UBE2J1,UBE2J2,UBE2K,UBE2L3,UBE2L6,UBE2M,UBE2N,UBE2O,UBE2Q1,UBE2Q2,UBE2R2,UBE2S,UBE2U,UBE2V1,UBE2V2,UBE2W,UBE2Z,UBE3A,UBE3B,UBE3C,UBE3D,UBE4A,UBOX5,UBR1,UBR2,UBR4,UFL1,UNKL,VAMP3,VAMP8,VHL,WSB1,WWP1,ZBTB16,ZNRF1,ZNRF2
REACTOME_ATF4_ACTIVATES_GENES_IN_RESPONSE_TO_ENDOPLASMIC_RETICULUM_STRESS	ASNS,ATF3,ATF4,ATF6,CCL2,CEBPB,CEBPG,CXCL8,DCP2,DDIT3,DIS3,EXOSC1,EXOSC2,EXOSC3,EXOSC4,EXOSC5,EXOSC6,EXOSC7,EXOSC8,EXOSC9,HERPUD1,IGFBP1,KHSRP,NFYA,NFYB,NFYC,PARN
HALLMARK_TNFA_SIGNALING_VIA_NFKB	ABCA1,ACKR3,AREG,ATF3,ATP2B1,B4GALT1,B4GALT5,BCL2A1,BCL3,BCL6,BHLHE40,BIRC2,BIRC3,BMP2,BTG1,BTG2,BTG3,CCL2,CCL20,CCL4,CCL5,CCN1,CCND1,CCNL1,CCRL2,CD44,CD69,CD80,CD83,CDKN1A,CEBPB,CEBPD,CFLAR,CLCF1,CSF1,CSF2,CXCL1,CXCL10,CXCL11,CXCL2,CXCL3,CXCL6,DENND5A,DNAJB4,DRAM1,DUSP1,DUSP2,DUSP4,DUSP5,EDN1,EFNA1,EGR1,EGR2,EGR3,EHD1,EIF1,ETS2,F2RL1,F3,FJX1,FOS,FOSB,FOSL1,FOSL2,FUT4,G0S2,GADD45A,GADD45B,GCH1,GEM,GFPT2,GPR183,HBEGF,HES1,ICAM1,ICOSLG,ID2,IER2,IER3,IER5,IFIH1,IFIT2,IFNGR2,IL12B,IL15RA,IL18,IL1A,IL1B,IL23A,IL6,IL6ST,IL7R,INHBA,IRF1,IRS2,JAG1,JUN,JUNB,KDM6B,KLF10,KLF2,KLF4,KLF6,KLF9,KYNU,LAMB3,LDLR,LIF,LITAF,MAFF,MAP2K3,MAP3K8,MARCKS,MCL1,MSC,MXD1,MYC,NAMPT,NFAT5,NFE2L2,NFIL3,NFKB1,NFKB2,NFKBIA,NFKBIE,NINJ1,NR4A1,NR4A2,NR4A3,OLR1,PANX1,PDE4B,PDLIM5,PER1,PFKFB3,PHLDA1,PHLDA2,PLAU,PLAUR,PLEK,PLK2,PLPP3,PMEPA1,PNRC1,PPP1R15A,PTGER4,PTGS2,PTPRE,PTX3,RCAN1,REL,RELA,RELB,RHOB,RIGI,RIPK2,RNF19B,SAT1,SDC4,SERPINB2,SERPINB8,SERPINE1,SGK1,SIK1,SLC16A6,SLC2A3,SLC2A6,SMAD3,SNN,SOCS3,SOD2,SPHK1,SPSB1,SQSTM1,STAT5A,TANK,TAP1,TGIF1,TIPARP,TLR2,TNC,TNF,TNFAIP2,TNFAIP3,TNFAIP6,TNFAIP8,TNFRSF9,TNFSF9,TNIP1,TNIP2,TRAF1,TRIB1,TRIP10,TSC22D1,TUBB2A,VEGFA,YRDC,ZBTB10,ZC3H12A,ZFP36
REACTOME_INTERFERON_GAMMA_SIGNALING	B2M,CAMK2A,CAMK2B,CAMK2D,CAMK2G,CD44,CIITA,FCGR1A,FCGR1BP,GBP1,GBP2,GBP3,GBP4,GBP5,GBP6,GBP7,HLA-A,HLA-B,HLA-C,HLA-DPA1,HLA-DPB1,HLA-DQA1,HLA-DQA2,HLA-DQB1,HLA-DQB2,HLA-DRA,HLA-DRB1,HLA-DRB3,HLA-DRB4,HLA-DRB5,HLA-E,HLA-F,HLA-G,HLA-

	H,ICAM1,IFI30,IFNG,IFNGR1,IFNGR2,IRF1,IRF2,IRF3,IRF4,IRF5,IRF6,IRF7,IRF8,IRF9,JAK1,JAK2,MAPK1,MAPK3,MID1,MT2A,NCAM1,OAS1,OAS2,OAS3,OASL,PIAS1,PML,PRKCD,PTAFR,PTPN1,PTPN11,PTPN2,PTPN6,RAF1,SMAD7,SOCS1,SOCS3,SP100,STAT1,SUMO1,TRIM10,TRIM14,TRIM17,TRIM2,TRIM21,TRIM22,TRIM25,TRIM26,TRIM29,TRIM3,TRIM31,TRIM34,TRIM35,TRIM38,TRIM45,TRIM46,TRIM48,TRIM5,TRIM6,TRIM62,TRIM68,TRIM8,VCAM1,YBX1
REACTOME_INTERLEUKIN_1_FAMILY_SIGNALING	AGER,ALOX5,ALPK1,APP,BTRC,CASP1,CASP8,CHUK,CTSG,CUL1,FBXW11,GSDMD,HMGB1,IKBIP,IKBKB,IKBKG,IL13,IL18,IL18BP,IL18R1,IL18RAP,IL1A,IL1B,IL1F10,IL1R1,IL1R2,IL1RAP,IL1RAPL1,IL1RL1,IL1RL2,IL1RN,IL33,IL36A,IL36B,IL36G,IL36RN,IL37,IL4,IRAK1,IRAK2,IRAK3,IRAK4,LRRC14,MAP2K1,MAP2K4,MAP2K6,MAP3K3,MAP3K7,MAP3K8,MAPK8,MYD88,N4BP1,NFKB1,NFKB2,NFKBIA,NFKBIB,NKIRAS1,NKIRAS2,NLRC5,NLRX1,NOD1,NOD2,PELI1,PELI2,PELI3,PSMA1,PSMA2,PSMA3,PSMA4,PSMA5,PSMA6,PSMA7,PSMA8,PSMB1,PSMB10,PSMB11,PSMB2,PSMB3,PSMB4,PSMB5,PSMB6,PSMB7,PSMB8,PSMB9,PSMC1,PSMC2,PSMC3,PSMC4,PSMC5,PSMC6,PSMD1,PSMD10,PSMD11,PSMD12,PSMD13,PSMD14,PSMD2,PSMD3,PSMD4,PSMD5,PSMD6,PSMD7,PSMD8,PSMD9,PSME1,PSME2,PSME3,PSME4,PSMF1,PTPN11,PTPN12,PTPN13,PTPN14,PTPN18,PTPN2,PTPN20,PTPN23,PTPN4,PTPN5,PTPN6,PTPN7,PTPN9,RBX1,RELA,RIPK2,RPS27A,S100A12,S100B,SAA1,SEM1,SIGIRR,SKP1,SMAD3,SQSTM1,STAT3,TAB1,TAB2,TAB3,TBK1,TIFA,TNIP2,TOLLIP,TP53,TRAF2,TRAF6,UBA52,UBB,UBC,UBE2N,UBE2V1,USP14,USP18
REACTOME_INTERLEUKIN_1_PROCESSING	CASP1,CTSG,GSDMD,IL18,IL1A,IL1B,NFKB1,NFKB2,RELA
REACTOME_INTERLEUKIN_1_SIGNALING	AGER,ALPK1,APP,BTRC,CASP8,CHUK,CUL1,FBXW11,HMGB1,IKBIP,IKBKB,IKBKG,IL1A,IL1B,IL1R1,IL1R2,IL1RAP,IL1RN,IRAK1,IRAK2,IRAK3,IRAK4,LRRC14,MAP2K1,MAP2K4,MAP2K6,MAP3K3,MAP3K7,MAP3K8,MYD88,N4BP1,NFKB1,NFKB2,NFKBIA,NFKBIB,NKIRAS1,NKIRAS2,NLRC5,NLRX1,NOD1,NOD2,PELI1,PELI2,PELI3,PSMA1,PSMA2,PSMA3,PSMA4,PSMA5,PSMA6,PSMA7,PSMA8,PSMB1,PSMB10,PSMB11,PSMB2,PSMB3,PSMB4,PSMB5,PSMB6,PSMB7,PSMB8,PSMB9,PSMC1,PSMC2,PSMC3,PSMC4,PSMC5,PSMC6,PSMD1,PSMD10,PSMD11,PSMD12,PSMD13,PSMD14,PSMD2,PSMD3,PSMD4,PSMD5,PSMD6,PSMD7,PSMD8,PSMD9,PSME1,PSME2,PSME3,PSME4,PSMF1,RBX1,RELA,RIPK2,RPS27A,S100A12,S100B,SAA1,SEM1,SKP1,SQSTM1,TAB1,TAB2,TAB3,TIFA,TNIP2,TOLLIP,TP53,TRAF2,TRAF6,UBA52,UBB,UBC,UBE2N,UBE2V1,USP14,USP18
REACTOME_INTERLEUKIN_6_FAMILY_SIGNALING	CBL,CLCF1,CNTF,CNTFR,CRLF1,CTF1,IL11,IL11RA,IL31,IL31RA,IL6,IL6R,IL6ST,JAK1,JAK2,LIF,LIFR,OSM,OSMR,PTPN11,SOCS3,STAT1,STAT3,TYK2

REACTOME_INTERLEUKIN_6_SIGNALING	CBL,IL6,IL6R,IL6ST,JAK1,JAK2,PTPN11,SOCS3,STAT1,STAT3,TYK2
REACTOME_TCR_SIGNALING	BCL10,BTRC,CARD11,CD101,CD247,CD3D,CD3E,CD3G,CD4,CDC34,CHUK,CSK,CUL1,ENAH,EVL,FBXW11,FYB1,GRAP2,HLA-DPA1,HLA-DPB1,HLA-DQA1,HLA-DQA2,HLA-DQB1,HLA-DQB2,HLA-DRA,HLA-DRB1,HLA-DRB3,HLA-DRB4,HLA-DRB5,IKBKB,IKBKG,INPP5D,ITK,LAT,LCK,LCP2,MALT1,MAP3K7,NCK1,NFKB1,NFKBIA,PAG1,PAK1,PAK2,PAK3,PDPK1,PIK3CA,PIK3CB,PIK3R1,PIK3R2,PLCG1,PLCG2,PRKCQ,PSMA1,PSMA2,PSMA3,PSMA4,PSMA5,PSMA6,PSMA7,PSMA8,PSMB1,PSMB10,PSMB11,PSMB2,PSMB3,PSMB4,PSMB5,PSMB6,PSMB7,PSMB8,PSMB9,PSMC1,PSMC2,PSMC3,PSMC4,PSMC5,PSMC6,PSMD1,PSMD10,PSMD11,PSMD12,PSMD13,PSMD14,PSMD2,PSMD3,PSMD4,PSMD5,PSMD6,PSMD7,PSMD8,PSMD9,PSME1,PSME2,PSME3,PSME4,PSMF1,PTEN,PTPN22,PTPRC,PTPRJ,RELA,RIPK2,RPS27A,SEM1,SKP1,TAB2,TRAF6,TRAT1,TRAV19,TRAV29DV5,TRAV8-4,TRBV12-3,TRBV7-9,UBA52,UBB,UBC,UBE2D1,UBE2D2,UBE2N,UBE2V1,VASP,WAS,ZAP70
SUPERCLASS_GO_OSTEOCLAST_DIFFERENTIATION	CAMK4,GPC3,SLC4A2,CSF1R,BGLAP,TNFRSF11A,TFE3,TLR4,POU4F1,CD81,CEBPB,TF,IFNG,IL23A,SRC,FOSL2,SH3PXD2A,IGSF23,FBN1,CARTPT,SFRP1,OSTM1,TCIRG1,LILRB1,OCSTAMP,PIK3R1,TNFAIP6,GAB2,CREB1,SLC9B2,MTOR,GPR137,TNFSF11,TREM2,CCR1,NEDD9,DCSTAMP,TOB2,FOS,IL17A,CTNNB1,CALCR,NF1,TFRC,TRAF6,TYROBP,TCTA,FSTL3,SIGLEC15,EPHA2,GPR137B,IREB2,FBXW7,LTF,IL23R,EEIG1,SBNO2,GPR68,CCN4,PIAS3,CD109,RASSF2,FSHB,JUNB,LRRK1,RPTOR,ERFE,OSCAR,ATP6AP1,LRRC17,EFNA2,IAPP,POU4F2,SNX10,GLO1,NOTCH2,PRXL2A,ZNF675,CCL3,FARP2,MAPK14,KLF10,TNF,GPR55,LILRB3,IL20,CLDN18,UBASH3B,LILRB4,IL4,MAFB,FAM20C,IL12B,PAFAH1B1,TMEM178A,TMEM64,INPP5D,PPARGC1B,GPR183,TLR3,TNFRSF11B,PPP3CA,TGFB1,ANXA2,FOXP1,P2RX5,BMP2,CSF1,MITF
REACTOME_INTERLEUKIN_23_SIGNALING	IL12B,IL12RB1,IL23A,IL23R,JAK2,P4HB,STAT3,STAT4,TYK2
REACTOME_INTERLEUKIN_1_PROCESSING	CASP1,CTSG,GSDMD,IL18,IL1A,IL1B,NFKB1,NFKB2,RELA
GOBP_OSTEOCLAST_DIFFERENTIATION	ANXA2,ATP6AP1,BGLAP,BMP2,CALCR,CAMK4,CARTPT,CCL3,CCN4,CCR1,CD109,CD81,CEBPB,CLDN18,CREB1,CSF1,CSF1R,CTNNB1,DCSTAMP,EEIG1,EFNA2,EPHA2,ERFE,FAM20C,FARP2,FBN1,FBXW7,FOS,FOSL2,FOXP1,FSHB,FSTL3,GAB2,GLO1,GPC3,GPR137,GPR137B,GPR183,GPR55,GPR68,IAPP,IFNG,IGSF23,IL12B,IL17A,IL20,IL23A,IL23R,IL4,INPP5D,IREB2,JUNB,KLF10,LILRB1,LILRB3,LILRB4,LRRC17,LRRK1,LTF,MAFB,MAPK14,MITF,MTOR,NEDD9,NF1,NOTCH2,OCSTAMP,OSCAR,OSTM1,P2RX5,PAFAH1B1,PIAS3,PIK3R1,POU4F1,POU4F2,PPARGC1B,PPP3CA,PRXL2A,RASSF2,RPTOR,SBNO2,SFRP1,SH3PXD2A,SIGLEC15,SLC4A2,SLC9

	B2,SNX10,SRC,TCIRG1,TCTA,TF,TFE3,TFRC,TGFB1,TLR3,TLR4,TMEM178A,TMEM64,TNF,TNFAIP6,TNFRSF11A,TNFRSF11B,TNFSF11,TOB2,TRAF6,TREM2,TYROBP,UBASH3B,ZNF675
GOBP_OSTEOCLAST_FUSION	CD109,CD81,DCSTAMP,SBNO2,SH3PXD2A,TCTA
GOBP_OSTEOCLAST_PROLIFERATION	CSF1,GREM1,JUNB,NMB,NMBR,NPR3,OCSTAMP,PTH,TCIRG1,TNFAIP3,TNFSF11

Figure E.2 scDRS-based disease association across cell types in SFMC
Heatmap showing scDRS-derived disease association scores across (A) T and NK cell subsets and (B) other immune populations, including myeloid cells, B cells, and additional minor subsets. Only cell types with more than 10 cells in total within the condition were included in the analysis. Colour scale represents the association Z-score, with higher values indicating stronger positive association with AxSpA. Statistical significance is denoted by adjusted p-values: *** < 0.001, ** < 0.01, * < 0.05.

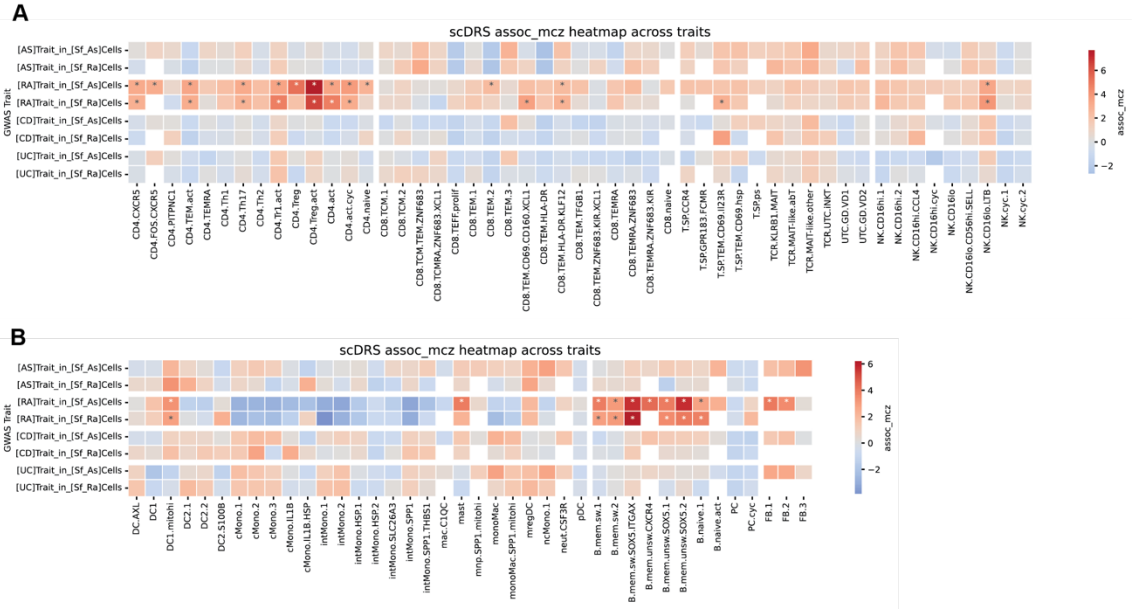


Figure E.3 scDRS-based disease association across cell types in PBMC
Heatmap showing scDRS-derived disease association scores across (A) T and NK cell subsets and (B) other immune populations, including myeloid cells, B cells, and additional minor subsets. Only cell types with more than 10 cells in total within the condition were included in the analysis. Colour scale represents the association Z-score, with higher values indicating stronger positive association with AxSpA. Statistical significance is denoted by adjusted p-values: *** < 0.001, ** < 0.01, * < 0.05.

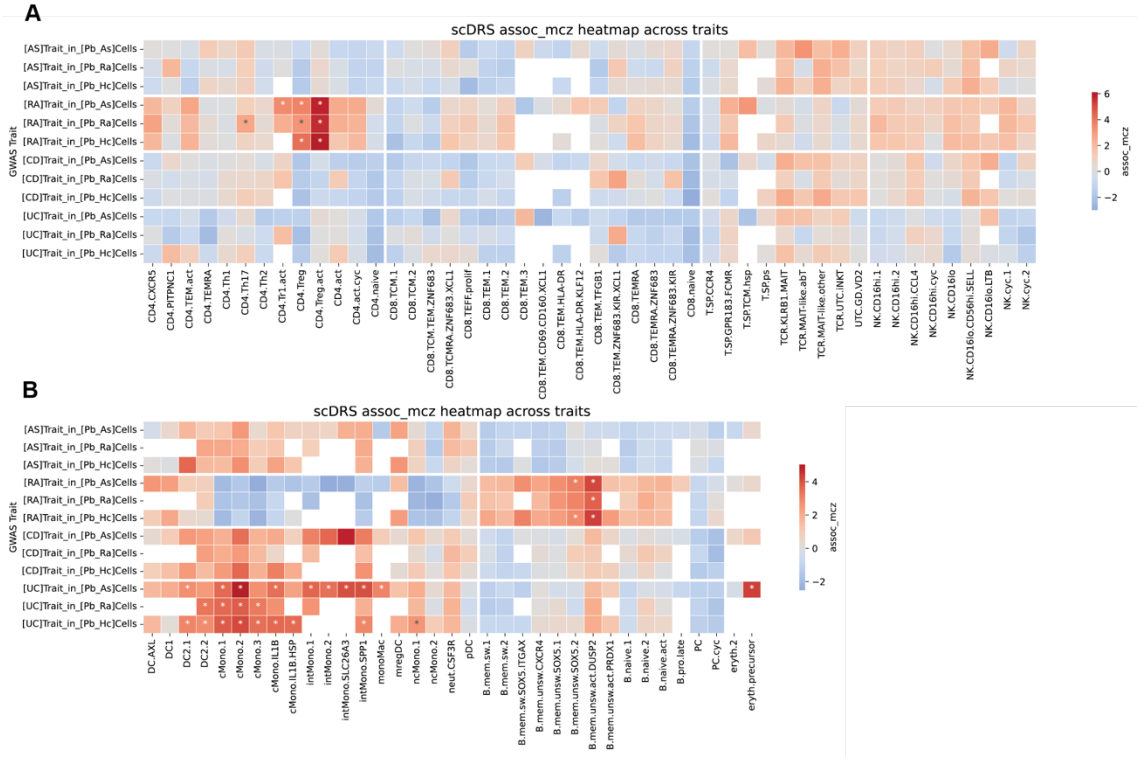


Figure E.4 Disease-associated pathway enrichment analysis in fresh ileum
Heatmap showing selected disease-associated pathways and their scDRS-derived enrichment Z-scores in the fresh ileum. (A) T cell compartments. (B) Myeloid-cell compartments. Colour represents the pathway enrichment Z-score, with higher values indicating stronger positive association with the selected pathway. Major cell-type groups are annotated. Significance thresholds: *** < 0.001, ** < 0.01, * < 0.05, + < 0.1.

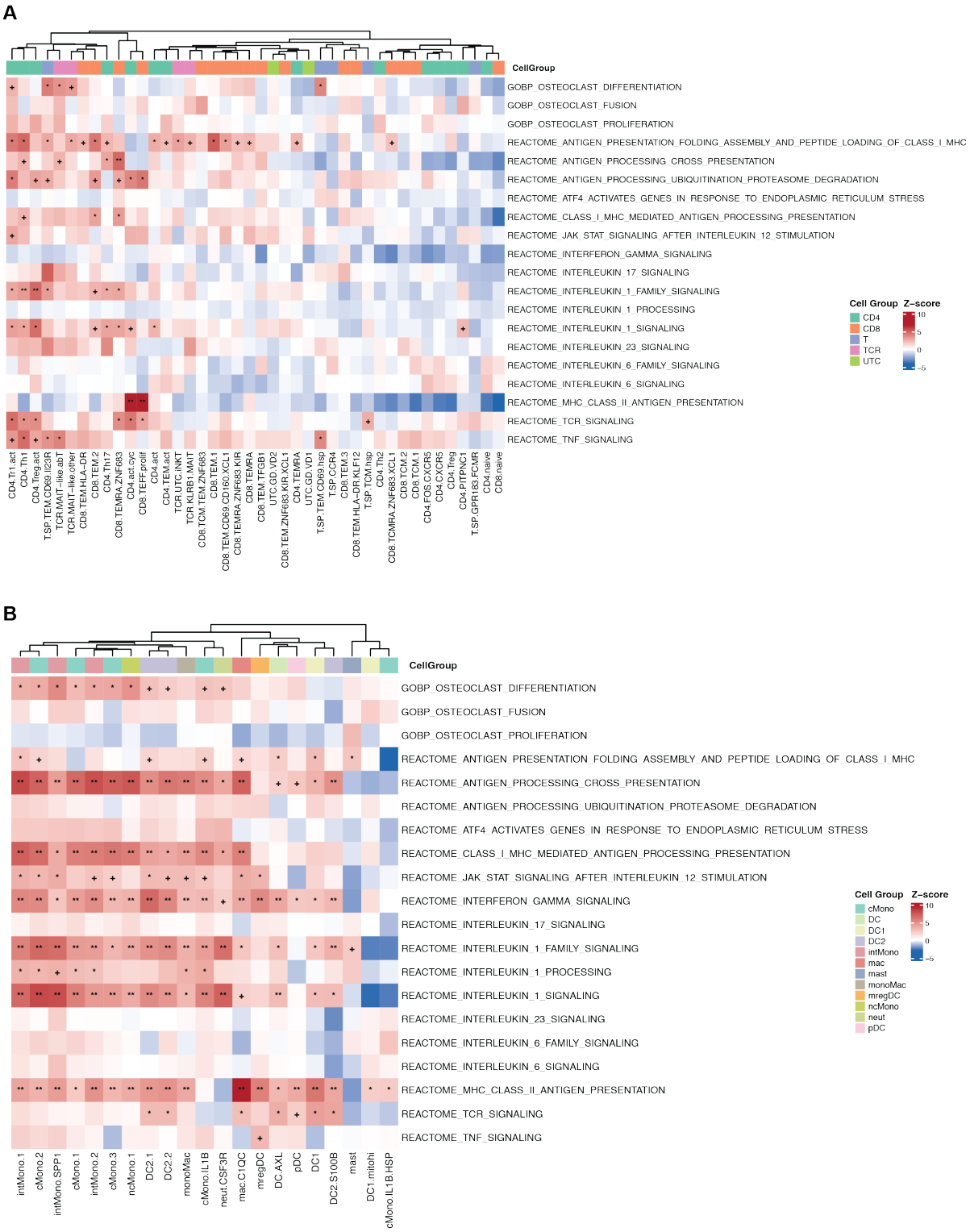


Figure E.5 Disease-associated pathway enrichment analysis in fresh synovial fluid
Heatmap showing selected disease-associated pathways and their scDRS-derived enrichment Z-scores in the fresh ileum. (A) T cell compartments. (B) Myeloid-cell compartments. Colour represents the pathway enrichment Z-score, with higher values indicating stronger positive association with the selected pathway. Major cell-type groups are annotated. Significance thresholds: *** < 0.001, ** < 0.01, * < 0.05, + < 0.1.

